

Characterization of MTP8 as a tonoplast Fe/Mn transporter essential for Fe efficiency and for Fe and Mn localization in the subepidermis of Arabidopsis embryos

Dissertation
zur Erlangung des
Doktorgrades der Naturwissenschaften (Dr. rer. nat.)

der

Naturwissenschaftlichen Fakultät I
– Biowissenschaften –

der Martin-Luther-Universität
Halle-Wittenberg

vorgelegt

von Herrn Seckin Eroglu

geb. am 30.08.1985 in Izmir/Türkei

verteidigung am 10.07.2015

Gutachter

1. Prof. Dr. Nicolaus von Wirén
2. Prof. Dr. Klaus Humbeck
3. Prof. Dr. Thomas Buckhout

Table of contents

1. Summary.....	5
2. General Introduction.....	6
2.1. Metabolic functions of Fe.....	6
2.2. Plant strategies to enhance Fe acquisition from soils	7
2.2.1. Strategy I.....	7
2.2.2. Strategy II.....	8
2.2.3. Fe deficiency and heavy metal toxicity	9
2.2.4. Mn-induced Fe deficiency	11
2.3. Fe translocation from roots to shoots	12
2.4. Post-phloem transport and storage of Fe, Mn and Zn in seeds.....	13
2.4.1. Post-phloem transport of Fe to the seed coat.....	13
2.4.2. Route of metal transport from the seed coat to the embryo	14
2.4.3. Use and storage of metals in the embryo	15
2.5. The Cation Diffusion Facilitator (CDF) family.....	17
2.6. Aims of the thesis.....	18
3. Materials and Methods	20
3.1. Plant lines, plasmids, and transformation	20
3.2. Plant growth conditions, media, and mutant screening.....	22
3.3. Elemental Analysis.....	22
3.4. GUS Histochemical Analyses.....	22
3.5. Chlorophyll Measurements.....	23
3.6. Observation of root fluorescence.....	23
3.7. Quantitative RT-PCR.....	23
3.8. Yeast strains, plasmids, transformation, and growth methods	23
3.9. Ferric chelate reductase activity and rhizosphere acidification assays	24
3.10. Perls staining and DAB/H ₂ O ₂ intensification.....	24
4. Results	25
4.1. Design and establishment of the screening medium.....	25
4.1.1. Optimization of growth parameters.....	25
4.1.2. Induction of Fe deficiency on Fe28/Mn40 medium	26
4.1.3. Validation of the medium and screening process	27
4.2. Involvement of MTP8 in Fe and Mn homeostasis in Fe-deficient Arabidopsis plants	

4.2.1.	<i>mtp8</i> mutant lines are susceptible to Fe deficiency-induced chlorosis	31
4.2.2.	Subcellular localization of MTP8.....	33
4.2.3.	Metal transport specificity of MTP8.....	33
4.2.4.	Sensitivity of the Arabidopsis <i>mtp8-1</i> mutant to high Mn	35
4.2.5.	Regulation of <i>MTP8</i> on high media in a <i>FIT</i> -dependent manner.....	36
4.2.6.	Tissue localization	37
4.2.7.	Effect of Mn on the Fe deficiency phenotype of <i>mtp8-1</i>	38
4.2.8.	Characterization of the Fe-deficiency response in the <i>mtp8-1</i> mutant	40
4.3.	A function of MTP8 in Mn localization in developing Arabidopsis embryos	45
4.3.1.	<i>In silico</i> analysis of <i>MTP8</i> and <i>VIT1</i> expression during embryo development ..	45
4.3.2.	<i>MTP8</i> and <i>VIT1</i> promoter activity during seed development.....	46
4.3.3.	Metal localization in <i>mtp8</i> mutant seeds by synchrotron X-ray fluorescence ...	47
4.3.4.	Phenotypic analysis of a <i>mtp8 vit1</i> double knock-out line	50
4.3.5.	Metal concentrations in rosette leaves and seeds of soil-grown plants.....	54
5.	Discussion.....	56
5.1.	Screening Arabidopsis mutant lines on high-pH, low-Fe agar medium as a novel approach to isolate genes involved in Fe homeostasis	56
5.2.	The vacuolar manganese transporter MTP8 determines tolerance to Fe deficiency-induced chlorosis in Arabidopsis	57
5.2.1.	MTP8 localizes to the tonoplast and transports Mn and Fe into the vacuole....	58
5.2.2.	MTP8 is part of the Fe acquisition machinery in Arabidopsis.....	59
5.2.3.	MTP8 prevents Mn from inhibiting Fe(III) reduction under Fe deficiency	60
5.3.	MTP8 is responsible for the specific Fe and Mn localization in subepidermal cells of the Arabidopsis embryo	62
6.	References.....	64
7.	Abbreviations	69
8.	Affirmation	70
9.	Acknowledgements	71

1. Summary

Although iron (Fe) is a highly abundant element in the earth's crust, plants often suffer from Fe deficiency when grown on alkaline soils, in which Fe availability is low. To increase Fe acquisition from soils, plants have developed different strategies, which are not yet fully understood at the molecular level. Therefore, the aim of the present thesis was to identify genes involved in the Fe deficiency response employing a forward-genetics approach in *Arabidopsis*.

In a first step, a high-pH, low-Fe agar medium was developed, which mimics the pH-dependent Fe limitation observed in alkaline soils. Using this medium, a collection of *Arabidopsis* T-DNA insertion lines was screened allowing to identify severely chlorotic plants, which regreened by the supplementation of Fe. These lines carried an insertion in *MTP8*, encoding a member of the MTP family of Mn transporters which belong to the superfamily of Cation Diffusion Facilitators. Since a MTP8-EYFP fusion protein localized to the tonoplast, *MTP8* complemented growth of a Mn-sensitive yeast mutant, and *mtp8* knockout lines were hypersensitive to low Fe availability only in the presence of Mn, MTP8 was attributed a role in Mn detoxification. Expression of *MTP8* was confined to outer root cell layers and strongly induced by low Fe and high Mn supplies in the medium, which was strictly dependent on the transcription factor FIT, a master regulator of Fe-deficiency responses. Fe deficiency-induced chlorosis observed in *mtp8* mutants depended on the presence of Mn in the medium and was correlated with low Fe but high Mn concentrations in shoots. Investigating other components of the Fe deficiency response revealed that the *mtp8* mutant was defective in enhancing ferric chelate reduction, although the corresponding *FRO2* gene was upregulated at the transcript level. These findings indicate that sequestering Mn to the root vacuoles by MTP8 is an important component of the Fe deficiency response, which is essential to increase Fe reduction rate in the presence of Mn.

Mn and Fe have previously been reported to take in a distinct cell type-specific localization in mature seeds, whereby Mn is primarily localized in the subepidermis of the abaxial side of cotyledons. In the present work, the question was addressed whether this localization pattern is dependent on MTP8. In cooperation with a Japanese partner laboratory, *mtp8* mutant seeds were analyzed by synchrotron X-ray fluorescence, showing that Mn localization in the subepidermis of the abaxial side of the cotyledons and hypocotyl was abolished. Instead, Mn co-localized with Fe around the vascular strands of the embryo. Consistent with a previous study showing that Fe localizes to the abaxial side of the cotyledons in the embryo when tonoplast Fe transporter VIT1 is lacking, it was assumed that Fe localization to the abaxial side of the cotyledons in *vit1* also depended on MTP8. To verify this hypothesis, a *mtp8 vit1* double knock-out line was generated and Fe was stained by Perls/DAB. As expected, stained Fe was detected in the abaxial side of the cotyledons in *vit1* and this distribution was abolished in the double knock-out line. A yeast complementation approach further showed that MTP8 is able to transport Fe besides Mn. However, germination experiments conducted with *mtp8* and *mtp8 vit1* mutants under Fe or Mn limitation failed to detect any phenotype related to the mislocalization of Fe and Mn. These findings indicate that the interplay between VIT1 and MTP8 determines the cell type-specific localization of Fe and Mn in the embryo of mature seeds.

2. General Introduction

2.1. Metabolic functions of Fe

Iron (Fe) is an essential element involved in the synthesis of many important proteins, especially those which participate in oxygen binding or electron transport. A major reason behind this is the versatile nature of Fe due to its ability to easily change its oxidation state between Fe(III) and Fe(II) and to form octa- and tetrahedral complexes with various ligands (Marschner, 2012). According to the form in which Fe binds to proteins, three classes have been described: heme-bound Fe, Fe-S clusters or Fe bound in any other form.

The heme structure consists of a tetrapyrrole ring, surrounding an Fe ion localised in the center which is coordinated by 4 N atoms (Chance et al., 1966; Kadish et al., 1999). This structure is called porphyrine group and binds to proteins belonging to the group of heme proteins. Cytochromes which have essential roles in the electron transport chain in chloroplasts and mitochondria are well-known examples. Besides, heme proteins have functions in various processes, such as the reduction of nitrate or detoxification of reactive oxygen species (ROS). In Fe-S proteins, Fe either creates a bond with thiol groups of cysteine or binds to inorganic S leading to the formation of Fe-S clusters or both. In proteins, Fe-S clusters can occur in the form of Fe_2S_2 , Fe_3S_4 or Fe_4S_4 . An example for a protein carrying an Fe_2S_2 cluster is the ferredoxin protein, which is involved in the photosynthetic electron transport chain. An Fe_3S_4 cluster, which is found e.g. in aconitase, becomes active when its cluster is converted to Fe_4S_4 by increasing Fe concentration *in vitro* (Kennedy et al., 1983). Other important examples of enzymes possessing Fe-S domains are nitrate reductase or Fe-dependent superoxide dismutase (FeSOD), the latter being involved in the detoxification of oxygen radicals. Besides these Fe-binding proteins, diiron-carboxylate proteins represent another group having a binuclear center (Kurtz Jr, 1997). Fe atoms in their center are at least partially coordinated by carboxyl groups of aspartate or glutamate. Examples include the ferritin protein which can store large amounts of Fe in nanocages, the stearyl-acyl carrier protein desaturase which mediates plant lipid desaturation or the ribonucleotide reductase which reduces ribonucleotides. In addition to diiron-carboxylate-containing proteins, there are proteins in which a single Fe atom is coordinated by either cysteines, histidines or the carboxyl groups of aspartate and glutamate (Glusker, 1991). These are less characterized compared to the other groups of Fe-binding proteins. Lipoygenases, which catalyze dioxygenation of fatty acids in lipids are examples for proteins containing one Fe atom (Brash, 1999).

Following O, Si, and Al, Fe is the fourth-most abundant element in the earth's crust, yet it is mostly found in precipitated forms of insoluble Fe(III)-hydroxides, -oxides, or -phosphates. In general, the solubility of these complexes decreases as the pH increases. Accordingly, in calcareous soils where the pH is high, Fe is often insoluble and not readily available to plants. In this case, the Fe concentration in the soil solution cannot meet the Fe demand by the plant, which provokes Fe deficiency. This low Fe solubility can be overcome by two main strategies which were evolved in plants to improve Fe acquisition.

2.2. Plant strategies to enhance Fe acquisition from soils

Fe-deficient plant roots show morphological and physiological differences to Fe-sufficient ones. Under Fe deficiency, plant roots can undergo a series of morphological adaptations including the swelling of root tips, an increase in the number of root hairs and the formation of transfer cells. These responses are accompanied by physiological changes including an increased ferric reductase activity at the root plasma membrane, an increased synthesis and stability of the Fe²⁺ uptake protein IRT1, an enhanced capacity for proton extrusion, and the release of phenolic compounds or phytosiderophores (Abadía et al., 2011). Looking to Fe-deficient roots at the molecular level, transcriptional profiling using the RNA sequencing showed that in *Arabidopsis* approximately 10% of the total number of transcripts and according to an iTRAQ approach 2% of the accumulated proteins are differentially regulated under Fe deficiency (Lan et al., 2011; Rodríguez-Celma et al., 2013). A large part of these differences account for the mechanisms which are induced in roots to increase Fe acquisition. Two distinct strategies, called Strategy I and II, have been described by which plants acquire precipitated Fe (Figure 1) (Marschner and Römheld, 1994).

2.2.1. Strategy I

Strategy I is confined to dicotyledonous and non-graminaceous monocotyledonous plant species. The most important characteristic of strategy I-type Fe acquisition is the reduction of Fe(III) to Fe(II) prior to root uptake. This strategy comprises of three main steps, which are all induced under Fe deficiency: Fe(III) mobilization, Fe(III) reduction, and Fe²⁺ uptake.

Fe(III) is mostly mobilized by the secretion of protons (Santi and Schmidt, 2009), coumarins and flavins (Fourcroy et al., 2014; Rodríguez-Celma et al., 2013; Schmid et al., 2014) into the rhizosphere. Proton secretion leads to an acidification of the rhizosphere, mobilizing Fe(III) from hydroxides (Zinder et al., 1986). Proton secretion is of major importance, considering that a decrease by one pH unit results in an approximately 1000-fold increase in Fe solubility (Santi and Schmidt, 2009). This acidification takes place via proton-pumping ATPases (AHAs). Accordingly, *aha2* knock-out seedlings of *Arabidopsis* showed a diminished capacity for proton secretion compared to the wild type under Fe deficiency, indicating that rhizosphere acidification under Fe deficiency is AHA2-dependent (Santi and Schmidt, 2009). Acidification of the rhizosphere is not efficient in mobilizing Fe(III) in calcareous soils, mostly due to the buffering capacity of bicarbonate. However, under this condition, some strategy I plants solubilize Fe better than others, indicating that there are other mechanisms involved in Fe mobilization. Recently, it has been shown that plants secrete flavins and phenolics, which are both involved in the mobilization of Fe(III) (Rodríguez-Celma et al., 2013; Schmid et al., 2014). Among the phenolics that *Arabidopsis* secretes into the rhizosphere, a class of coumarins has been shown to be essential for chlorosis-free growth on calcareous soils. These coumarins include mostly scopoletin and to a lesser extent esculin and esculetin. Among those, based on *in vitro* assays, only esculetin was shown to chelate and mobilize Fe(III) (Schmid et al., 2014). It is possible that esculetin is also generated from the demethylation of scopoletin after its secretion. Scopoletin synthesis is greatly reduced in *f6'h1* mutants, which are defective in enzymes involved in synthesis of coumarins via the phenylpropanoid pathway (Kai et al., 2008). Coumarin synthesis and secretion increases greatly under Fe deficiency. As coumarins

emit fluorescence under UV light, this enhanced secretion can be visualized on agar plates by an increase in fluorescence in the rhizosphere of Fe-deficient plants (Schmid et al., 2014). Loss-of-function mutants of a gene belonging to Plant Pleiotropic Resistance (PDR) family, called *PDR9* showed a different fluorescence pattern in the roots compared to the wild type. While wild-type plants showed fluorescence in both, the roots and the rhizosphere, fluorescence in *pdr9* mutants was restricted only to the roots, indicating that PDR9 mediates the release of coumarins to the rhizosphere (Fourcroy et al., 2014).

Fe(III) reduction is a prerequisite for Fe acquisition by strategy I plants because only Fe²⁺ is transported across the plasma membrane. Reduction mainly depends on the activity of the ferric chelate reductase enzyme, encoded by *FRO2* (Robinson et al., 1999). Furthermore, analysis of *FRO2* mutants showed that reduction is the rate-limiting step in Fe acquisition (Connolly et al., 2003). Fe(III) reduction is strongly dependent on rhizosphere acidification because the ferric chelate reductase activity is pH-dependent (Schaaf, 2004). Finally, some Fe(III) may be reduced by phenolics, since some of the phenolics are known to be strong reducing agents and their secretion is upregulated under Fe deficiency (Mladěnka et al., 2010).

The major importer for Fe²⁺ is IRT1, which localizes to the plasma membrane of rhizodermal and cortical root cells. It is strikingly upregulated under Fe deficiency (Vert et al., 2002). Absence of the protein in loss-of-function mutants leads to Fe deficiency-induced chlorosis, even under Fe-sufficient conditions. IRT1 transports not only Fe²⁺ but also other divalent heavy metals when expressed in yeast (Korshunova et al., 1999) or *in planta*, explaining why Fe-deficient plants accumulate other heavy metals in roots and shoots. Consistently, such an accumulation is not seen in the absence of a functional IRT1 protein (Korshunova et al., 1999; Vert et al., 2002). Taken together, IRT1 is at the center of Fe acquisition, but also responsible for excess accumulation of heavy metals due to the lack of specificity for Fe.

2.2.2. Strategy II

Graminaceous plants use Strategy II for Fe acquisition (Figure 1). They secrete a class of ligands, phytosiderophores (PS), which chelate Fe(III) by means of their amine and carboxyl groups, leading to the solubilization of rhizosphere Fe (Takagi et al., 1984; Weber et al., 2002). PS are synthesized from L-methionine in a series of reactions which are catalyzed by enzymes including S-adenosylmethionine synthetase, nicotianamine synthase, nicotianamine aminotransferase and deoxymugineic acid synthase (Higuchi et al., 1999; Takahashi et al., 1999). Not surprisingly, genes encoding for these enzymes and genes involved in methionine recycling by the Yang cycle are rapidly induced under Fe deficiency and required for increased PS synthesis (Kobayashi and Nishizawa, 2012; Ma et al., 1995). Nine different types of PS have been identified in graminaceous plants until now (Kobayashi and Nishizawa, 2012), which form complexes with Fe(III), Zn(II), and Cu(II) with different affinities. PS are secreted into the rhizosphere through TOM1-type transporters (Murata et al., 2006). Release of PS and their uptake as a metal complex are diurnally regulated, being highest soon after the onset of light (Marschner and Römheld, 1994). Fe(III)-PS chelates are then taken up without prior reduction of Fe(III) via YS1/YSL-type proton-coupled symporters in the plasma membrane of root cells (Curie et al., 2001; Mori, 1999; Schaaf et al., 2004; von Wirén et al., 1995). Zn(II)- or Cu(II)-PS complexes are also transported into root cells by this transporter family, but at lower affinity and capacity (White and Broadley, 2009).

Major key elements in Fe deficiency signaling in strategy II plants are the *cis*-acting iron deficiency–responsive element 1 (IDE1) and IDE2 (Kobayashi et al., 2003), as well as the corresponding IDE-binding factor 1 (IDEF1) and IDEF2, which bind specifically to IDE1 and IDE2, respectively (Kobayashi et al., 2007; Ogo et al., 2008). IDEF1 regulates most of the known Fe deficiency-inducible genes under Fe sufficiency and upon early Fe deficiency (Kobayashi et al., 2009), whereas IDEF2 regulates *OsYSL2* and is responsible for a balanced distribution of Fe between the root and shoot (Ogo et al., 2008).

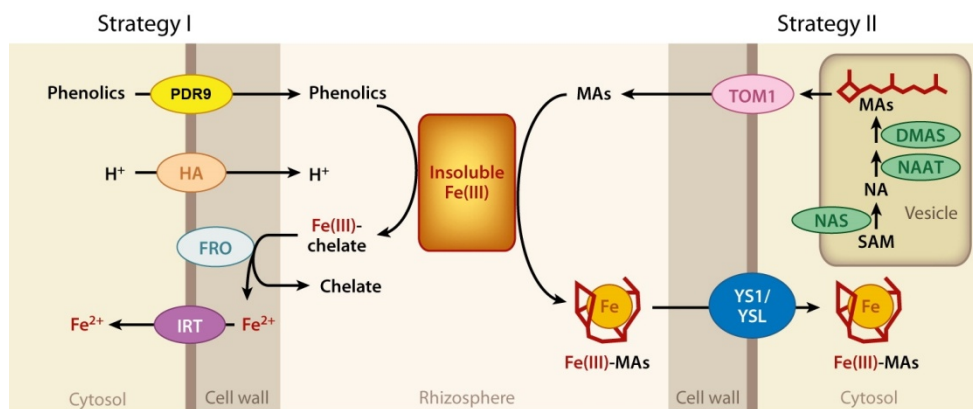


Figure 1. Scheme of Fe acquisition strategies I and II. In strategy I, Fe(III) is solubilized by proton secretion by HA and by secretion of phenolics via PDR9. Fe is reduced to Fe²⁺ by FRO, before it is taken up into the cytosol by IRT1. In strategy II, Fe(III) is chelated by mugineic acids which are derived from a series of reactions: NA is synthesized by NAS from SAM. NA then acts as a precursor for the synthesis of MAs after being modified by NAAT and DMAS. Once Fe(III) is chelated by MAs, it is transported into the cytosol by YS1/YSL-type proteins without a need for a reduction. Abbreviations: DMAS, deoxymugineic acid synthase; FRO, ferric-chelate reductase oxidase; HA, H⁺-ATPase; IRT, iron-regulated transporter; MAs, mugineic acid family phytosiderophores; NA, nicotianamine; NAAT, nicotianamine aminotransferase; NAS, nicotianamine synthase; PEZ, Phenolics efflux zero; SAM, S-adenosyl-L-methionine; TOM1, transporter of mugineic acid family phytosiderophores 1; YS1/YSL, Yellow stripe 1/Yellow stripe 1-like. The model was taken from Kobayashi and Nishizawa (2012) and slightly modified.

2.2.3. Fe deficiency and heavy metal toxicity

Plants have to tightly control their Fe uptake. While a lack of Fe causes severe impairments in growth, excess of free Fe results in oxidative stress through the production of reactive oxygen species (ROS) by the Fenton reaction. Furthermore, another risk arises as potentially toxic heavy metals are taken up into the cells in excess under Fe deficiency. As a result, plants need a concerted action of proteins controlling i) Fe acquisition and ii) the detoxification of Fe-accompanying heavy metals (this term is now introduced for those heavy metals whose entry is due to the non-specific nature of the major Fe uptake machinery).

i) Control of Fe acquisition

IRT1 is the best-characterized component of Fe acquisition. The IRT1 protein accumulates in the plasma membrane under Fe deficiency and is rapidly degraded upon Fe resupply, which indicates its tight regulation by Fe.

Transcriptional regulation of *IRT1* under Fe deficiency is mediated by FIT, the key regulator of Fe deficiency responses (Bauer et al., 2007; Jakoby et al., 2004; Ling et al., 2002). Overexpression of *FIT* does neither lead to the induction of *IRT1* nor of other downstream

genes under Fe sufficiency, unless it is coexpressed constitutively with *bHLH38* or *bHLH39* (Yuan et al., 2008), showing that FIT action is dependent on the interaction with these transcription factors (Yuan et al., 2008). At the protein level, FIT interacts also with EIN3 and EIL1, which are central components of ethylene signaling (Lingam et al., 2011). This interaction is proposed to increase the stability of the FIT protein, since the *ein3 eil1* double knock-out line leads to a decrease in FIT protein accumulation following a suppression of the Fe deficiency response, which is probably due to an increase in the rate of 26S proteasome-dependent degradation of FIT (Sivitz et al., 2011). *FIT* itself is upregulated under Fe deficiency, indicating that there should be transcription factors upstream of it, but these have not yet been discovered. Possible upstream elements should also include proteins with an Fe-sensing function. Such Fe-sensing proteins have recently been identified in rice, namely OsHRZ1 and OsHRZ2. Rice plants in which both genes are knocked out show a higher accumulation of Fe in the shoots, suggesting that those proteins downregulate Fe acquisition under Fe sufficiency (Kobayashi et al., 2012, 2013). An ortholog of these proteins, BTS, which is found in Arabidopsis, has been shown to possess hemerythrin with Fe in the center and to interact with another protein, PYE, to regulate Fe deficiency responses (Kobayashi et al., 2012, 2013; Long et al., 2010). However, if these genes act upstream of FIT is not clear. In summary, *IRT1* is transcriptionally controlled by FIT, which, in turn, is transcriptionally and posttranscriptionally controlled by other upstream regulators, indicating the complexity of transcriptional control of *IRT1*.

It has been reported that the IRT1 protein does not accumulate when *IRT1* is ectopically expressed under Fe sufficiency (Connolly et al., 2002). Later, another group has reported that IRT1 is not subjected to Fe-dependent degradation but overaccumulates under Fe sufficiency (Barberon et al., 2011). They suggested the finding of Connolly et al. was due to the ectopic expression of an unstable truncated version of *IRT1*. Posttranslational control over IRT1 has been reported to have an impact on the subcellular localization of IRT1. According to the proposed model (Barberon et al., 2011), IRT1 accumulates in the *trans*-Golgi network and in early endosomes of rhizodermal and cortical cells and cycles to the plasma membrane to mediate Fe uptake. After releasing Fe to the cytoplasm, it is targeted to the vacuole for degradation. This cycling depends on monoubiquitination of several cytosol-exposed residues (Barberon et al., 2011). Ubiquitination of IRT1 for degradation is mediated by a RING E3 ubiquitin ligase, IDF1, which has been shown by reduced accumulation of the IRT1 protein when *IRT1* was coexpressed with *IDF1* in yeast or *Xenopus laevis* oocytes (Shin et al., 2013). However, although ubiquitin-mediated degradation of IRT1 slows down in the loss-of-function mutant of IDF1, it still exists, indicating that other ubiquitin ligase proteins are also involved in this process. Degradation of the IRT1 protein further related to correct trafficking and stability of IRT1 in the plasma membrane which requires SNX1 (Ivanov et al., 2014), based on the analysis of *snx1* loss-of-function mutants which showed enhanced IRT1 protein degradation and reduced Fe uptake efficiency.

Transcriptional and posttranslational multi-level control of IRT1 is an example of how complex an Fe acquisition protein may be regulated. Therefore, it may be assumed that similar control mechanisms are likely to exist also for other proteins involved in Fe acquisition. Accordingly, overexpression of *FRO2* in Arabidopsis does not lead to an increase in ferric reductase activity under Fe sufficiency, indicating the interference of posttranscriptional regulation (Connolly et al., 2003). Taken together, there is a very strict regulation of the components of Fe acquisition and further investigations in this direction are needed in order to generate a complete picture.

- ii) Detoxification of Fe-accompanying heavy metals under Fe deficiency

Due to the lack of specificity of IRT1 for Fe, other heavy metals like Zn, Ni, Co and Mn, may accumulate to high levels in the roots and shoots of Fe-deficient plants (Connolly et al., 2002; Korshunova et al., 1999; Vert et al., 2002). Under Fe deficiency there is a continuous import of those metals into the cytoplasm where they can cause toxicity unless being chelated or removed from the cytosol. Zn, Ni and Co are sequestered to the vacuole in epidermal and cortical cells of roots by tonoplast transporters which are upregulated under Fe deficiency (Figure 2) (Arrivault et al., 2006; Schaaf et al., 2006). If Zn, Co and Ni are not sequestered into root vacuoles, as it is in the case of the corresponding loss-of-function mutants, they do not accumulate predominantly in the root anymore, but are instead translocated to the shoot. This increases the sensitivity of Fe-deficient plants to these heavy metals.

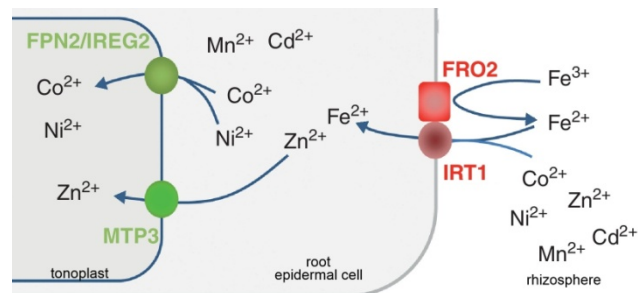


Figure 2. Uptake and sequestration of Fe-accompanying heavy metals in root epidermal cells of *Arabidopsis*. IRT1 takes up not only Fe but also Co, Ni, Mn, Zn and Cd. Under Fe deficiency *IRT1* is upregulated causing an excess influx of Fe-accompanying heavy metals. Ni and Co are sequestered to the vacuole by IREG2, while Zn is transported by MTP3. Genes encoding both proteins are upregulated under Fe deficiency. Modified model according to Thomine and Vert (2013).

2.2.4. Mn-induced Fe deficiency

Fe acquisition by plants is affected by the external availability of Mn. There are numerous examples where an increase of Mn availability coincided with Fe deficiency in plants, both under field (Gile, 1916; Johnson, 1917; Kelley, 1909) or laboratory (Rippel, 1923; Tottingham and Beck, 1916) conditions. For example, plants growing on a Hawaiian island soil suffered from Fe deficiency due to excess Mn (Johnson, 1917). Pineapple trees grown in this soil showed Fe deficiency-dependent chlorosis, although the soluble Fe concentration in the soil was high. Accordingly, Fe deficiency symptoms were more severe where the Mn concentration of the soil was higher (Johnson, 1917). As another example, soybeans which were grown hydroponically contained less soluble Fe as the concentration of Mn in the medium increased (Somers and Shive, 1942). However, some of these reports claim that plant Fe concentration may not be reduced upon increasing Mn, although plants began to show Fe-deficiency symptoms, which were even alleviated by foliar Fe application, indicating that a disturbed Fe/Mn balance can cause Fe deficiency in plants (Lindner and Harley, 1944). However, the processes and mechanisms causing this disturbed Fe/Mn balance and the Fe-deficiency symptoms are still unclear. Several researchers have suggested an antagonism between Fe and Mn based on their redox activity (Alvarez-Tinaut et al., 1980; Hopkins, 1930a, 1930b; Shive, 1941). For example, Somers and Shive (1942) argued that reduction of ferric to ferrous Fe is impaired in the presence of oxidized Mn, because ferrous Fe can be precipitated by the

oxidizing potential of Mn(IV), leading to precipitation of Fe. Others suggested that Mn competes for chelators involved in Fe mobilization (Hewitt, 1948; Klimovitskaya et al., 1969; Schmid and Gerloff, 1961; Sideris and Young, 1949; Twyman, 1951). Lastly it has been suggested that, due to the very similar atomic radius and charge of Fe and Mn, many proteins involved in the homeostasis of both metals can be shared (Hewitt, 1948) such as IRT1, which may lead to a competition between these metals at the plasma membrane of root epidermal cells.

Mn availability in Fe-deficient soils is not only determined by the absolute amount of Mn being present, but also by soil conditions. Just like Fe, the speciation of Mn determines its availability to the plant. Soluble ionic forms of Fe and Mn become prevalent if the pH and redox potential of the soil decrease. Dominant forms of Fe or Mn in dependence of the pH and redox status of the soil are shown in Figure 3. Both metals behave similarly (Figure 3A,B): they tend to precipitate as oxides and hydroxides when pH or redox potential increase. However, with increasing pH or redox potential, Fe precipitates much earlier than Mn (Figure 3C).

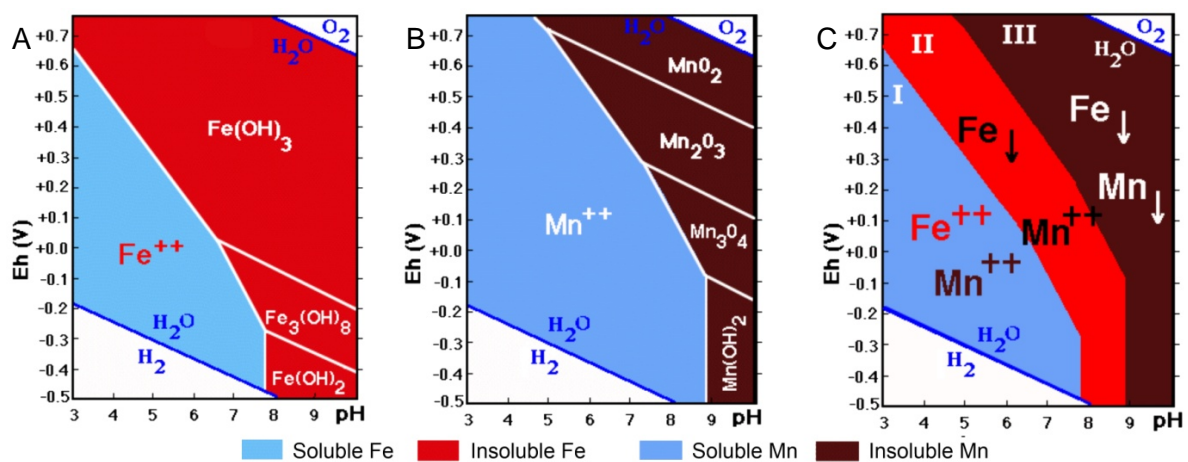


Figure 3. Forms and mobility of Fe and Mn complexes in relation to the redox conditions and the pH of the soil. The diagrams show the stability fields of the forms of Fe and Mn as a function of Eh and pH for each element (A, B) and for both elements combined (C). The graphs show that for Fe, the precipitation zone (red) is much larger than the solubility zone (blue), whereas for Mn (brown) it is the opposite. Picture taken from <http://edafologia.ugr.es/hidro/conceptw.htm> and modified.

2.3. Fe translocation from roots to shoots

After it is taken up, Fe must be translocated to the shoot and distributed to the individual shoot organs. During its pathway from the soil to the shoot Fe translocation requires the following steps: radial transport from the root epidermis to the xylem, xylem loading, axial translocation, uptake by shoot cells, and for retranslocation: phloem loading, transfer, and unloading and symplastic movement to the sink (Kim and Guerinot, 2007). Throughout its translocation, Fe must be kept soluble and restricted from producing free radicals. This is achieved via chelation (von Wirén et al., 1999). Fe is chelated by citrate, which can bind Fe^{3+} , and NA which can bind both Fe^{2+} and Fe^{3+} . The binding of Fe to these chelators is strictly pH dependent. Citrate binds Fe(III) in the xylem sap which has a pH between 5.5 to 6. In roots, citrate is exported into the xylem by the FRD3 protein. In *frd3* loss-of-function mutants, shoots are Fe deficient while Fe accumulates in roots around the xylem vessels, indicating the

importance of citrate for xylem transport of Fe (Durrett et al., 2007; Roschztardt et al., 2011). NA preferentially binds Fe in the phloem sap, considering the mutual existence of NA and Fe^(III) in the phloem sap and the higher affinity of NA to Fe^(III) at the more alkaline pH found in the phloem sap (von Wirén et al., 1999). Further evidence supporting that NA chelates and mobilizes Fe came from studies conducted with the tomato mutant *chloronerva*, which has a mutation in the NA synthetase gene and suffers from Fe deficiency-induced chlorosis. In *chloronerva*, the Fe deficiency machinery is continuously upregulated in roots, although Fe accumulates at high levels in shoots and roots. External application of NA rescues the phenotype (Stephan and Scholz, 1993), indicating the importance of Fe binding to NA for long-distance translocation of Fe. NA-bound Fe is most likely transported by YSL proteins, which have been shown to complement Fe uptake in an Fe uptake-defective yeast mutant if Fe(II) is co-supplied with NA (DiDonato et al., 2004; Waters et al., 2006). Since YSL genes are strongly expressed in vascular tissues, pollen grains, and seeds, Fe may be translocated to these organs in the form of Fe-NA complexes (Curie et al., 2009).

2.4. Post-phloem transport and storage of Fe, Mn and Zn in seeds

A successful establishment of the seedling in the soil is directly related to the nutrients that are contained in the seed. Seeds represent the major part of the human diet, as edible parts of most of the staple food crops are seeds. Considering micronutrient deficiencies as one of the biggest problems in human nutrition (Ramakrishnan, 2002), increasing micronutrient contents of seeds is an important aim in agricultural food production, as on the long run, it is a more sustainable and economic way to deliver essential nutrients in adequate amounts to the people with what they eat rather than providing micronutrient supplements.

Attempts to manipulate seed nutrient contents by exogenous applications or by selecting mutants that accumulate more nutrients often resulted in increased nutrient concentrations in the vegetative organs of the plants but not in the seeds. For example, a pea mutant accumulating 36-times more Fe in the leaves had similar Fe levels as wild-type seeds (Grusak, 1994). Therefore, specific bottlenecks exist in the loading of seeds with micronutrients, and the knowledge on molecular players involved in seed loading with nutrients is very scarce. The model plant *Arabidopsis* has become the major focus of seed micronutrient research with emerging imaging techniques like synchrotron X-ray fluorescence that allow the local mapping of metals in plant organs (Punshon et al., 2013; Wu and Becker, 2012).

2.4.1. Post-phloem transport of Fe to the seed coat

A single vascular bundle connects the silique to the seeds. This bundle ends in the integumental region of the seed below the chalazal endosperm. In this region, minerals are symplastically unloaded from the phloem and loaded into the seed coat cells. Minerals can diffuse through the seed coat, which is a maternal tissue and symplastically isolated from the filial tissues, i.e. the endosperm and embryo. Therefore, transfer of minerals from the seed coat to the endosperm and from the endosperm to the embryo requires crossing the apoplast at least once. According to microarray analysis genes from the HMA, ZIP, MTP, NRAMP, NAS, and YSL families are active in barley grain transfer cells of the maternal vascular bundle,

aleurone, endosperm, and embryo (Tauris et al., 2009); therefore candidate genes having roles in facilitating the transport of metals into seeds of *Arabidopsis* may belong to these families. YSLs in particular seem to play a very important role in loading NA-metal complexes into the seeds, based on the high expression of the corresponding genes during seed development. Consistently, a loss-of-function mutant of YSL1 showed less Fe and NA in the seeds (Jean et al., 2005). Furthermore, *ysl1 ysl3* seeds accumulated less Fe, Zn, and Cu. YSLs may transport Mn-NA complexes in *Arabidopsis* as well, based on a report of a rice YSL protein that transports Mn-NA in *Xenopus laevis* oocytes (Koike et al., 2004).

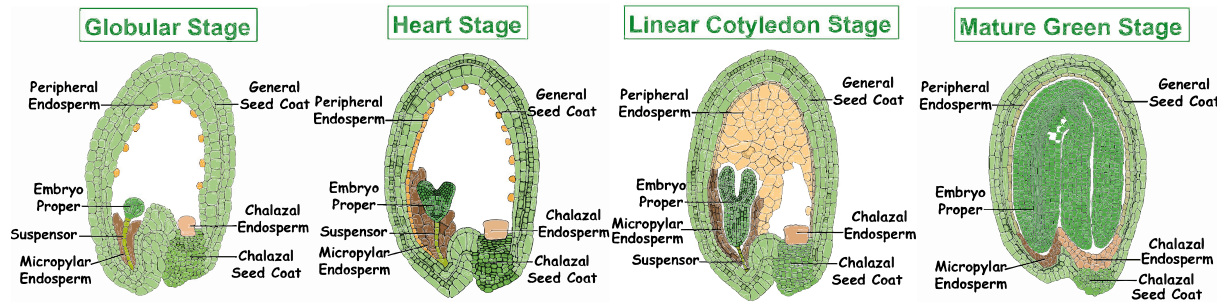


Figure 4. Developmental stages of an *Arabidopsis* embryo. At the globular stage, cotyledons have not been developed yet and the embryo is spherical, carrying at its end a structure called the suspensor. The suspensor connects the embryo to the seed coat and the endosperm. There is a large central vacuole between the chalazal endosperm and embryo. At heart stage, embryonic cotyledons begin to appear. The suspensor reaches its maximal size and nourishes the embryo. The endosperm starts cellularization. At the linear cotyledon stage, the embryo continues to grow. Now, the embryo is green and photosynthetically active. The symplastic connection between the embryo and the seed coat through suspensor is getting lost. The endosperm is cellularized except the chalazal endosperm and rapidly increases and occupies most of the seed volume. In mature green stage the embryo divides very fast and occupies most of the volume. Cotyledons are bent and store nutrients. Nutrients in the endosperm are depleted by the developing embryo (Berger, 1999, 2003; Olsen, 2004; Otegui et al., 2002a; Yeung and Meinke, 1993). Picture is taken from www.seedgenenetwork.org.

2.4.2. Route of metal transport from the seed coat to the embryo

Minerals can be loaded from the seed coat into the embryo directly through the suspensor or the endosperm. The suspensor is symplastically connected to the embryo proper and able to transport nutrients to the embryo (Yeung and Meinke, 1993) (Figure 4). However, this connection gets lost as the embryo matures; therefore, minerals can only be loaded through the suspensor to the embryo during early embryo development (Stadler et al., 2005). Alternatively, metals can be first loaded to the endosperm and afterwards from the endosperm to the embryo, which are symplastically not connected (Patrick and Offler, 2001). Metals are transported through the chalazal endosperm which has a central role in nutrient loading to the embryo, based on its structure and on high concentrations of nutrients found in its vacuoles (Otegui et al., 2002). Metals can be transported from the chalaza to chalazal vacuoles, which in the early seed development are connected directly to the central vacuole between embryo and chalaza (white space in the seed in globular and heart stages in Figure 4). Therefore, in the early seed, the central vacuole may represent a quick route for metals to be transferred from the chalazal to the micropylar domain, where the embryo is located (Otegui et al., 2002).

The routes and time point by which nutrients reach the embryo can be different for different metals. Zn and Mn but not Fe have been shown to transiently accumulate in the chalazal

endosperm as complexes of phytate before entering to the embryo in the early seed (Otegui et al., 2002). The accumulation of Zn and Mn has a specific pattern, as they accumulate in different organelles and are released asynchronously. Mn accumulates in large amounts in the form of crystals in the endoplasmic reticulum of the chalazal and micropylar endosperms and not released from there before the linear cotyledon stage (Otegui et al., 2002). Contrary to Mn, Zn accumulates in the form of crystals in vacuolar structures of the chalazal endosperm, and these Zn crystals disappear earlier than the Mn crystals. Disappearance of Mn and Zn crystals coincides with the increase of their concentrations in the embryo (Otegui et al., 2002). Zn and Fe entry into the embryo have been reported to be delayed in *vit1-1* mutants (Punshon et al., 2013), although VIT1 is supposed not to transport Zn (Kim et al., 2006). How VIT1 contributes to the Fe and Zn loading of the embryo is not yet known. The differential uptake of metals by the embryo suggests the existence of specific transport systems for the individual metals.

In order to identify the molecular players and bottlenecks for metal seed loading, information on the speciation of metals in seeds is essential. However, the current knowledge on metal speciation in different seed tissues is mostly limited to Fe. Grillet et al. used pea in order to search for chelators and forms of Fe in the embryo sac liquid, which are supplied to the developing embryo (Grillet et al., 2014). Almost all of the Fe in the embryo sac liquid was found in the form of Fe(III) complexed to citrate and malate, as represented by the major complexes $\text{Fe(III)}_3\text{Cit}_3\text{Mal}_2$, $\text{Fe(III)}_3\text{Cit}_3\text{Mal}_1$ and to a minor extent Fe(III)Cit_2 . The citrate found in embryo sac liquid may have been released by FRD3, which is expressed in the aleurone and the protodermis of the embryo during seed maturation in Arabidopsis (Durrett et al., 2007; Roschztardt et al., 2011). Although the embryo sac liquid is dominated by Fe(III), a reduction step is necessary before the embryo can take up Fe. Surprisingly, ascorbate appears to be essential for Fe uptake by the embryo (Grillet et al., 2014). Ascorbate which is secreted from pea embryos has been found to reduce ferric Fe, and ascorbate synthesis-deficient mutants of Arabidopsis embryos contained less Fe and a lower Fe(III) reduction capacity compared to the wild type. The identity of transporters involved in Fe uptake from the embryo sac liquid is not yet known. However, OPT3 may be a promising candidate for this, because it has been recently shown that it localizes to the plasma membrane and transports Fe in *Xenopus* oocytes (Zhai et al., 2014), and the promoter of the corresponding gene is active during seed development (Stacey et al., 2008).

2.4.3. Use and storage of metals in the embryo

The embryo needs metals i) to meet the need of its metabolism during development, and ii) for long-term storage in order to use these metals during the first few days of germination. After fertilization, embryonic cells divide very fast and the embryo requires 14 days to reach the mature stage, indicating a high demand for metals as they are cofactors in proteins involved in multiple metabolic reactions. Particularly, developing embryos are photosynthetic, indicating that Fe and Mn must be needed in large amounts to synthesize proteins involved in water splitting or in the electron transport chain. Recently, developing embryos have been analyzed by confocal microscopy to detect chlorophyll fluorescence (Tejos et al., 2010). Torpedo stage embryos showed a line of intense fluorescence just under the shoot apex, similar to the Prussian blue-stained Fe as shown by Roschztardt et al (2009). This indicates that a considerable part of the stainable Fe in the embryo can be associated with chloroplasts just under the shoot apex in this stage. From the torpedo stage onwards, stainable Fe is almost

exclusively found in endodermal vacuoles, which provide the main storage compartment until Fe is remobilized for germination.

i) Role of the vacuole in building metal storage reserves in seeds

Mature Arabidopsis embryo cells do not possess a central vacuole; instead, the only type of vacuole existing in embryo tissues are protein storage vacuoles (PSVs) (Hunter et al., 2007; Otegui et al., 2002). Either Arabidopsis generate PSVs from existing lytic vacuoles or *de-novo* during embryo maturation. However, how PSVs develop from lytic vacuoles at the onset of germination in order to mobilize nutrients is not clear (Frigerio, 2008; Frigerio et al., 2008). Recently, it has been proposed that PSVs of dry and germinating Arabidopsis seeds possess distinct lytic vacuolar compartments, indicating that storage and lytic compartments can be found together (Bolte et al., 2011). PSVs contain globoid crystals made of phytate which are the major storage form for phosphorus as well as metals (Raboy, 2003). Consistently, PSVs in Arabidopsis seeds have been reported to contain Mn, Ca, Zn (Donner et al., 2012), and Fe (Lanquar et al., 2005; Roschztardt et al., 2009).

The accumulation patterns of the transition metals Fe, Mn and Zn in the embryo are remarkably different from each other (Kim et al., 2006). Based on X-ray synchrotron analysis and Fe staining by Perls/DAB, Fe is localized in the endodermal cells surrounding the vascular tissue (Donner et al., 2012; Roschztardt et al., 2009), whereas Mn is in the subepidermis of the abaxial side of the cotyledons, and Zn is more or less homogeneously distributed throughout the embryo. Based on quantitative measurements conducted by μ PIXE, Ramos et al. (2013) reported that at least half of the Fe in the Arabidopsis seed is found outside of the cells surrounding the endodermal veins (Ramos et al., 2013).

The tissue-specific expression of tonoplast transporters appears to determine the final localization of metals in the embryo. VIT1 is a Fe/Mn influxer expressed in the prevascular tissue of Arabidopsis embryos and is responsible for the Fe localization around the vascular strands (Kim et al., 2006). As Fe was mislocalized in *vit1* seedlings and seedlings became chlorotic when grown on a calcareous soil, the Fe localization in the endodermis of vascular bundles has been proposed as being highly critical (Kim et al., 2006) Furthermore, in *vit1-1* Fe colocalizes with Mn in the subepidermal cell layer of the abaxial side of the cotyledons and the hypocotyl. Unlike Fe and Mn, Zn is distributed quite evenly throughout the seed.

ii) Roles of chloroplasts and mitochondria in metal storage

In legume seeds, most of the Fe is stored in the plastids in the form of ferritin during seed development and consumed during the first few days of germination (Lobreaux and Briat, 1991). In contrast, in Arabidopsis seeds ferritin-bound Fe accounts for only about 5% of the total Fe and the physiological function of ferritin is more associated with Fe detoxification rather than building Fe storage reserves. The Arabidopsis genome encodes 4 isoforms of ferritin but among them only FER2 is found in the seeds (Ravet et al., 2009)

As mentioned before, large amounts of Fe and Mn are found in chloroplasts and mitochondria during seed development. These metals are no longer needed in large amounts when respiration and photosynthesis decrease during desiccation. Consequently, metals are released from these organelles in order to be stored in PSVs. The release of Fe, and most likely also of Mn, from the chloroplast is mediated by YSL4 and YSL6, which are highly active at later stages of the maturing embryo (Divol et al., 2013).

2.5. The Cation Diffusion Facilitator (CDF) family

Transport of metals in the plant across organellar and plasma membranes is essential and needs to be tightly controlled by transporters because nutritive and toxic metals should be separated and carried to their final destinations. While toxic metals can be detrimental even in small concentrations, nutritive metals which are used for the biosynthesis of proteins can cause toxicity at elevated concentrations or when improperly partitioned inside the cell. Metals are transported by metal-transporting proteins which are encoded by genes of different families including heavy metal ATPases (HMAs), natural resistance-associated macrophage proteins (NRAMPs), cation diffusion facilitators (CDFs), the ZRT-, IRT-like proteins (ZIPs), Cation/H⁺ antiporters (CAXs), proteins from the iron-regulated gene (IREG) family, multi drug and toxic compound extrusion (MATE) family or others. These transporters differ in their expression patterns, membrane localization, metal specificity and transport mechanisms and have been proposed to take over diverse functions in plants (Clemens, 2006; Hall and Williams, 2003).

Cation diffusion facilitator family (CDF) proteins have been identified in all three kingdoms: archaea, eubacteria and eukaryotes. They transport divalent cations, contain 6 putative transmembrane domains and an N-terminal amino acid sequence with the CDF signature (Nies and Silver, 1995; Paulsen and Saier Jr, 1997). The three-dimensional protein structure of an *E. coli* CDF protein, together with other pieces of evidence, support that CDFs act as homodimers (Blaudez et al., 2003; Gustin et al., 2011; Lu and Fu, 2007; Wei and Fu, 2006). CDF proteins generally function as exporters of cations out of the cytosol for sequestration into intracellular compartments or for transport out of the cell. Plant CDFs are involved in heavy metal tolerance, and plant CDF members have thus been named metal tolerance proteins (MTPs) (Mäser et al., 2001; van der Zaal et al., 1999). In a phylogenetic analysis, 273 CDF sequences from all kingdoms of life have been analyzed for sequence similarities (Montanini et al., 2007). Those that had already been characterized for their transport activities have been grouped together with those that have similar sequences. This approach resulted in the separation of three subfamilies of CDFs: Zn-CDFs, Fe/Zn-CDFs, and Mn-CDFs and was suggested to be helpful for predicting metal specificity of yet uncharacterized plant MTPs (Figure 5)(Migeon et al., 2010; Montanini et al., 2007). According to this classification, Zn-CDFs transport specifically Zn and maybe Co, Cd and Ni with a lower affinity. Fe/Zn-CDFs are expected to transport Fe, Zn, Co, Cd and Ni. Mn-CDFs appear to be specific for Mn, based on the fact that heterologous expression of Mn-CDFs only rescued Mn-sensitive yeast mutants under high Mn supply but not other metal-hypersensitive strains under high concentrations of the corresponding metals (Migeon et al., 2010; Montanini et al., 2007).

Of the 12 Arabidopsis MTPs (Ricachenevsky et al., 2013), only MTP1, MTP3 and MTP11 have been characterized so far. MTP1 localizes to the tonoplast, complements Zn hypersensitivity in yeast and increases plant tolerance to excess Zn (Bloss et al., 2002; Kobae et al., 2004). Another member, which shares the same phylogenetic group with MTP1 is MTP3 (Arrivault et al., 2006; Haydon and Cobbett, 2007). MTP3 is very similar to MTP1, but differs in tissue localization and in the regulation by metals. MTP1 is expressed ubiquitously and constitutively, whereas MTP3 is confined to the root and upregulated under Fe deficiency and excess Zn. More recently, MTP11 has been characterized in Arabidopsis. It also complements Mn-hypersensitive yeast when heterologously expressed, contributes to Mn tolerance in the plant, and localizes to the prevacuolar compartment and the trans-Golgi network. It has been suggested that MTP11 is involved in vacuolar sequestration or exocytosis of excess Mn from the cytoplasm as a way to deal with Mn toxicity (Delhaize et al., 2007; Peiter et al., 2007). A

close relative to Arabidopsis MTP8, is the vacuolar Mn transporter ShMTP8 which is thought to contribute to the high Mn tolerance of *Stylosanthes hamata*. Recently, other orthologs of Arabidopsis MTP8 have been characterized in cucumber (CsMTP8) and rice (OsMTP8.1) with a similar function to ShMTP8, as these proteins increase Mn tolerance of the plants under excess Mn supplies (Chen et al., 2013; Migocka et al., 2014).

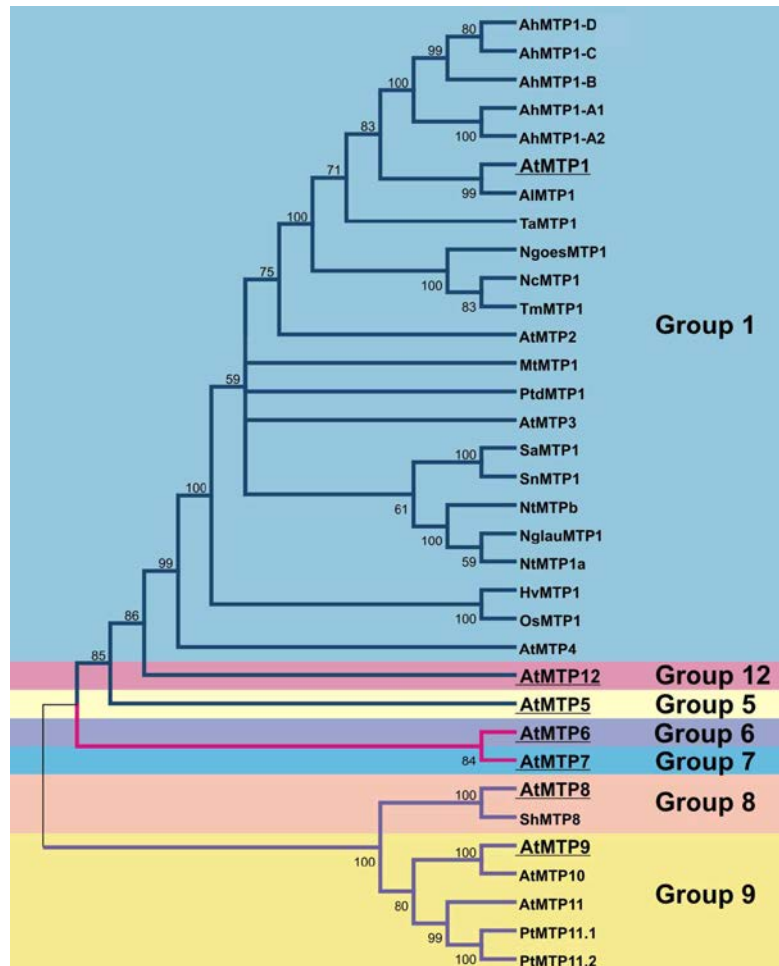


Figure 5. Phylogenetic groups of characterized MTPs from Arabidopsis and other plants. The tree is constructed using all sequences of functionally characterized members, plus all MTP proteins from *A. thaliana*, and each subgroup was named after its first *A. thaliana* member. Founding members of each group are highlighted. Colors of branches are in blue for Zn-CDF group proteins; pink for Fe/Zn-CDF proteins; and purple for Mn-CDF proteins. Figure from Ricachenevsky et al. (2013)

2.6. Aims of the thesis

Several transcription factors including PYE, FIT, bHLH38/39 and bHLH101 have been shown to be involved in the adaptation to Fe deficiency by regulating the expression of downstream genes required for enhanced Fe acquisition or improved Fe utilization. However, many of these downstream target genes have not yet been characterized for their physiological function. In order to identify the physiological role of these genes and proteins in the Fe deficiency response, T-DNA insertion lines of genes that are targets of the transcription factors PYE and FIT were phenotypically screened under low Fe availability in order to select lines suffering from Fe deficiency-induced chlorosis. As commonly used media to grow Fe-deficient

plants were not considered as suitable for such a forward-genetics screening approach, a new medium composition had to be developed. The first chapter of the results part of this thesis therefore describes the approach how the medium was designed and the screening was performed.

The screening procedure revealed the Mn-CDF protein MTP8 to be essential for chlorosis-free growth under Fe deficiency. The second part of the Results set out to characterize the function and physiological importance of MTP8 in the Fe deficiency response.

Independent from its role under Fe deficiency, *MTP8* was also found to be highly expressed during embryo development. Therefore, the third chapter in the Results part describes the localization of Mn and Fe in wild type and *mtp8* mutant seeds. Since a previous study showed the involvement of VIT1 in Fe localization in *Arabidopsis* embryos, a *mtp8 vit1* double insertion line was generated and employed for further analyses.

3. Materials and Methods

3.1. Plant lines, plasmids, and transformation

All *Arabidopsis thaliana* genotypes used in this study were derived from the Columbia-0 ecotype. More than 120 *Arabidopsis* insertional mutant lines (Figure 5 in Results section) were obtained from the SALK collection (Alonso et al., 2003) and used in a screen for hypersensitivity to low Fe. All of those lines carried a T-DNA insertion in a gene up-regulated under Fe deficiency. Insertions in *mtp8* mutant lines were confirmed by PCR and sequencing of left borders (Ülker et al., 2008) (Figure 6). To construct the pART7-AtMTP8 plasmid, an *AtMTP8* cDNA was amplified from Col 0 cDNA using Xma I-containing primers and cloned into the pART7 vector (Gleave, 1992) downstream of a *CaMV35S* promoter (Bastian Meier, unpublished). To construct the pART7-AtMTP8-EYFP plasmid, the *AtMTP8* cDNA without stop codon was amplified from Col 0 cDNA using Xma I-containing primers and cloned into the pART7-EYFP vector (Peiter et al., 2007) in frame with *EYFP* (Bastian Meier, unpublished). For stable transformation of *Arabidopsis*, an expression cassette (including *CaMV35S* promoter and *ocs* terminator) was Not I-excised from pART7-derived constructs and inserted into the binary plant transformation vector pBART (Gleave, 1992). To construct the pBI101-PrAtMTP8-GUS plasmid, the promoter and 5'-untranslated region (-2046 to -1bp) of the *AtMTP8* gene was amplified from Col-0 genomic DNA using Xma I-containing primers and cloned into the pBI101 vector upstream of the *uidA* gene (Jefferson et al., 1986) (Bastian Meier, unpublished).

Stable transformation of *Arabidopsis* was carried out by the floral dip method with *Agrobacterium tumefaciens* GV3101 (Clough and Bent, 1998). pBART and pBI101-PrMTP8-GUS transformants were selected by spraying with BASTA or by germination on kanamycin-containing plates, respectively. Transient transformation of *Arabidopsis* mesophyll protoplasts was performed as described previously (Peiter et al., 2005a).

vit1-1 (SALK_020596C) and two *promoterVIT1:GUS* lines (Kim et al., 2006) were obtained from Mary-Lou Guerinot (Dartmouth College, Hanover, USA). The *vit1-2* (SALK_123591C) T-DNA insertion line was identified from the SALK collection. *vit1-2* showed mislocalization of Fe in the embryos when stained by Perls/DAB. A *mtp8-1 vit1-2* line was generated and its homozygosity was confirmed by PCR based segregation analysis.

Name	Purpose	Sequence
MTP8_494_F	T-DNA screen <i>mtp08-1</i> forward	ACGCGCTGATGTGAGCA TT
MTP8_494_R	T-DNA screen <i>mtp08-1</i> reverse	CCCAATTTGAGATTTGCA TGG
MTP8_226_F	T-DNA screen <i>mtp08-2</i> forward	CGCAACCGCTATTA AACTCGT
MTP8_226_R	T-DNA screen <i>mtp08-2</i> reverse	GATTCA CCAATCGCATGAGC
SALK_LBa1	T-DNA screen	TGGTTCA CGTAGTGGGCCATCG
SALK_RBb	T-DNA screen	CAGTCA TAGCCGAATAGCCTCTCC
MTP8_F-NotI	cloning in pFL61 forward	AAAAAA GCGGCCGCA TGAAGTCAATTA TTGTCCGGA
MTP8_R-NotI	cloning in pFL61 reverse	AAAAAA GCGGCCGCTCA TAAATCGTTGGGGATTGTAGA
MTP8_F-XmaI	cloning in pART7-EYFP forward	AAAAAA CCCGGGATGGAAGTCAATTA TTGTCCGGA
MTP8_R-XmaI (nostop)	cloning in pART7-EYFP (gene N-terminal of EYFP) rev	AAAAAA CCCGGGTGCTAAA TCGTTGGGGATTGTAGA
MTP8_R-XmaI	cloning in pART7-EYFP (gene C-terminal of EYFP) rev	AAAAAA CCCGGGTCA TAAATCGTTGGGGATTGTAGA
MTP8_gDNA_F-XmaI	cloning in pBI101 forward	AAAAAA CCCGGGGCA TTCCTCCTGTAAACGGAAGC
MTP8_gDNA_R-XmaI	cloning in pBI101 reverse	AAAAAA CCCGGGTCTTGAAAA TTA TTAACAAATCATCG
MTP8_rt_F	qRT-PCR forward	TTGTGCA GGTGGATA TAGAACTGCC
MTP8_rt_R	qRT-PCR reverse	GGAA TGTTCAGGCTTGTGATGACA
At4g05320_rt_F	qRT-PCR forward	CACACTCCA CTGGTCTTGCGT
At4g05320_rt_R	qRT-PCR reverse	TGGTCTTTCCGGTGAGAGTCTTCA
At3g18780_rt_F	qRT-PCR forward	TCCCTCAGCACA TTCCAGCAGAT
At3g18780_rt_R	qRT-PCR reverse	AACGATTCCTGGACCTGCCTCATC
At5g60390_rt_F	qRT-PCR forward	TGAGCA CGCTCTTCTTGCTTTCA
At5g60390_rt_R	qRT-PCR reverse	GGTGGTGGCATCCA TCTTGTTACA
bhlh38_F	qRT-PCR forward	AATCAA TACGAAAGCTATTA CCGT
bhlh38_R	qRT-PCR reverse	TAA GCTCTTTGAAACCGTTTC
bhlh101_F	qRT-PCR forward	CTTTCTGA TCAAAAGAGGAA GCTGAG
bhlh101_R	qRT-PCR reverse	GAAA CAGATGTCCA TTTGACGT
PYE_F	qRT-PCR forward	CAGGACTTCCCA TTTTCCAA
PYE_R	qRT-PCR reverse	CTTGTGTCTGGGATCAGGT
BTS_F	qRT-PCR forward	GCTCTGGCACAAGTCAATCA
BTS_R	qRT-PCR reverse	CGTTCA TCAAA TGCCGATAA
at3g12900_F	qRT-PCR forward	GCGGAGCATAGGGTTCGAA
at3g12900_R	qRT-PCR reverse	GGGATTTGGTGCCGTGAA
MYB72_F4	qRT-PCR forward	TCA TGA TCTGCTTTTGTGCTTTG
MYB72_R4	qRT-PCR reverse	ACGAGATCAAAAACGTGTGGAAC
IRT1_F	qRT-PCR forward	CGGTTGGACTTCTAAA TGC
IRT1_R	qRT-PCR reverse	CGATAA TCGACATTTCCACCG
FIT_F	qRT-PCR forward	GGAGAA GGTGTGCTCCA TCTC
FIT_R	qRT-PCR reverse	GTCTCGAA TTTGAA CCGATTGG
AtNAS4_F	qRT-PCR forward	ATCGGTTTA TCA CCGTACCG
AtNAS4_R	qRT-PCR reverse	TACCGTGGATCTTGGAACAG
UBQ2F	qRT-PCR forward	CCAAGA TCCAGGACAAA GAAGGA
UBQ2R	qRT-PCR reverse	TGGAGACGAGCATAA CACTTG
SALK_LBb1.3	T-DNA screen <i>vit1-2</i> forward	ATTTTGCCGATTTCCGGAAC
vit1-2_RP	T-DNA screen <i>vit1-2</i> reverse	GAA GAGAA GGCTCTGCAACTG
vit1-2_LP3	T-DNA screen <i>vit1-2</i> forward	CGAA GAAGA TCA TTA CCGCGAG
vit1-2_LP3	T-DNA screen <i>vit1-2</i> forward	CGAA GAAGA TCA TTA CCGCGAG

Figure 6. List of primers used in the thesis

3.2. Plant growth conditions, media, and mutant screening

Arabidopsis seeds were surface sterilized using a solution of 70% ethanol and 0.05% Triton X100. 1 mL of this solution was added to approximately 100 μL seeds and then shaken at room temperature for 20 min at 1400 rpm. The supernatant was aspirated, seeds were washed two times with 100% ethanol and left to dry for at least 4 h. Plates were oriented vertically in a growth cabinet (Percival Scientific, USA) set to 22°C day and 19°C night temperature and a 10 h light period with a light intensity of 120 $\mu\text{mol photons m}^{-2} \text{ s}^{-1}$ after seeds were incubated for two days in the dark at 4 °C for stratification.

In order to develop an agar medium with low Fe availability, half-strength Murashige and Skoog (MS) medium without FeSO_4 and MnSO_4 (Duchefa Biochemie; Haarlem, The Netherlands), containing 1.5% agar (Difco) and 0.5% sucrose, was used as a basal medium. To decrease the Fe availability, the medium was buffered with 10 mM MES adjusted to pH 6.7 with NaOH. Fe was added to the medium as NaFe(III)-EDTA and Mn as MnCl_2 in the concentrations indicated. In experiments where plants were cultivated on standard $\frac{1}{2}$ MS medium, the pH of the medium was buffered to 5.5 with 2.5 mM MES.

To observe growth on soil, seeds were sown onto standard potting soil (Substrat 1; Klasmann-Deilmann GmbH, Geeste, Germany) supplemented with 20 g kg^{-1} CaCO_3 and 12 g kg^{-1} NaHCO_3 . After 13 days of pre-culture, seedlings were watered for six days either with a solution containing 120 μM MnCl_2 or with dH_2O and photographed thereafter. For soil pH measurements, 2.5 g of soil was suspended in 25 ml of a 10 mM CaCl_2 solution. After filtration, the pH of the solution was determined by a pH meter.

3.3. Elemental Analysis

Roots and shoots were separated, rinsed with deionized water, and dried at 65°C for a week. The dried shoots and roots were weighed into PTFE digestion tubes and digested in HNO_3 under pressure using a microwave digester (UltraCLAVE IV; MLS, Germany). Elemental analysis was undertaken using inductively coupled plasma optical emission spectroscopy (iCAP 6500 dual OES spectrometer; Thermo Fisher Scientific, Germany).

3.4. GUS Histochemical Analyses

Root and shoot samples were incubated at 37°C in a GUS reaction buffer containing 0.4 mg mL^{-1} 5-bromo-4-chloro-3-indolyl- β -D-glucuronide, 50 mM sodium phosphate (pH 7.2), and 0.5 mM ferrocyanide. Five promoterMTP8:GUS lines were examined and showed the same staining patterns under standard growth conditions. Of those lines, two were analyzed in more detail. Shoot samples were cleared and mounted according to the method described by Malamy and Benfey (1997). For microscopic observations of root and embryo cross sections, samples were fixed in 2% formaldehyde, 2% glutaraldehyde in 50 mM cacodylate buffer (pH 7.2), dehydrated in an ethanol series (30%, 40%, ..., 100%), and embedded in Spurr's resin. 5 μm cross sections of stained roots and embryos were obtained by cutting the fixed and resin-

embedded samples using a microtome (Ultracut; Leica, Nussloch, Germany) and observed under a light microscope (Axioskop; Carl Zeiss, Jena, Germany).

3.5. Chlorophyll Measurements

Chlorophyll concentrations were determined by extracting shoot samples with spectrophotometric grade N,N'-dimethyl formamide (Sigma-Aldrich) at 4°C for 48 h. The absorbance at 647 and 664 nm was measured in extracts according to Porra et al. (1989).

Chlorophyll fluorescence parameters were obtained using an IMAGING-PAM fluorometer (Heinz Walz GmbH, Effeltrich, Germany). The device was equipped with the standard-measuring head. Seedlings were dark adapted for at least 30 min and subsequently illuminated for 12 min at an irradiance of 108 $\mu\text{mol quanta m}^{-2} \text{s}^{-1}$ so that steady state photosynthesis was achieved. Maximum fluorescence yield in the dark- (F_m) as well as in the light- adapted state (F_m') was measured during 800 ms exposure of a saturating light pulse. Fluorescence parameters were calculated according to Baker (2008).

3.6. Observation of root fluorescence

Root fluorescence was imaged as described elsewhere (Schmid et al., 2014) by using a fluorescence imaging system (Quantum ST4). Excitation by epi-UV was adjusted to 365 nm and the emitting light was filtered by a 440 nm filter (F-440M58). The images were taken with the help of the "Quantum-capt version 15.17" software.

3.7. Quantitative RT-PCR

RNA was isolated by using a modified version of the single-step method (Chomczynski and Sacchi, 1987). For reverse transcription of RNA into cDNA, the RevertAid First Strand cDNA Synthesis Kit (Fermentas), oligo(dT)-primers, and RNA samples treated with RQ1 RNase-free DNase (Promega) were used. Gene expression was analyzed by quantitative realtime PCR using a Mastercycler ep realplex (Eppendorf) and iQ SYBR Green Supermix (Bio-Rad Laboratories). Relative expression was calculated according to Pfaffl (2001) and normalized to *UBQ2* as constitutively expressed control.

3.8. Yeast strains, plasmids, transformation, and growth methods

The *Saccharomyces cerevisiae* deletion mutants Y04534 (*pmr1* Δ), Y04069 (*ycf1* Δ), Y00829 (*zrc1* Δ), Y01613 (*cot1* Δ), Y04533 (*cup2* Δ), Y04169 (*ccc1* Δ), and their parental strain BY4741 were obtained from the Euroscarf collection (Winzeler et al., 1999). To construct the pFL61-AtMTP8 plasmid, the *AtMTP8* cDNA was amplified from Col-0 cDNA using *NotI*-containing primers and cloned into the pFL61 shuttle yeast expression vector (Minet et al.,

1992) downstream of a *PGK* promoter (Bastian Meier, unpublished). Yeast transformation was carried out according to Elble (1992). Transformants were selected on synthetic complete (SC) plates lacking the appropriate selective markers. Yeast drop assays were performed as described previously (Peiter et al., 2005b).

3.9. Ferric chelate reductase activity and rhizosphere acidification assays

Seedlings were cultivated on Fe14/Mn0 for 11 days, and similar-sized ones were transferred to Fe100/Mn0, Fe0/Mn0, or Fe14/Mn320. After 0, 24, 48, and 72 h, seedlings were assayed for ferric chelate reductase activity as described by Waters et al. (2006). Three to five plants were pooled, and roots were placed into 2.0 mL buffer solution containing 0.2 mM CaSO₄, 5 mM MES (pH 5.5), 0.2 mM Ferrozine, and 0.1 mM Fe-EDTA in a 24 well-plate. The reaction was allowed to continue for 1-2 h. Seedlings were then removed from the solution, and roots were excised, quickly dried on tissue paper and weighed. Absorbance of the solutions at 562 nm was measured by using a UV-VIS spectrophotometer (Uvikon XL; Biotek).

For the rhizosphere acidification assay, plants were cultivated according to the same protocol that was used for the ferric chelate reductase activity assay. The assay was conducted as previously described (Yi and Guerinot, 1996). In brief, the seedlings that were cultivated for 24, 48 or 72h on Fe100/Mn0, Fe0/Mn0, or Fe14/Mn320 were re-transferred to a 1% agar plate containing 0.006% bromocresol purple and 0.2 mM CaSO₄ (pH adjusted to 6.5 with NaOH) and incubated in the growth chamber for 24 h.

3.10. Perls staining and DAB/H₂O₂ intensification

Perls staining and DAB/H₂O₂ intensification was performed according to Roschttardt et al. (2009). Embryos were dissected from seeds previously imbibed in distilled water for 3 h, using a binocular magnifying lens. The isolated embryos were vacuum-infiltrated with equal volumes of 4% (v/v) HCl and 4% (w/v) K-ferrocyanide (Perls stain solution) for 15 min and incubated for 30 min at room temperature (Stacey et al., 2008). DAB intensification was applied as described in Meguro et al. (2007). After washing with distilled water, the embryos were incubated in a methanol solution containing 0.01 M NaN₃ and 0.3% (v/v) H₂O₂ for 1 h, and then washed with 0.1 M phosphate buffer (pH 7.4). For the intensification reaction the embryos were incubated between 10 and 30 min in a 0.1 M phosphate buffer (pH 7.4) solution containing 0.025% (w/v) DAB (Sigma), 0.005% (v/v) H₂O₂, and 0.005% (w/v) CoCl₂ (intensification solution). The reaction was stopped by rinsing with distilled water.

For the *in situ* Perls/DAB/H₂O₂ intensification isolated embryos were vacuum-infiltrated with fixation solution containing 2% formaldehyde, 2% glutaraldehyde in 50 mM cacodylate buffer (pH 7.2), dehydrated in an ethanol series (30%, 40%, 50%, 60%, 80%, 100%), and embedded in resin. 5 µm cross sections of stained roots and embryos were obtained by cutting the fixed and resin-embedded samples using a microtome. The sections were deposited on glass slides that were incubated for 45 min in Perls solution. The intensification procedure was then applied as described above.

4. Results

4.1. Design and establishment of the screening medium

4.1.1. Optimization of growth parameters

In order to screen for T-DNA insertion lines with enhanced susceptibility to Fe deficiency-induced chlorosis, a high-pH and low-Fe agar medium was developed by adding MES to half-strength MS medium containing 40 μM Mn but no Fe. The effect of changing medium parameters on the severity of the Fe deficiency-induced chlorosis of the plants is shown in a summarized way in the chart of Figure 1A. As expected, an increase in the NaFeEDTA concentration resulted in recovery of the chlorotic phenotype, while an increase in buffer concentration and pH increased the severity of the chlorosis. An increase in agar concentration did not change the severity of chlorosis, indicating that the Fe contamination derived from the agar did not have a significant impact on the Fe availability to the plant at high pH. However, a decrease in the agar concentration in the medium below 1.5% did not allow sufficient gelling when the pH of the medium was high.

Fe deficiency-dependent chlorosis in *Arabidopsis* plants only developed when the medium was buffered (Figure 1B), showing that an induction of Fe deficiency-dependent chlorosis in seedlings was pH-dependent in this growth system. Sowing density appeared as another factor affecting growth and chlorosis on the high-pH and low-Fe medium. Seeds were either sown at a distance of approximately 1 cm or closer to each other. Seedlings that were sown closer to each other had longer roots and bigger shoots (Figure 1C). In addition, light had a strong impact on the severity of Fe deficiency-dependent chlorosis of the seedlings. An increase in light intensity resulted in extensive chlorosis (Figure 1D). Furthermore, the Fe deficiency status of the seedlings that were subjected to different light intensities was monitored by visualization of the fluorescence emission by the roots under UV light. This fluorescence is an indicator of the synthesis and secretion of coumarins, and is strongly upregulated under Fe deficiency (Schmid et al., 2014). Seedlings that were subjected to 350 $\mu\text{mol m}^{-2} \text{s}^{-1}$ light intensity had smaller roots and the fluorescence was confined to the subapical zone of the root tips (Figure 1E). When the light intensity was set to 120 $\mu\text{mol m}^{-2} \text{s}^{-1}$, fluorescence was more homogeneously distributed over the root. In order to verify if Fe deficiency could be rescued by decreasing the intensity of the light, light intensity was set to 30 $\mu\text{mol m}^{-2} \text{s}^{-1}$. Indeed, root fluorescence decreased dramatically and plants developed greener shoots (data not shown), indicating that the plants were not Fe-deficient anymore. Therefore, it was concluded that an increase in light intensity decreases the Fe availability to the plant in the present system.

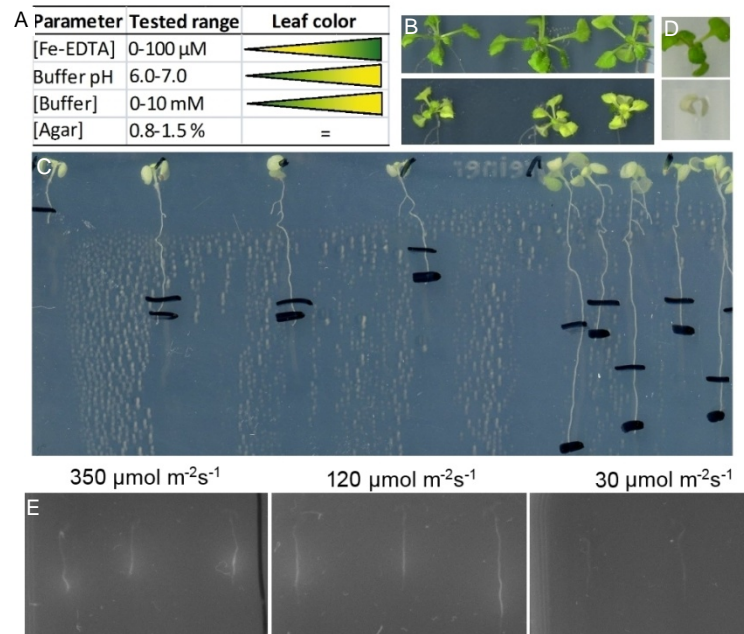


Figure 1. Critical factors in the establishment of a screening medium for the identification of genes involved in Fe deficiency-induced chlorosis

A, chart of the parameters which were optimized and their impact on the severity of Fe deficiency-induced chlorosis under high-pH and low-Fe conditions. B, effect of buffer on the development of chlorosis, not buffered (top) or buffered with 10 mM MOPS at pH 6.7 (bottom). C, effect of sowing density on root and shoot growth under low Fe availability. Seeds were either sown at a distance of approx. 1 cm or closer to each other. D, effect of light intensity on chlorosis development. Plants were subjected to 120 $\mu\text{mol m}^{-2}\text{s}^{-1}$ (top) or 350 $\mu\text{mol m}^{-2}\text{s}^{-1}$ (bottom). E) Effect of light intensity on fluorescence emission by plant roots.

4.1.2. Induction of Fe deficiency on Fe28/Mn40 medium

Several conditions were tested to induce a mild chlorosis in *Arabidopsis* wild-type seedlings which sustained for several days. These expectations were met when 28 μM NaFeEDTA was added to the medium which contained 40 μM Mn (hereafter called Fe28/Mn40) (Figure 2). In Fe28/Mn40, Col-0 seedlings grew in a chlorotic state for more than two weeks. After 17d, plants which grew on Fe28/Mn40 partially recovered from chlorosis, but were still slightly chlorotic compared to the ones which were grown on medium containing 100 μM NaFeEDTA (hereafter called Fe100/Mn40). After 21d, plants grown on Fe28/Mn40 fully recovered from chlorosis. On Fe-sufficient control plates, seedlings did not develop any chlorotic leaves.

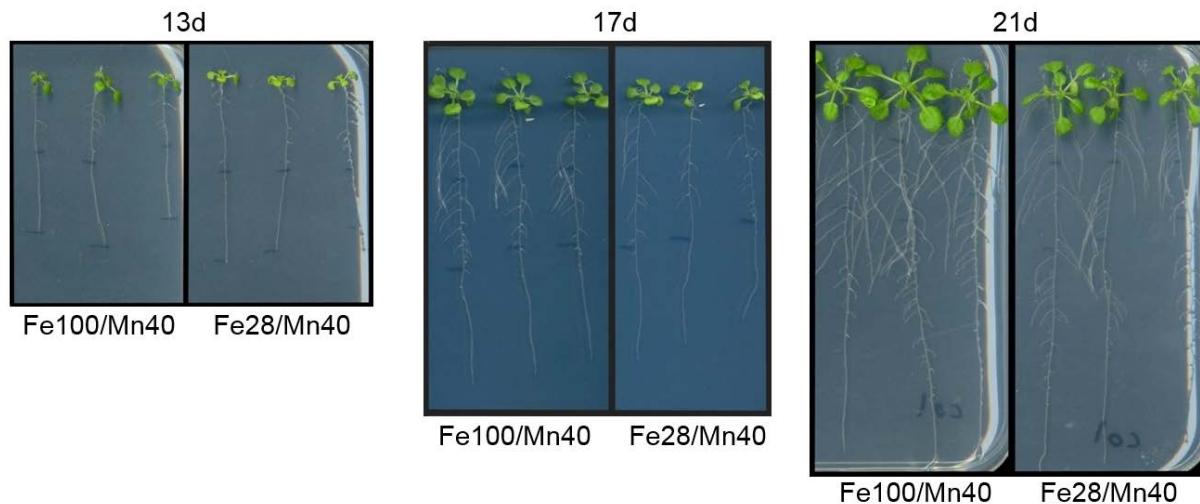


Figure 2. Development of Fe deficiency-induced chlorosis in Arabidopsis seedlings after germination on Fe-deficient (Fe28/Mn40) agar medium

Arabidopsis wild-type seedlings were cultivated on either Fe100/Mn40 or Fe28/Mn40. Plates were scanned after 13, 17 and 21 days after cultivation.

4.1.3. Validation of the medium and screening process

Before starting the screening, previously characterized mutants in Fe deficiency response-related genes were grown on Fe28/Mn40 or Fe100/Mn40 in order to validate the high-pH and low-Fe medium (Figure 3). On Fe100/Mn40, which was supposed to provide Fe sufficient conditions, *pve* and *frd3* grew similar to or were a bit more chlorotic than Col-0. *irt1* and *fro2* mutants showed extensive chlorosis and retarded growth. On Fe28/Mn40, which was supposed to provide Fe-deficient conditions, *frd3* was severely chlorotic; *irt1* and *fro2* grew even worse and almost died. *pve* grew similar to Col-0, except that it showed necrotic lesions.

The Fe status of the *fro2* mutant was further examined by comparing its root fluorescence to that of the wild type (Figure 3). Wild type root fluorescence was low under Fe100/Mn40 and higher in Fe28/Mn40, as expected. However, root fluorescence of *fro2* grown on Fe100/Mn40 was similar or even higher than in the wild type grown under Fe28/Mn40, indicating that in *fro2* the Fe deficiency response was upregulated even on Fe100/Mn40. Taken together, Fe deficiency-susceptible mutants showed differential growth on Fe100/Mn40 and Fe28/Mn40. On Fe28/Mn40, all mutants were suffering more severely from Fe deficiency than Col-0 and developed more severe leaf chlorosis or necrosis.

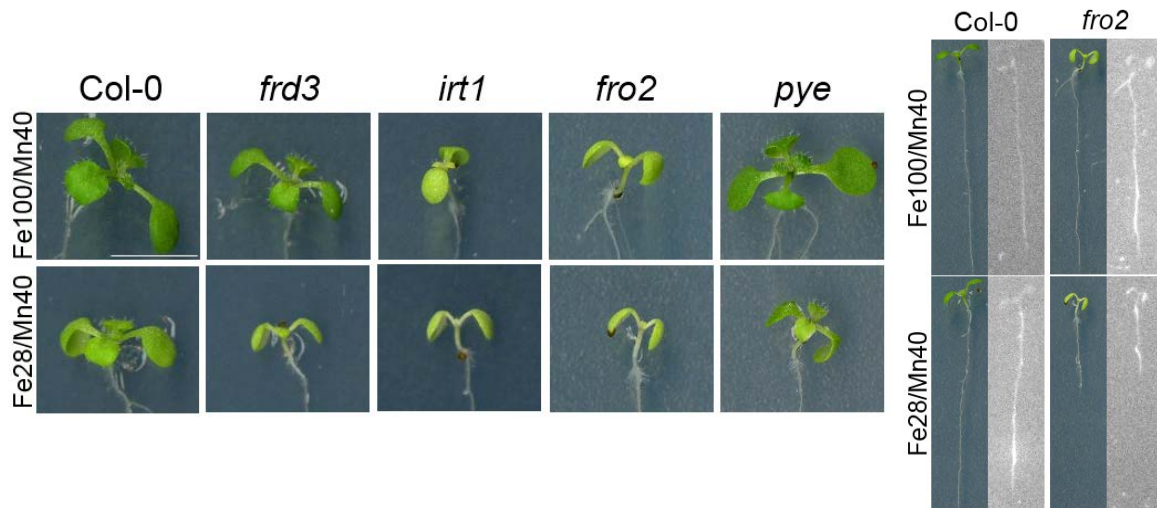


Figure 3. Growth, chlorosis and root fluorescence of Fe deficiency-sensitive mutants.

Seedlings were cultivated for 12 days on Fe100/Mn40 or Fe28/Mn40. Left, shoots of Col-0 and Fe deficiency-sensitive mutants *frd3*, *irt1*, *fro2*, and *pye*. Right, seedling growth and fluorescence emission by the wild type and the *fro2* mutant.

The screening was started using gain-of-function mutants to identify seedlings which grew better than the wild type on Fe28/Mn40. For this purpose, FOX lines were selected as screening material (Ichikawa et al., 2006). These lines express ectopically one to two independent Arabidopsis full-length cDNAs and are advantageous over other gain-of-function lines especially because the cDNA causing the phenotype can be identified simply by PCR. However, the seedlings of the FOX seed pool showed inconsistent growth on Fe28/Mn40. Approximately 15% of the seedlings showed non-chlorotic growth whereas the rest showed extensive chlorosis, eventually resulting in death (Figure 4). The inserted cDNAs of several of those lines which showed vigorous growth on Fe28/Mn40 were amplified by PCR and sequenced (data not shown). Sequencing results showed that these cDNAs encoded various proteins, which were unlikely to be related to Fe deficiency responses. It was concluded that the screening of FOX lines under the present conditions led to many false positives. Therefore, it was decided to change the screening material.



Figure 4. Phenotypic variability of seedlings from the FOX seed pool when grown on Fe28/Mn40.

Seeds obtained from the FOX seed pool were sown on Fe28/Mn40 and cultivated for three weeks before the plates were scanned.

Homozygous SALK T-DNA insertion lines (Alonso et al., 2003) were used in a next attempt to identify Fe deficiency-related genes. These seedlings grew more consistently on Fe28/Mn40. To restrict the number of lines to be screened, lines carrying T-DNA insertions in genes reported to be upregulated under Fe deficiency via FIT or PYE were selected. The list of genes and the corresponding lines which were screened are shown in Figure 5. Lines that showed more severe chlorosis compared to the wild type on Fe28/Mn40 were selected for further analysis.

	Line Code	Gene Code		Line Code	Gene Code		Line Code	Gene Code
1	SALK_144164C	At1g09790	40	SALK_080688C	At4g38950	80	SALK_103699C	At1g11840
2	SALK_147451C	At3g46900	41	SALK_011913C	At4g29220	81	SALK_058904C	At3g47650
3	SALK_109396C	At5g47910	42	SALK_107939C	At3g51200	82	SALK_040185C	At1g23020
4	SALK_132418C	At3g13610	43	SALK_042794C	At3g61930	83	SALK_017016C	
5	SALK_121565C	At5g13740	44	SALK_048526C	At1g05700	84	SALK_135507C	At1g56430
6	SALK_082635C	At2g30660	45	SALK_085412C	At4g21910	85	SALK_096228C	At3g47420
7	SALK_118446C	At3g48450	46	SALK_085412C	At4g21910	85	SALK_096539C	At3g47630
8	SALK_080218C	AT1G19000	47	SALK_136932C	At1g60610	86	SALK_043140C	At5g45410
9	SALK_088311C	At2g47000	48	SALK_008958C	At4g02330	87	SALK_151290C	At1g03080
10	SALK_057638C	At3g53280	49	SALK_015054C	At1g74770	88	SALK_051706C	
11	SALK_043881C	At4g14680	50	SALK_146998C	At5g53450	89	SALK_053278C	At5g03140
12	SALK_009007C	At1g05300	51	SALK_018370C	At5g55620	90	SALK_204565C	At3g55430
13	SALK_036012C	At3g18290	52	SALK_035416	At1g57560	91	SALK_149052C	
14	SALK_003255C	At4g26890	53	SALK_048470C	At1g18910	92	SAIL_74_B07	At1g74780
15	SALK_074896C	At5g37260	54	SALK_040332C	At5g38820	93	SALK_110010C	
16	SALK_140266C	At3g58060	55	SALK_094426	At1g09560	94	SALK_113040C	At3g57070
17	SALK_133841C	At2g35930	56	SALK_078702	At3g50740	95	SALK_131929C	At5g03210
18	SALK_133954C	At1g49820	57	SALK_128043C	At2g45400	96	SALK_030632 C	
19	SALK_057798C	At4g25640	58	SALK_080627C	At1g68650	97	SAIL_1255_G10	At1g74790
20	SALK_147453C	At4g25640	59	SALK_023292C	At5g67370	98	SALK_029828C	
21	SALK_025900	At1g11670	61	SALK_081645C	At4g10510	99	SALK_200963C	At1g23030
22	SALK_019139C	At2g36885	62	SALK_132418C	At3g13610	100	SALK_006284C	At3g48140
23	SALK_023076C	At1g33090	63	SALK_019569C	At1g17260	101	SALK_204374C	
24	SALK_066923C	At2g20030	64	SALK_095937C	At3g06890	102	SALK_003991C	At3g55440
25	SALK_035704C	At3g53480	65	SALK_016715C	At4g31950	103	SALK_100762C	At2g30090
26	SALK_071767C	At5g05250	66	SALK_130376C	At3g21690	104	SALK_093190C	At5g14960
27	SALK_107837C	At1g77280	67	SALK_140776C	At2g19410	105	SALK_071809 C	
28	SALK_045057C	At3g58810	68	SALK_076701C	At1g75200	106	SALK_090862C	At3g47660
29	SALK_110829C	At1g01570	69	SALK_118350C	At2g18960	107	SALK_063364C	
30	SALK_063184	AT1G49960	70	SALK_120680C	AT4G22880	108	SALK_107945C	At3g47430
31	SALK_034026	At5g36890	71	SALK_105742C	AT3G60330	109	SALK_005625C	At2g14850
32	SALK_140776C	At2g19410	72	SALK_131820 C	At3g48450	110	SALK_141935C	
33	SALK_073511C	At4g30120	73	SALK_054106C	At4g14680	111	SALK_054389C	At5g03230
34	SALK_020101C	At5g04730	74	SALK_121588 C	AT4G22880	112	SALK_052443C	
35	SALK_138196	At3g11750	75	GABI_797 D03	At3g59030	113	SALK_141821C	At5g14950
36	SALK_012767	At3g07720	76	SALK_106967C	AT1G49960	114	SAIL_703_C10	
37	SALK_099407C	At4g10510	77	SALK_127844C	AT2G24520	115	SAIL_1214_C01	At2g30100
38	SALK_072019C	At3g61410	78	SALK_048598C	At1g17260	116	SALK_052766C	
39	SALK_123168C	At1g34760	79	SALK_052070C	At5g53450	117	SALK_073451C	At1g72460
				SALK_063470C	At2g35930	118	SALK_136462	
						119	SAIL_1156_C06	At1g72450
							SAIL_267_C12	At1g68580
							SALK_045661C	
							SALK_111412C	At2g46060
							SAIL_813_E05	At3g13710
							SAIL_1254_A07	At2g24550
							SALK_025606C	At1g72440
							SALK_130654C	At2g15440
							SALK_205573C	
							SALK_205342C	At4g23010
							SALK_205869C	At4g00590
							SAIL_768_F02	At3g02140
							SALK_137966C	At1g03090
							SALK_073394C	
							SALK_200761C	At3g15210
							SALK_120395C	At2g24545
							SALK_094145 C_S	At5g45307

Figure 5. List of the homozygous Arabidopsis lines selected for screening on Fe28/Mn40.

Given are SALK, SAIL or GABI identifiers of the lines and the corresponding gene identifiers. All lines carry T-DNA insertions in genes reported to be upregulated under Fe deficiency via FIT or PYE.

Among the screened T-DNA insertion lines, nine lines exhibited lower biomass or more severe chlorosis compared to the wild type on Fe28/Mn40. Only three of these lines showed consistently more chlorotic growth when the growth assay was repeated. These three lines, when grown on Fe100/Mn40, either did not show the phenotype or showed to a lesser extent, indicating that the phenotype was Fe-deficiency related. For instance, the SALK_019569C line, carrying a T-DNA insertion in *AHA10* (At1g17260) showed extensive primary root growth repression when grown on Fe28/Mn40, but much less so when grown on Fe100/Mn40 (Figure 6). Lateral root length was not different from that of the wild type, neither on Fe100/Mn40 nor on Fe28/Mn40. However, the phenotype could not be confirmed by using a new generation of seeds of the same line or by using an independent knock-out allele of the same gene, SALK_048598C (data not shown).

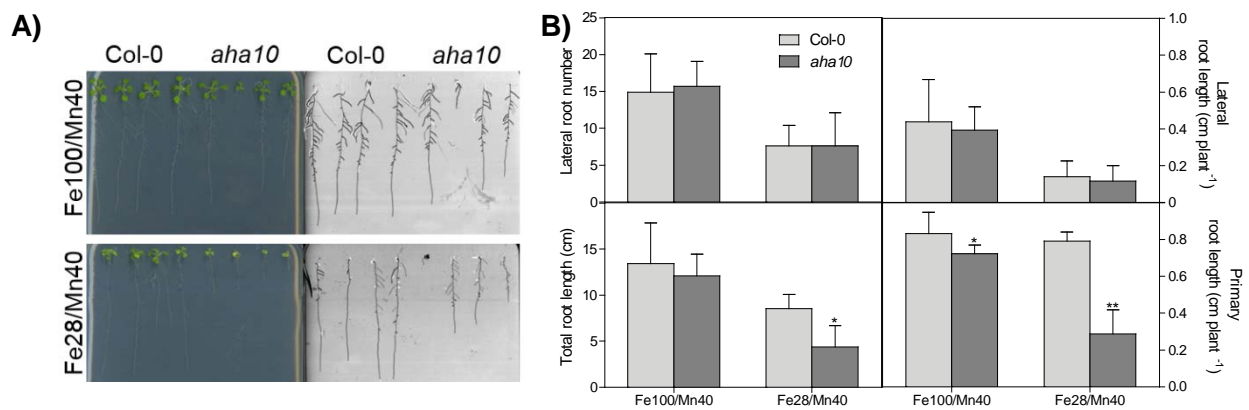


Figure 6. Growth and root phenotype of the homozygous *aha10* (SALK_019569C) line on Fe100/Mn40 and Fe28/Mn40.

A, plants were cultivated for 21 days either on Fe100/Mn40 or Fe28/Mn40, and plates were scanned (left). After scanning, shoots were excised and plates were scanned again in black and white to increase contrast (right). B, quantitative measurement of root parameters. (N=10, error bars represent SEM). An asterisk above a bar indicates that the corresponding mean of the mutant line is significantly different (*, $P < 0.05$; **, $P < 0.01$) from the mean of the Col-0 line according to Student's t-test.

4.2. Involvement of MTP8 in Fe and Mn homeostasis in Fe-deficient Arabidopsis plants

4.2.1. *mtp8* mutant lines are susceptible to Fe deficiency-induced chlorosis

Screening for chlorotic phenotypes of more than 120 homozygous T-DNA insertion lines grown on Fe28/Mn40 identified two lines which carried a T-DNA insertion in *MTP8*, a gene that had not yet been associated with Fe deficiency-induced chlorosis (Figure 7). On Fe100/Mn40, mutants grew similar to wild-type plants. However, on Fe28/Mn40, both mutant lines showed extensive chlorosis, which could be reverted by spraying 100 μ M FeEDTA. This regreening indicated that the mutants were susceptible to Fe deficiency and not to the lack or the toxicity of another element. When grown on a calcareous potting substrate, seedlings of the *mtp8-1*

mutant were smaller and extremely chlorotic. This demonstrated that the mutant phenotype was not limited to the screening conditions on agar, but also relevant on soil.

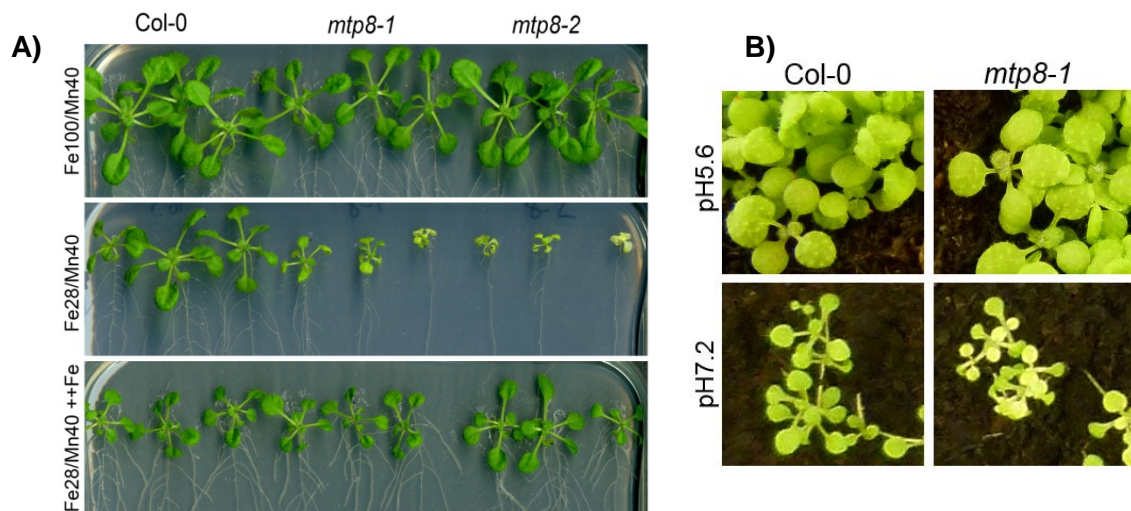


Figure 7. Tolerance of *mtp8-1* and *mtp8-2* to high pH-induced low-Fe availability.

A, Growth of *mtp8-1* and *mtp8-2* mutants on Fe100/Mn40, Fe28/Mn40, or Fe28/Mn40 with foliar application of Fe. Seedlings were cultivated for 23 days. In the resupply treatment, a solution containing 100 μ M Fe-EDTA was sprayed after 9 days of cultivation on Fe28/Mn40 medium. B, Growth of the *mtp8-1* mutant on non-limed (pH5.6) and limed potting soil (pH7.2), watered with 160 μ M MnCl₂ solution. Plants were photographed after 19 days of cultivation.

The genomic sequence of *MTP8* has seven exons (Figure 8). In one of the mutant lines of the SALK collection, SALK_068494, a T-DNA was inserted in the first exon. This line was named *mtp8-1*. In the second mutant line, SALK_140266, a T-DNA was inserted in the 6th exon. This line was named *mtp8-2*. RT-PCR amplification of RNA from both mutants and the wild type using *MTP8*-specific primers only produced a visible band for the wild type, but not for the mutants, indicating that *mtp8-1* and *mtp8-2* were knock-out lines for *MTP8*.

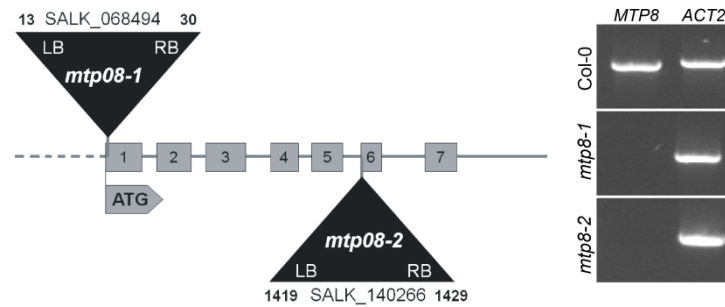


Figure 8. Genetic characterization of *mtp8-1* and *mtp8-2*.

A, diagram showing the insertion sites of T-DNAs in *mtp8* mutants. The location of T-DNA insertions is shown by triangles. Coding regions are presented as grey boxes; introns are shown by a line. Numbers indicate the last remaining nucleotide before and the first nucleotide after the T-DNA, counting from the ATG. LB, left T-DNA border; RB, right T-DNA border. B, products of RT-PCR amplification of wildtype and *mtp8* mutants RNA using *MTP8*-specific primers. *ACT2* was used as a positive control. (Experiment: Bastian Meier)

4.2.2. Subcellular localization of MTP8

MTP8 is the closest ortholog of ShMTP8 which was characterized as a vacuolar Mn transporter contributing to the high tolerance of *Stylosanthes hamata* to excess Mn (Delhaize et al., 2003). In order to identify the subcellular localization of MTP8, an MTP8-EYFP construct was generated to transform Arabidopsis protoplasts. EYFP fluorescence was observed at the vacuolar membrane only (Figure 9), showing that Arabidopsis MTP8, like ShMTP8, is localized to the vacuolar membrane.

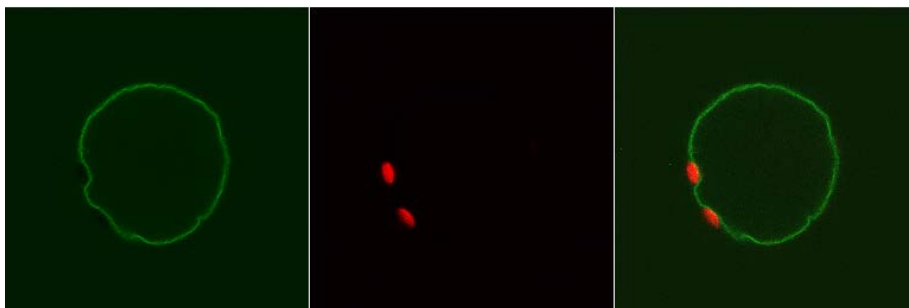


Figure 9. *MTP8:EYFP* localization in mesophyll protoplasts.

Arabidopsis Col-0 mesophyll protoplasts were transformed with an *MTP8-EYFP* construct. Fluorescence was observed 24 h after transformation. A, *MTP8:EYFP* fluorescence. B, chlorophyll autofluorescence. C, merged image. (Experiment: Bastian Meier)

4.2.3. Metal transport specificity of MTP8

Since ShMTP8 and Arabidopsis MTP8 share a high degree of sequence similarity, including an amino acid signature specific for the Mn subgroup of CDFs (Montanini et al.,

2007), and since both are localized to the tonoplast, it was hypothesized that Arabidopsis MTP8 functions in sequestering Mn ions into the vacuole, and that this function is related to the Fe-deficient phenotype of the mutant. The metal selectivity of the transporter was determined by expressing the *MTP8* cDNA in metal-hypersensitive yeast strains. Growth of yeast mutants sensitive to Co (*cot1Δ*), Zn (*zrc1Δ*), and Cu (*cup2Δ*) on media containing high concentrations of the respective metals was not improved by expression of *MTP8* (Figure 10). In contrast, growth of the Mn-hypersensitive mutant *pmr1Δ* on elevated Mn and the Fe-sensitive mutant *ccc1Δ* on elevated Fe were considerably improved when transformed with *MTP8*. *PMR1* encodes a Ca/Mn-ATPase that confers Mn tolerance to yeast (Antebi and Fink, 1992), whereas *CCC1* encodes for a vacuolar Fe transporter. Both the *MTP8*-expressing *pmr1Δ* and *ccc1Δ* mutants grew well even on media containing concentrations of the respective metals that are strongly inhibitory to the wild type. This observation indicated that Arabidopsis MTP8 transports Mn and Fe into the vacuole.

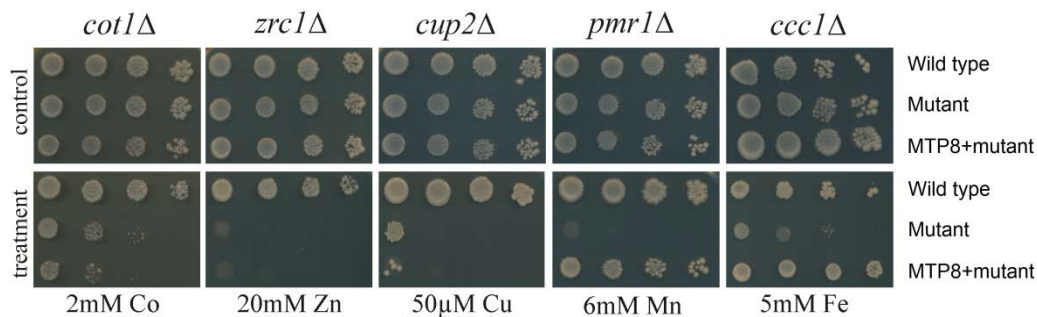


Figure 10. Complementation of metal-sensitive yeast strains with Arabidopsis *MTP8*

Cultures of yeast strains sensitive to Co (*cot1Δ*), Zn (*zrc1Δ*), Cu (*cup2Δ*), Mn (*pmr1Δ*) and Fe (*ccc1Δ*) were serially diluted and dropped onto SD medium plates supplied with the respective metals. (Experiment: Bastian Meier)

To further examine the function of the MTP8 protein in metal transport, overexpression lines were generated, in which the expression of *MTP8* is driven by the CaMV35S promoter. (Figure 11). Quantitative real time PCR analysis showed that in these lines, expression of the *MTP8* gene was strongly enhanced. The lines *35S::MTP8 OE2* and *35S::MTP8 OE4*, which expressed *MTP8* approximately 7000- and 3000- fold, were selected for further experiments. On standard ½ MS (pH 5.8) medium, containing 50 μM Fe, both overexpressors accumulated about three times higher Mn levels in the roots than the wild type (Figure 11), indicating that an overexpression of *MTP8* increases Mn sequestration in roots. In the shoot, there was a trend of lower Mn concentrations in the overexpressors, which was significant in *35S::MTP8 OE2*. This effect became more striking on Fe28/Mn40 medium. Here, the overexpressors contained less than half of the concentration of Mn in the shoot compared to the wild type. The Mn concentration in the root was not altered by *MTP8* overexpression, which was likely due to the large fraction of Mn bound in the root apoplast under those conditions. Taken together, these data further supported the notion that MTP8 is involved in controlling the long-distance translocation of Mn from roots to shoots.

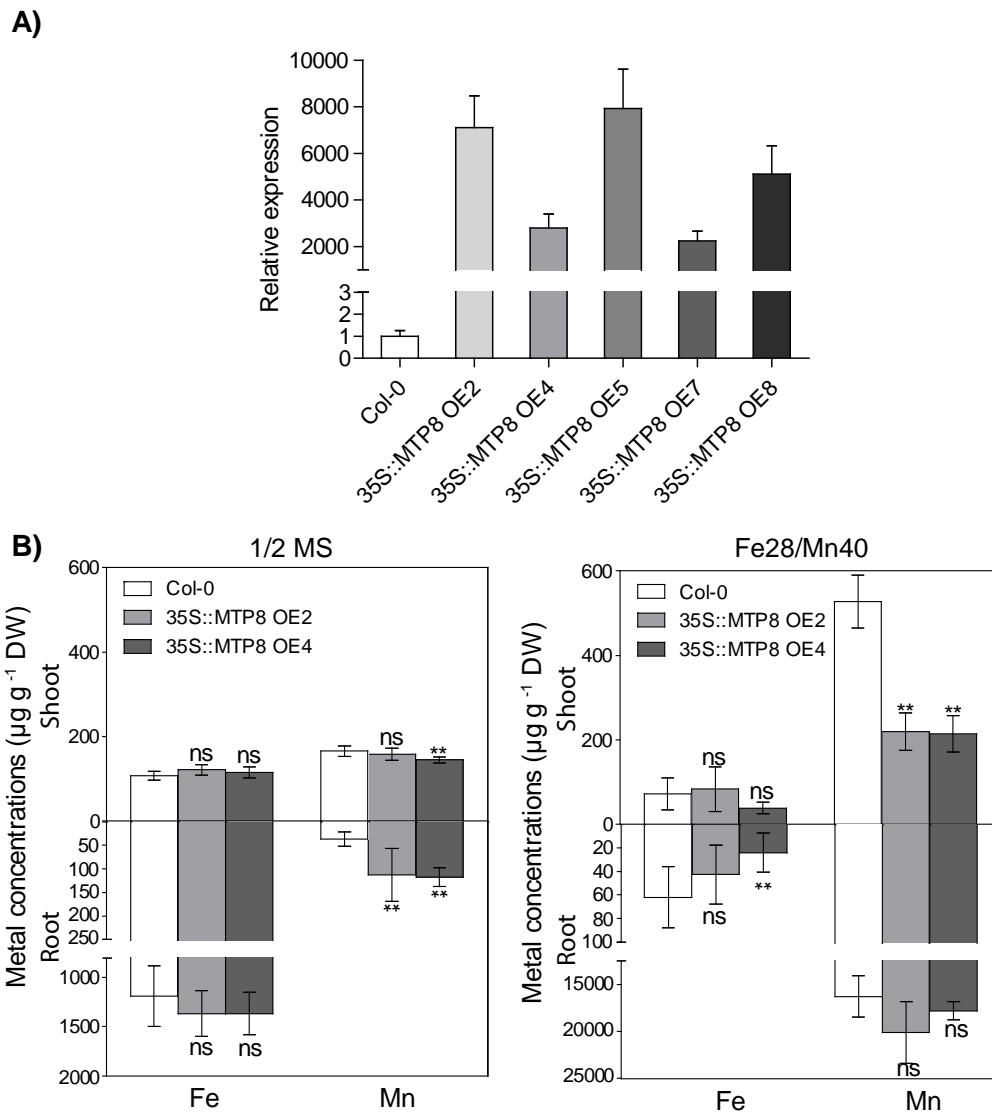


Figure 11. Accumulation of Fe and Mn in the roots and shoots of *MTP8* overexpressor lines.

A, expression of *MTP8* in 35S::AtMTP8 lines grown on 1/2 MS medium (Experiment: Bastian Meier). B, Fe and Mn concentrations of *MTP8* overexpressor lines grown on Fe-sufficient (1/2 MS) or Fe28/Mn40 medium. Seeds were precultured for one week on 1/2 MS or Fe28/Mn40, transferred to the same medium, and cultured for one more week. Data were obtained from pooling 4 plants with at least 4 replicates. The experiment was conducted twice with comparable results. An asterisk above a bar indicates that the corresponding mean of the mutant line is significantly different (*, $P < 0.05$; **, $P < 0.01$) from the mean of the Col-0 line according to Student's t-test. Error bars represent \pm SD

4.2.4. Sensitivity of the Arabidopsis *mtp8-1* mutant to high Mn

Expression of *Stylosanthes ShMTP8* in Arabidopsis increased the Mn tolerance of the plant. In order to test if Arabidopsis *MTP8* also confers tolerance to excess Mn, wild type and *mtp8-1* mutant seedlings were subjected to increasing concentrations of the metal. At elevated Mn supplies, root growth rates were repressed more strongly in the *mtp8-1* mutant than in the wild type (Figure 12A). Since repression of primary root growth is a typical Mn toxicity

symptom, the observation indicated that *MTP8* indeed increases the tolerance of *Arabidopsis* to excess Mn.

4.2.5. Regulation of *MTP8* on high media in a *FIT*-dependent manner

In order to investigate if *MTP8* is regulated by high Mn, its expression in seedlings which were subjected to increasing concentrations of Mn was analyzed. When the medium was supplemented with 1.5 or 2 mM Mn, *MTP8* expression was induced by 8- or 12-fold in the roots (Figure 12B). This finding confirmed a Mn-dependent transcriptional control.

In a transcriptome analysis of the *Arabidopsis fit* mutant, *MTP8* has been reported to be upregulated under Fe deficiency by the transcription factor FIT (Colangelo and Guerinot, 2004). In order to confirm this finding, wild type and *fit* mutant plants pre-cultured on ½ MS medium were transferred either to the same Fe-sufficient medium or to Fe-depleted medium (½ MS medium without Fe and containing 100 µM Ferrozine). After 5 days of cultivation, *MTP8* expression in Fe-sufficient roots was low in both, wild type and *fit* mutant plants (Figure 12C). As expected, *MTP8* expression in the wild type was induced approximately 50-fold under Fe deficiency. In contrast, *MTP8* transcript levels remained unaltered in the Fe-deficient *fit* mutant. This result confirmed that under Fe deficiency, *MTP8* is upregulated in a FIT-dependent manner.

In order to verify whether the increased expression of *MTP8* under high Mn stress was also dependent on FIT, wild type and *fit* mutant plants pre-cultured on ½ MS medium were transferred either to the same medium or to ½ MS medium supplemented with 2 mM Mn. After five days on basal ½ MS medium, expression of *MTP8* was similar in wild type and *fit* mutant plants (Figure 12D). Supplementation of the medium with 2 mM Mn caused a 10-fold increase of *MTP8* expression in the wild type, whereas *MTP8* transcript abundance did not change in the *fit* mutant. This indicated that the transcriptional upregulation of *MTP8* under high Mn is regulated by FIT.

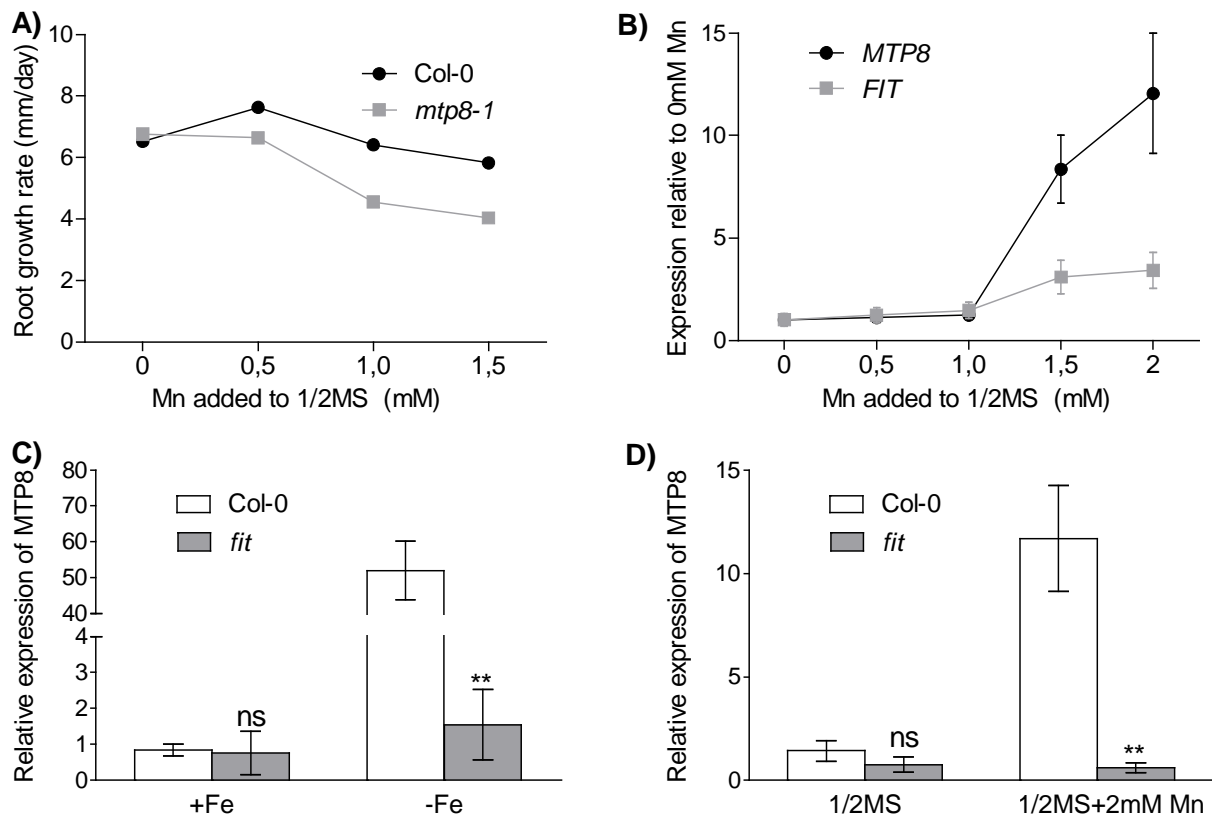


Figure 12. Growth of a *mtp8* mutant on media containing high Mn concentrations and regulation of *MTP8* on high-Mn medium and low-Fe medium in a *FIT*-dependent manner

A, root growth rate of Col-0 and *mtp8-1* seedlings on 1/2 MS agar supplemented with extra MnSO₄. B, expression of *MTP8* and *FIT* in the roots of the seedlings. Seedlings were grown for 21 days on near-vertical 1/2 MS plates supplemented with extra MnSO₄ as indicated. Expression of *MTP8* and *FIT* in roots is displayed relative to the expression level of these when grown on 0 Mn control plates. (n=4, error bars represent SD). C, *FIT*-dependence of *MTP8* expression on low-Fe medium. Seedlings were cultivated on 1/2 MS agar medium for 10 days and then transferred either to fresh 1/2 MS medium or to Fe-free 1/2 MS medium supplemented with 100 μM ferrozine. Plants were harvested after 5 days. 5 roots were pooled as one sample (n=4, error bars represent SD). D, *FIT*-dependence of *MTP8* expression on high-Mn medium. Seedlings were cultivated on 1/2 MS agar medium for 10 days and then transferred either to fresh 1/2 MS medium or 1/2 MS medium supplemented with 2 mM Mn. Plant roots were harvested after 5 days. 5 roots were pooled as one sample (n=4, error bars represent SD). (Experiment in A and B: Bastian Meier)

4.2.6. Tissue localization

PromoterMTP8::GUS lines were generated to characterize the expression pattern of *MTP8*. In order to further confirm that the gene was induced under Fe deficiency, seedlings were transferred from 1/2 MS agar after 10 days of cultivation to either 1/2 MS plates or 1/2 MS plates without Fe supplemented with 100 μM ferrozine. Seedlings were cultivated for 2 days. After two hours of incubation in GUS staining solution, the Fe-deficient roots but not the Fe-sufficient ones showed an intense blue staining (Figure 13A). The staining was evident all over the root except for the meristematic regions and oldest part of the main root. Cross sections of the root revealed that only epidermis, root hairs and outer cortex were stained, indicating that *MTP8* expression in the root is limited to the outer cell layers (Figure 13B). After an overnight incubation of the shoot, only cotyledons were stained (Figure 13C), and staining intensity did not change under Fe deficiency (not shown). The staining in the cotyledons was not as intense

as in the root although the shoot was incubated in GUS solution much longer, indicating that *MTP8* expression was predominant in the roots under Fe deficiency.

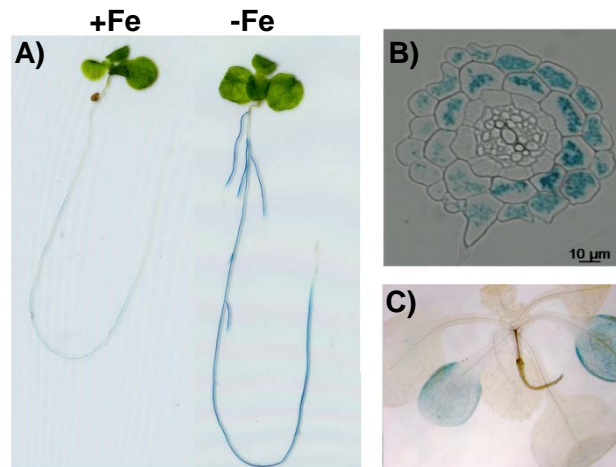


Figure 13. Activity of the Arabidopsis *MTP8* promoter in roots and shoots upon Fe deficiency.

Col-0 plants transformed with the *promoterMTP8::GUS* construct were grown on ½ MS agar for 10 days, transferred to plates supplemented with 100 µM ferrozine to render Fe unavailable, or to control plates. Plants were cultivated further for two days. A, staining of *promoterMTP8::GUS*-transformed seedlings grown on Fe-sufficient (left) and Fe-deficient (right) media after incubation for 2 h in GUS staining solution. B, cross section of a root of a *promoterMTP8::GUS*-transformed seedling grown on Fe-deficient media. The pictures shown are representative, and the staining patterns were confirmed in at least one other independent *promoterMTP8::GUS* line. C, staining of *promoterMTP8::GUS*-transformed shoot grown on Fe-deficient media after incubation for 24 h in GUS staining solution and removal of chlorophyll.

4.2.7. Effect of Mn on the Fe deficiency phenotype of *mtp8-1*

Arabidopsis *mtp8* mutants showed severe chlorosis on Fe-limiting medium (Figure 7), and *MTP8* plays a role in Mn tolerance which is dependent on FIT (Figure 12). It was therefore hypothesized that the *MTP8*-dependent chlorosis observed on medium with low Fe availability is related to a disturbed Mn homeostasis. To assess the effect of Mn supply, plants were precultured on Fe28/Mn0 (Fe28 devoid of Mn) for one week, transferred to either the same medium, to Fe28/Mn40, or to Fe28/Mn160, and cultivated further for one week. On Fe28/Mn40, *mtp8* mutants became chlorotic as observed before, which was also reflected in a decreased chlorophyll content (Figure 14). Shoot fresh weight of the mutants was lower than that of the wild type, whereas primary root length did not differ significantly in *mtp8-1* and was only slightly shorter in *mtp8-2* (Figure 14).

In contrast to the plants on Fe28/Mn40 medium, mutants transferred to medium not supplemented with Mn (Fe28/Mn0) neither showed chlorosis symptoms nor differed from the wild type in chlorophyll concentration, shoot fresh weight, or primary root length (Figure 14). On the other hand, increasing the medium Mn concentration by four times (Fe28/Mn160) yielded an opposite effect. All lines, including the wild type, showed extensive chlorosis on newly emerging leaves, resulting in similarly low chlorophyll concentrations. Besides a decreased shoot fresh weight, both mutants now also showed a far stronger repression of primary root growth than the wild type.

Based on this experiment it was concluded that the Fe deficiency phenotype of *mtp8* mutants strongly depends on the medium concentration of Mn. Furthermore, the Mn-induced exacerbation of the chlorosis in the wild type growing on Fe-limiting medium clearly underlined the antagonistic relationship between Fe and Mn.

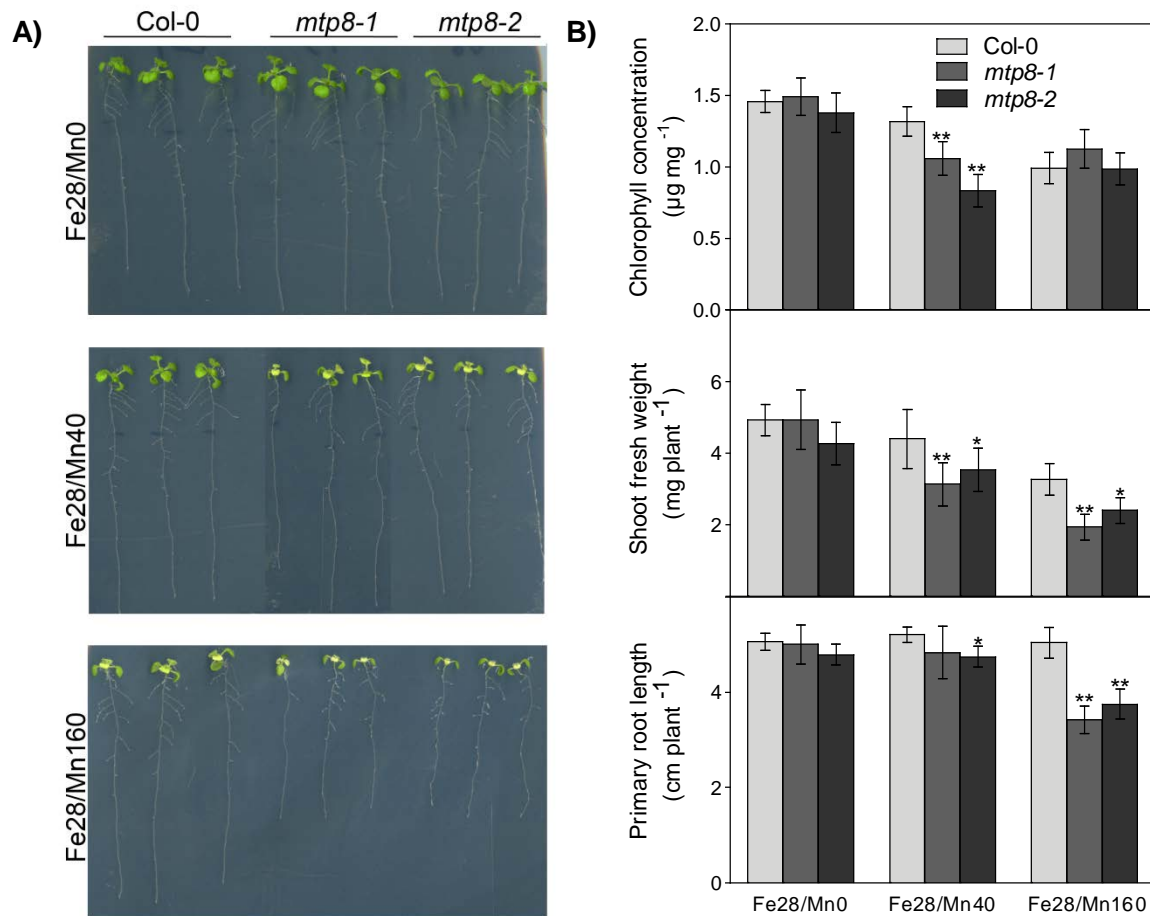


Figure 14. Effect of Mn concentration on Fe deficiency-induced chlorosis, primary root elongation, and shoot fresh weight of *mtp8-1* and *mtp8-2* mutants.

A, growth of *mtp8* mutant lines on low-Fe medium containing different concentrations of Mn. Seedlings were precultured on Fe28/Mn0 for one week, transferred to Fe28/Mn0, Fe28/Mn40, or Fe28/Mn160, and cultivated for one more week. B, chlorophyll concentration, shoot fresh weight, and primary root length of seedlings treated as shown in (A). Shoots were separated from roots, and shoot FW was determined before chlorophyll measurements. Three seedlings were pooled ($n \geq 5$). Data are from five replicate pools. An asterisk above a bar indicates that the corresponding mean of the mutant line is significantly different (*, $P < 0.05$; **, $P < 0.01$) from the mean of the Col-0 line according to Student's t-test. Error bars represent \pm SD.

Since the increased vulnerability of the *mtp8* mutants to Fe deficiency depended on the Mn concentration in the medium (Figure 14), the concentration and distribution of both elements in plants grown at different Fe and Mn levels were determined. Plants were precultured for one week either on (i) Fe100/Mn0 and transferred to the same medium or to Fe100/Mn40, or on (ii) Fe28/Mn0 and transferred to either the same medium or to Fe28/Mn40. Fe and Mn concentrations in roots and shoots were determined by ICP-OES after one week of treatment. As shown in Figure 15, on media not supplemented with Mn, wild type and mutant plants did not differ in their Fe and Mn concentrations at sufficient or low Fe supply. In contrast, when Mn

was included in the low or high Fe media, Mn and Fe concentrations in the mutant were distinct from those in the wild type. The most drastic difference was observed for the Mn concentration in the roots of plants grown on Fe28/Mn40, which was approximately five times higher in the wild type than in the *mtp8-1* mutant, whereas the shoot Mn concentration was more elevated in the mutant. Hence, when grown on the Mn40 media, the *mtp8-1* mutant did not only sequester less Mn in the roots than the wild type, but also translocated a higher proportion of Mn to the shoot.

In contrast to Mn, the concentration of Fe in mutant shoots grown on Fe28/Mn40 was only half of that of the wild type (Figure 15), indicating that Fe uptake and/or translocation were inhibited. This lower Fe concentration in the mutant was well below the threshold level to meet the requirement for chlorophyll synthesis (Gruber et al., 2013) and confirmed that the chlorotic phenotype was due to Fe deficiency. Fe concentrations in mutants cultivated on high Fe medium (Fe100/Mn40) were also lower than those in the wild type, but were still in the sufficient range.

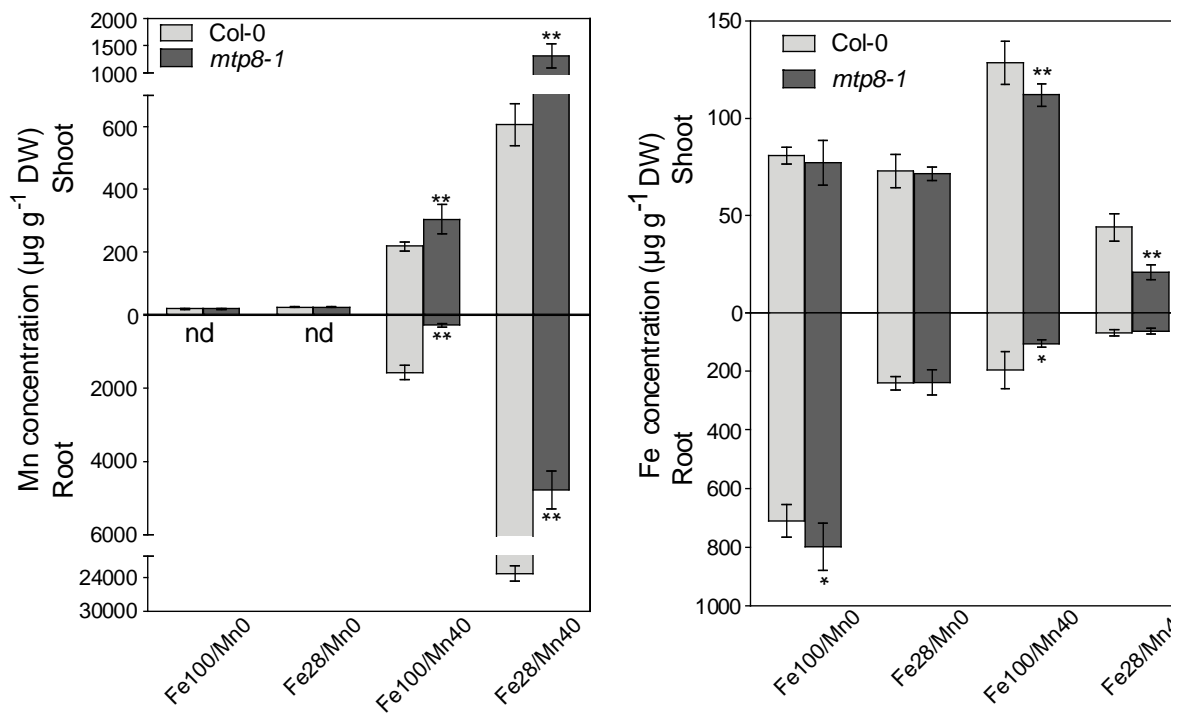


Figure 15. Shoot and root Mn and Fe concentrations of Arabidopsis *mtp8-1* seedlings under Fe deficiency or sufficiency in the presence or absence of Mn.

Seedlings of Col-0 and *mtp8-1* were precultured on Fe100/Mn0, Fe28/Mn0, Fe100/Mn40, or Fe28/Mn40 agar for one week. Seedlings of similar size were transferred to the same media and cultivated for one more week. Concentrations of Mn and Fe were determined by ICP-OES. Data are from four replicate pools, each consisting of four seedlings. The experiment was conducted twice with comparable results. An asterisk above a bar indicates that the mean of the mutant line is significantly different from the mean of the Col-0 line according to Student's t-test (*, $P < 0.05$; **, $P < 0.01$). Error bars represent \pm SD. nd: not detectable.

4.2.8. Characterization of the Fe-deficiency response in the *mtp8-1* mutant

The higher susceptibility to chlorosis and the decreased Fe translocation in the *mtp8-1* mutant in the presence of Mn could have been caused by an inhibition of the transcriptional Fe deficiency response. Therefore, the expression of genes known to be required for Fe acquisition and upregulated by Fe deficiency was analyzed on Fe28 medium containing 40 μ M or no Mn. In the wild type, addition of Mn to low-Fe medium led to an increased expression of the transcription factor genes *FIT*, *bHLH38*, *bHLH101*, and *MYB72*, the nicotianamine synthase gene *NAS4*, as well as the acquisition genes *IRT1* and *FRO2* (Figure 16). The transcriptional response of all analyzed genes was more pronounced in the *mtp8-1* knockout line. These data indicate that Mn triggers Fe deficiency responses and that a loss of *MTP8* exacerbates this antagonism, but that the transcriptional response to the perceived Fe deficiency is not hampered in the mutant.

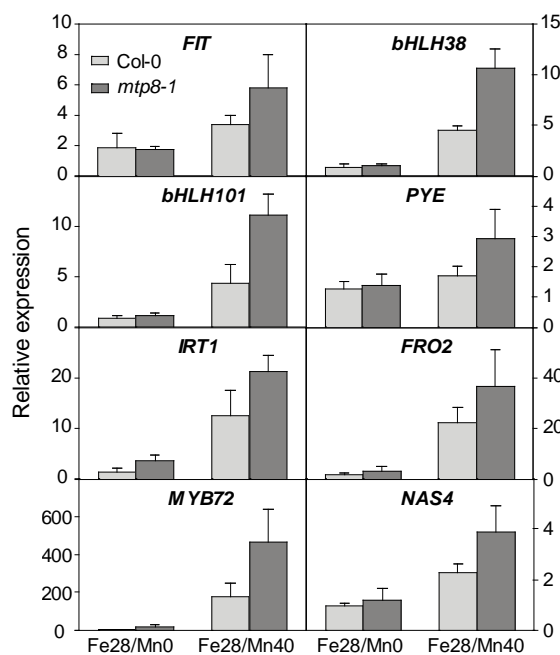


Figure 16. The transcriptional Fe deficiency response of *mtp8-1* under Fe deficiency in the presence or absence of Mn.

Real-time PCR analysis of roots of wildtype and *mtp8-1* plants which were cultivated on either Fe28/Mn0 or Fe28/Mn40 for 7 days. The expression of the Fe-deficiency responsive genes *FIT*, *bHLH38*, *bHLH101*, *PYE*, *IRT1*, *FRO2*, *MYB72*, and *NAS4* in roots was determined by qRT-PCR. Data are the means \pm SD of four samples, each consisting of three roots. The experiment was repeated three times with comparable results.

A hallmark of the response of strategy I species to Fe deficiency is an increased fluorescence emission in the rhizosphere which can be detected under UV light. This fluorescence emission is caused by scopoletin and other coumarins which are accumulated in the roots and secreted to the rhizosphere to chelate Fe under low Fe availability (Schmid et al., 2014). Since the *mtp8-1* mutant is Fe-deficient when grown on Fe28/Mn40 (Figure 15, Figure 16), it was expected for mutant roots to be more fluorescent under UV compared to the wild type. When seedlings were grown on Fe28/Mn0, root fluorescence levels were apparently not different from each other. However, in the presence of Mn, although wild-type roots were highly fluorescent, mutant root fluorescence stayed low (Figure 17). This data set indicated that coumarin-based root fluorescence in Fe-deficient *mtp8-1* roots is inhibited by Mn.

When Arabidopsis plants are grown on calcareous soil, coumarins are essential to mobilize Fe for chlorosis-free growth. Accordingly, mutant seedlings such as *f6'h1* and *myb72* which are impaired in coumarin synthesis developed chlorosis when grown on calcareous soil (Schmid, 2014). In order to investigate if coumarin accumulation is an essential step for chlorosis-free growth on low-Fe and high-Mn medium, *f6'h1* and *myb72* mutant seedlings were cultivated on Fe28/Mn40. Both *f6'h1* and *myb72* mutants exhibited non-chlorotic growth similar to the wild type (Figure 17). It was concluded that coumarin secretion strategy is not critical for

Fe uptake on agar plates, most probably because in the agar medium, Fe is already supplemented in a chelated form, FeEDTA. This experiment indicated that inhibition of coumarin accumulation or secretion by Mn did not explain the Fe deficiency phenotype of *mtp8-1* seedlings.

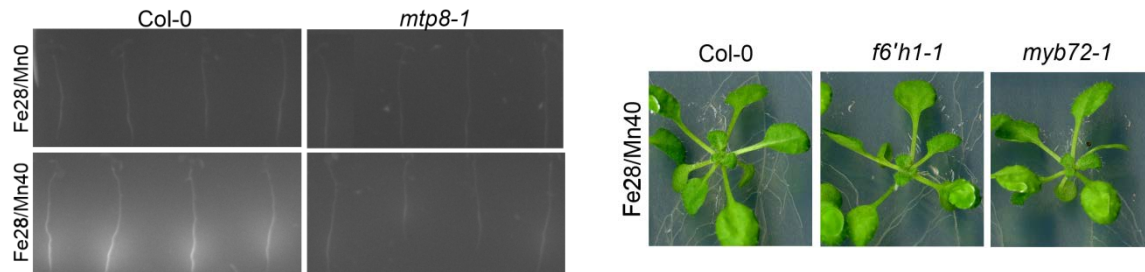


Figure 17. Fe deficiency dependent coumarin-based fluorescence in *mtp8-1* roots and phenotype of Arabidopsis mutants impaired in coumarin biosynthesis on Fe28/Mn40 medium.

Left, fluorescence emission by roots of wild-type and *mtp8-1* plants under UV light. Seedlings were cultivated for 7 days on low-Fe medium in either in the presence or the absence of Mn. Right, mutants that are impaired in the Fe deficiency-induced biosynthesis of coumarins were grown on Fe28/Mn40 for 18 days.

In order to investigate the interference of Mn with Fe availability to the plant in a wide range of Fe and Mn concentrations, wild type and *mtp8-1* were cultivated on media containing a series of concentrations of Fe (ranging from 0 μM to 100 μM) and Mn (ranging from 0 μM to 320 μM) for one week. The Fe status of the wild-type plants was assessed by the intensity of coumarin dependent-fluorescence emission of the roots. When Mn was excluded from the medium, fluorescence was very low in all plates, except where also Fe was excluded (Figure 18). Contrastingly, an increase of Mn to 320 μM resulted in wild-type plant roots to emit fluorescence even if 42 μM of Fe was added. These data confirmed that an increase in Mn concentration in the medium increased the Fe deficiency-dependent, coumarin-based root fluorescence of wild-type seedlings.

As expected, the presence of Mn in the medium inhibited fluorescence emission by *mtp8-1* roots. However, the possibility that *mtp8-1* might have been unable to accumulate coumarins was excluded because roots of *mtp8-1* seedlings grown on Fe0/Mn0 were highly fluorescent. These data confirmed that *mtp8-1* seedlings are able to increase coumarin-based fluorescence emission under Fe deficiency only in the absence of Mn (Figure 18).

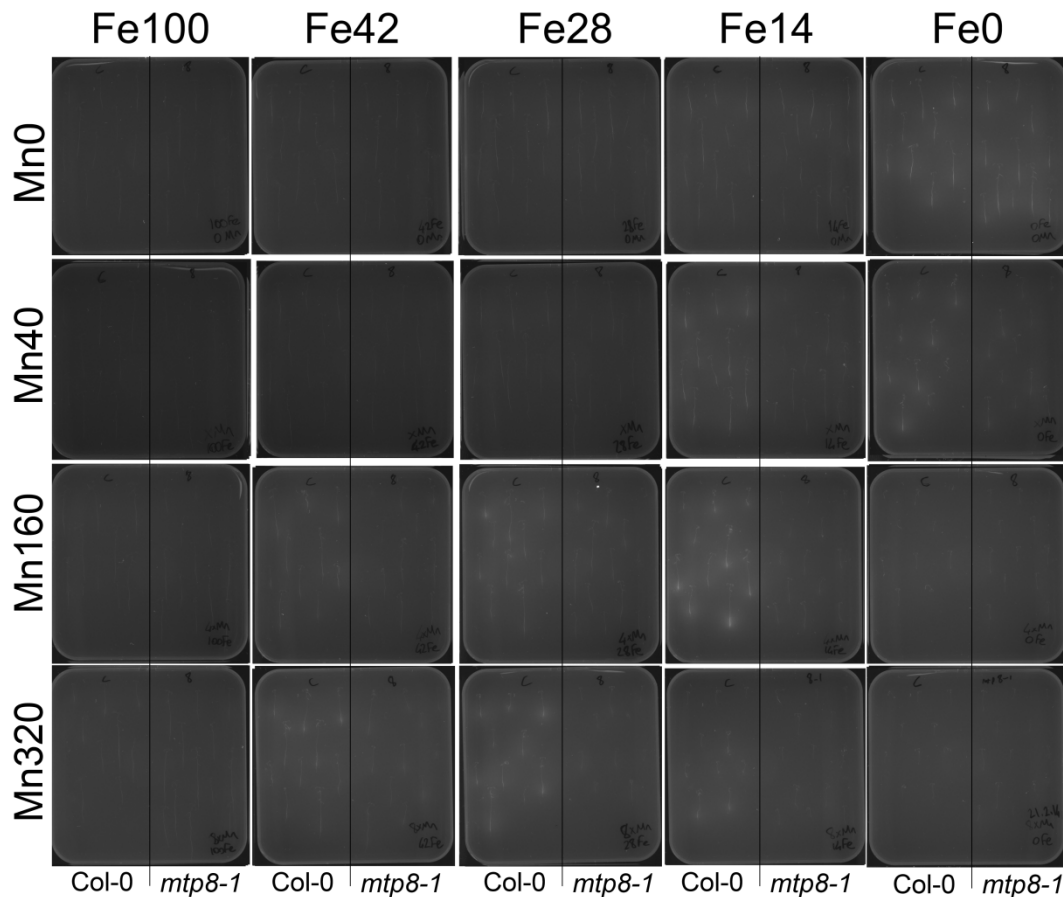


Figure 18. Visualization of coumarin-based root fluorescence emission of wild type and mutant plants which were grown under different Mn and Fe regimes

Agar plates were prepared according to the recipe of Fe28/Mn40 medium with the indicated concentrations of Fe or Mn. Col-0 seeds were sown on the left half and *mtp8-1* seeds on the right half of the plates and cultivated for 7 days. Fluorescence was visualized under 365 nm UV light.

Since the Fe deficiency response was induced at the transcriptional level (Figure 16), but neither coumarin-based fluorescence emission (Figure 18) nor the Fe concentration increased in *mtp8-1* plants (Figure 15), it was reasoned that a posttranscriptional step in the Fe acquisition machinery may be defective in the mutant.

To be able to analyze direct physiological adaptations of *mtp8-1* to Fe deficiency in the presence of Mn, it was aimed to omit possible side effects arising from long-term stress. Consequently, Fe and Mn concentrations in the medium were modified in order to increase stress intensity, which finally led the chlorotic phenotype of *mtp8-1* to appear 24h after treatment. Seedlings were precultured on Fe14/Mn0 medium for 11 days and transferred to Fe100/Mn0, Fe0/Mn0, or Fe14/Mn320 media and cultivated further for 72h. None of the plants developed chlorotic shoots, except for the *mtp8-1* seedlings grown on Fe14/Mn320 medium (Figure 19). Hence, an increased Mn-to-Fe ratio in the medium exacerbated the chlorotic phenotype of the mutant quite rapidly.

As a strategy I plant, Arabidopsis requires a ferric chelate reductase to reduce Fe(III) for uptake and the activity of this reductase is upregulated under Fe deficiency (Bauer et al., 2007; Robinson et al., 1999). Accordingly, when seedlings were transferred from Fe14/Mn0 to Fe0/Mn0, reductase activity increased strongly in the first 24 h of treatment to the same extent

in the wild type and *mtp8-1* mutant, confirming that both lines responded similarly to Fe deficiency in the absence of Mn (Figure 19). However, when plants were grown on Fe14/Mn320, ferric chelate reductase activity of the *mtp8-1* mutant did not increase over time although mutant seedlings developed a Fe deficiency-dependent chlorosis. Reductase activity of the mutant was at comparable levels to that of the non-chlorotic wild type. These data indicated that Mn inhibits ferric chelate reductase activity of Fe-deficient *mtp8-1* seedlings.

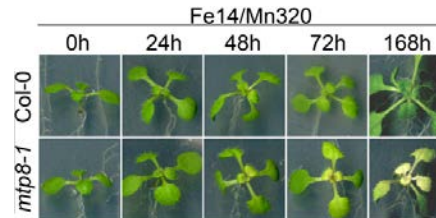
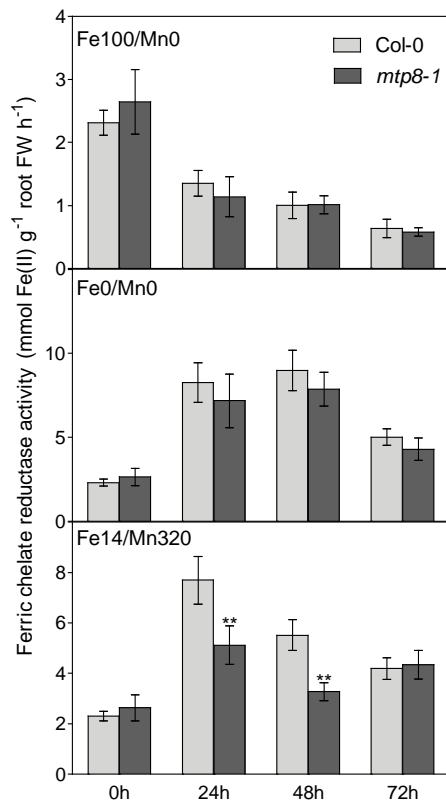


Figure 19. Ferric chelate reduction capacity of the *mtp8-1* mutant under Fe deficiency in the presence of Mn

Seedlings were grown for 11 days on Fe14/Mn0 medium and transferred to Fe100/Mn0, Fe0/Mn0, or Fe14/Mn320 media. A, phenotype of Col-0 and *mtp8-1* mutant plants on Fe14/Mn320 medium. B, temporal development of ferric chelate reduction capacity under varied Fe/Mn regimes. Three plants for each treatment and genotype were pooled, and the roots were dipped into the ferric chelate reductase assay solution in a 12 well plate (n=4). The data point 0 h corresponds to seedlings harvested just before the transfer. The experiment was conducted twice with comparable results. An asterisk above a bar indicates that the corresponding mean of the mutant line is significantly different from the mean of the Col-0 line according to Student's t-test (*, P<0.05; **, P<0.01). Error bars represent \pm SD.

The Fe deficiency-induced ferric chelate reductase has a low pH optimum (Susin et al., 1996). In order to confirm that the diminished ferric chelate reduction capacity of the *mtp8-1* mutant is not a consequence of a decreased rhizosphere acidification, rhizosphere acidification capacity of the *mtp8-1* mutant was assessed. Plants that were treated in the same way as in the ferric chelate reductase assay were transferred to an agar medium that contained bromocresol purple as pH indicator. The only roots that produced a marked yellow coloration of the agar, i.e. an acidified rhizosphere, were those of *mtp8-1* seedlings grown on Fe14/Mn320 (Figure 20). A yellowing of the external medium was observed already after 48 h of treatment (not shown) and was even more pronounced with 72 h-treated *mtp8-1* mutant seedlings. This observation confirmed that rhizosphere acidification was not limiting ferric chelate reductase activity in *mtp8-1*, but was instead even increased, reflecting the aggravated Fe deficiency of the mutant.

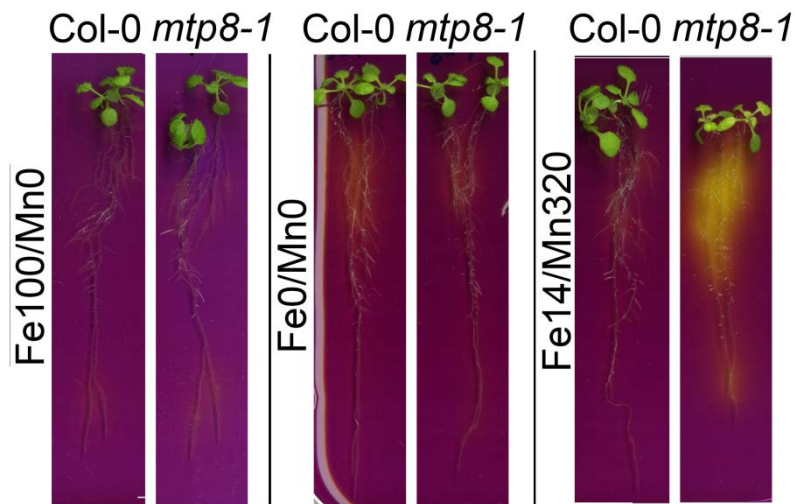


Figure 20. Rhizosphere acidification by *mtp8-1* roots under Fe deficiency in the presence of Mn.

Seedlings were grown for 11 days on Fe14/Mn0 medium and transferred to Fe100/Mn0, Fe0/Mn0, or Fe14/Mn320 media and further cultivated for 72 h. The plants were subsequently transferred to nutrient-free agar plates containing bromocresol purple, and incubated for 24 h. Yellow color around the roots indicates acidification.

4.3. A function of MTP8 in Mn localization in developing Arabidopsis embryos

Kim et al. (2006) showed that in Arabidopsis wild-type embryos Fe localizes to the vacuoles of the cells surrounding provascular strands, but colocalizes with Mn in subepidermal layers of the abaxial side of cotyledons in a *vit1* mutant. Since MTP8 is suggested to be a Fe/Mn vacuolar influxer (Figure 9, Figure 10), it was hypothesized that MTP8 is the transporter responsible for the specific Mn localization in the cotyledons of wild-type embryos as well as for Fe localization in *vit1*. This hypothesis raised three expectations about this protein: (i) *MTP8* is expressed during embryo development; (ii) in *mtp8* loss-of-function mutants Mn and (iii) in *mtp8 vit1* double knockout lines Fe may not predominantly localize anymore to the abaxial side of the cotyledons.

4.3.1. *In silico* analysis of *MTP8* and *VIT1* expression during embryo development

An *in silico* analysis of the expression profiles of *MTP8* and *VIT1* by using the efp browser indicated that both genes are expressed during seed development (Le et al., 2010; Schmid et al., 2005) (Figure 21). Based on Schmid et al. (Figure 21A, top), *MTP8* expression is upregulated during late developmental stages and peaks at maturation. For comparison, *VIT1* expression is upregulated earlier than *MTP8* but downregulated during later stages of development. This study was conducted on mRNA extracted from whole seeds. Another independent study, which was conducted on mRNA derived directly from embryo, claimed that not only *MTP8*, but also *VIT1* was upregulated during later stages (Figure 21A, bottom).

Therefore, at later stages, although there is a consensus on the upregulation of *MTP8*, there are contradictory data regarding the regulation of *VIT1*.

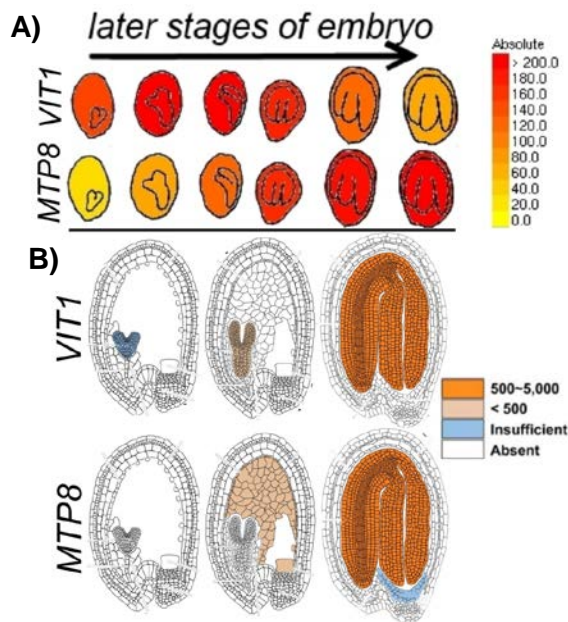


Figure 21. Developmental expression profile of *MTP8* and *VIT1* in Arabidopsis seeds based on microarray analysis.

Relative expression of *MTP8* and *VIT1* during seed development. A, *MTP8* and *VIT1* expression are presented relative to At3g27340 at signal threshold 200 (Schmid et al., 2005). B, relative expression of *MTP8* and *VIT1* during seed development in different layers of the seed (Le et al., 2010). Data obtained from efp browser, www.arabidopsis.org.

4.3.2. *MTP8* and *VIT1* promoter activity during seed development

In order to track promoter activity of *MTP8* during embryo development *promoterMTP8::GUS* lines were analyzed. *PromoterVIT1::GUS* lines were used as a reference, since *VIT1* was also active in embryo development and responsible for Fe localization to the provascular strands of the embryo (Kim et al., 2006). *GUS* activity of *promoterVIT1::GUS* lines started as soon as provascular tissues appeared in the heart stage and further increased at later stages, which is in accordance with the transcriptome study of Lee et al. (2010). Promoter activity of *MTP8* started at later stages of embryo development, i.e. the maturation and post-maturation stage. This observation was in close agreement with the *in silico* data (Figure 22A) (Le et al., 2010; Schmid et al., 2005). Cross and longitudinal sections of the mature embryo of *promoterMTP8::GUS* lines exhibited *GUS* staining in particular in the outer cell layers of the embryo on the adaxial and abaxial sides of the cotyledons, but clearly excluding the root apex, the hypocotyl apex as well as the cotyledon tips (Figure 22B and C).

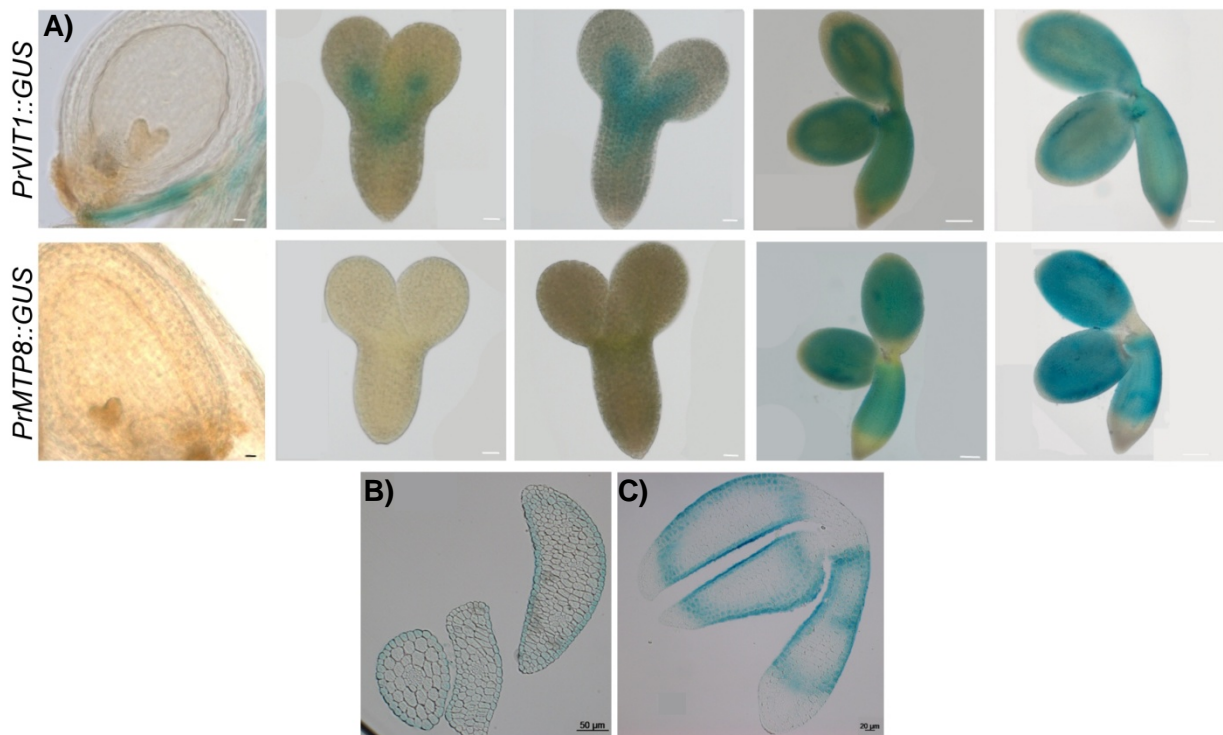


Figure 22. *MTP8* promoter activity during different stages of embryo development.

A, visualization of GUS staining in *promoterVIT1::GUS* and *promoterMTP8::GUS* lines at different stages of embryo development. (left to right) heart, torpedo, walking stick, mature, and post-mature embryo. Bar corresponds to 20 µm for heart, torpedo, walking stick stages, and to 100 µm for the mature green, post-mature stages. Embryos in heart, torpedo and walking stick stages were incubated overnight; mature green and postmature stages were incubated for 2 h in GUS solution. B, C cross and longitudinal sections of GUS-stained postmature embryos of *promoterMTP8::GUS* line.

4.3.3. Metal localization in *mtp8* mutant seeds by synchrotron X-ray fluorescence

To verify the metal localization reported by Kim et al. (2006) and to investigate the impact of *MTP8* on Fe and Mn localization in embryos, wild-type and *mtp8* mutant seeds were analyzed by X-ray synchrotron fluorescence in collaboration with Prof. Michiko Takahashi, (Utsunomiya University, Japan), using the Spring8 facility in Hyogo (Figure 23). In wild-type seeds, Cu was predominantly localized in the seed coat rather than in the embryo, whereas Ni localized more to the embryo than to the seed coat. Both of these metals were homogeneously distributed in the seed coat and the embryo. Zinc was not found in the seed coat but showed a rather homogeneous distribution in the embryo with enrichment in three tissues of the embryo: the adaxial side of the cotyledons, the provascular strand and the subepidermal cell layer of the hypocotyl. Like Zn, Fe was also enriched in the provascular tissue of the hypocotyl but in addition also restricted to the three provascular strands of the cotyledons. As the background of Fe-dependent X-ray signals in the remaining tissue was very low, the localization of Fe was highly confined. Most of the Mn was found in the embryo. The localization of Mn in the embryo was highly specific and confined to the abaxial sides of the subepidermis of the cotyledons as well as to the subepidermis of the hypocotyl. These observations were in close agreement with the X-ray analysis of wild-type seedlings as reported by Kim et al. (2006).

Analyzing the metal distribution in *mtp8* seeds showed that with the exception of Mn all other metals followed the same localization pattern as in wild-type seeds. Most interestingly, Mn lost its localization to the subepidermal layers of the cotyledons in *mtp8*, but now colocalized with Fe in the prevascular tissue. This observation indicated that Mn localization to the abaxial sides of the cotyledons in wild-type seeds is determined by MTP8. Furthermore, the result also indicated that, in *vit1*, the specific Fe localization which was overlapping with Mn (Kim et al., 2006) is most probably determined by MTP8.

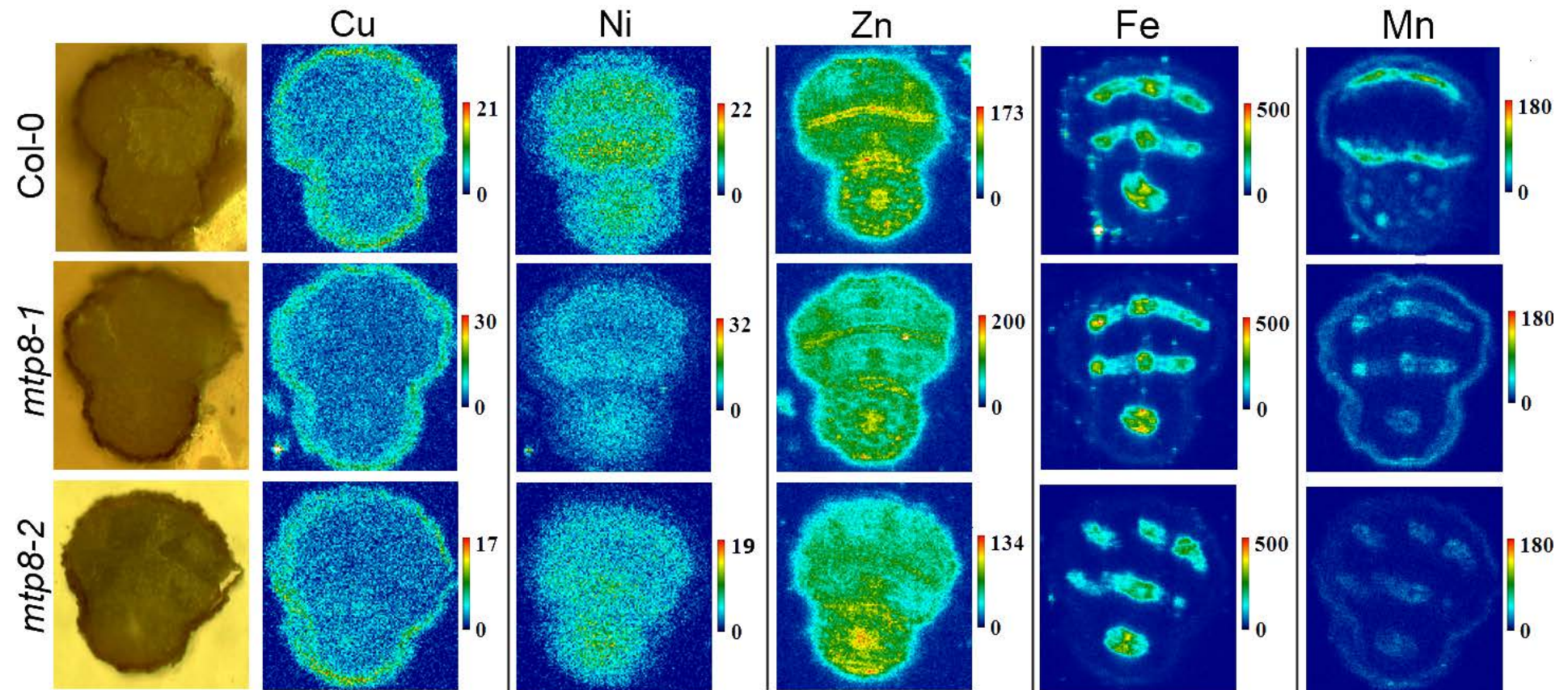


Figure 23. Synchrotron μ XRF analysis of wildtype, *mtp8-1*, and *mtp8-2* mutant seeds for metal localization. (Experiment: Michiko Takahashi, Yasuko Terada)

Dry seeds were imbibed in water for three hours and metal localization was analyzed. Seeds were propagated under the same conditions. At least three different seeds from each line were analyzed.

One of the most important functions of Mn in green plant tissues is in the water-splitting complex of photosystem II (Yi et al., 2005) and deficiency of the metal causes interveinal chlorosis (Marschner, 2012). As Mn was mislocalized in *mtp8* seeds, it was hypothesized that chlorophyll synthesis or photosynthetic efficiency may be compromised in germinating *mtp8* seedlings. Therefore, *mtp8* seeds were germinated under several different conditions including $\frac{1}{2}$ MS, $\frac{1}{2}$ MS without Mn or on wetted filter paper devoid of any nutrients. However, seeds of the *mtp8* mutants germinated without an apparent phenotype. Mutant seedlings developed similar to those of the wild type and no visible symptoms could be detected (Figure 24).

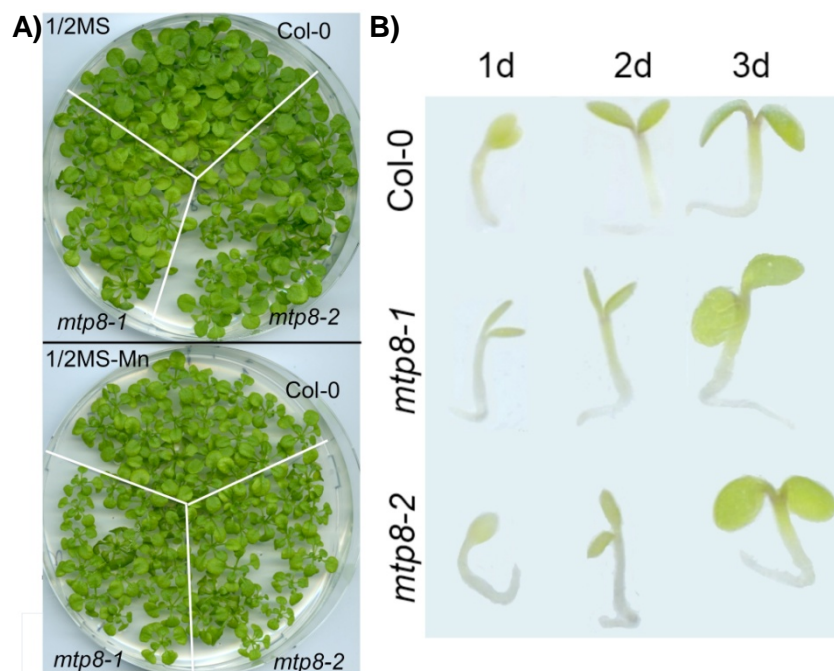


Figure 24. Phenotype of *mtp8-1* and *mtp8-2* mutants after germination with varying Mn supply.

Seedlings were germinated; A, on $\frac{1}{2}$ MS with (top) or without (bottom) addition of Mn and cultivated for three weeks, or B, on filter paper moistened with distilled water and cultivated for 1-3 days before photographs were taken.

4.3.4. Phenotypic analysis of a *mtp8 vit1* double knock-out line

In order to confirm the role of MTP8 in Fe distribution in *vit1* seeds, a *mtp8-1 vit1-2* double knock-out line was generated. Embryos were isolated from wild-type and mutant seeds and stained with Perls/DAB. The distribution of stainable Fe is shown in Figure 25A. In Col-0, *mtp8-1* and *mtp8-2*, Fe was clearly distributed throughout the veins, indicating that MTP8 has no influence on the preferential loading of Fe into endodermal vacuoles of the prevascular strands. In both *vit1-1* and *vit1-2*, stainable Fe was localized on the abaxial side of the cotyledons, which is consistent with the observations made by Roschztardt et al. (2009). However, in *mtp8-1 vit1-2* embryos, Fe staining was weaker and Fe was not predominantly localized to any

tissue or cell type, but instead homogenously distributed throughout the embryo (Figure 25A and Figure 25B). Since Fe localization to the abaxial side of the cotyledons in *vit1* single mutants was disrupted in *mtp8 vit1*, it is concluded that MTP8 is responsible for the preferential Fe enrichment on the abaxial side of the cotyledons in *vit1*.

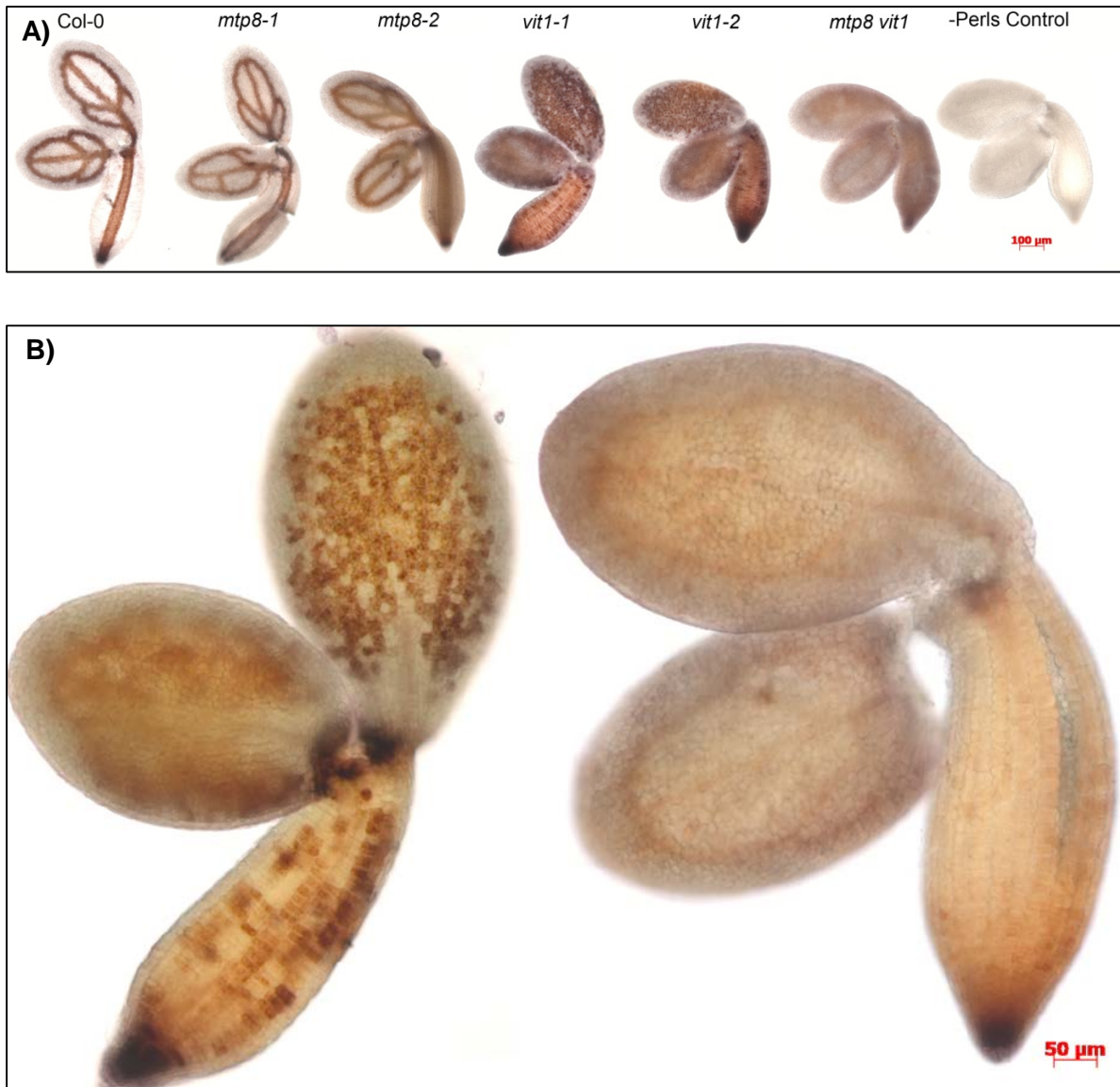


Figure 25. Fe distribution in post-mature embryos of wild-type, *mtp8* and *vit1* single and double mutant lines

A, post-mature embryos were stained with Perls/DAB. Mature seeds were incubated for 12 h in distilled water and embryos were isolated, stained and observed under a light microscope. B, Perls/DAB staining of embryos isolated from desiccating seeds of *vit1-2* (left) and *mtp8-1 vit1-2* (right).

Since i) both of the MTP8 and the VIT1 genes are expressed during embryo development, ii) both proteins encoded by those genes are involved in Fe and Mn homeostasis, and iii) the embryo makes photosynthesis which requires Fe and Mn, developing embryos of the *mtp8*

vit1 double mutant were isolated under the microscope to analyze a possible disruption in chlorophyll abundance and distribution (Figure 24). There was no visible difference in the chlorophyll distribution in developing embryos of the *mtp8 vit1* mutant when compared to those of the wild type. All embryos showed a similar chlorophyll-dependent green color. Early embryos (first three pictures from the left in Figure 26) exhibited chlorophyll all over but the color intensity was higher in a line at the apex of the hypocotyls (shown by red arrow). The intensity of chlorophyll was highest in mature embryos, and the distribution was homogeneous, except for the provascular strands and the basal root meristem, which had a lower intensity of the green color.



Figure 26. Chlorophyll distribution in embryos of wild type and *mtp8 vit1* double knock-out seeds

Developing embryos were isolated from wild-type and *mtp8 vit1* double mutant seeds at the following stages (from left to right): heart, torpedo, walking stick, green cotyledon, mature green. Embryos were observed under a light microscope. Red arrows show the darker green region at the apex of cotyledons.

In order to investigate if mislocalization of Fe or Mn caused a hypersensitivity to Fe or Mn deficiency, several chlorophyll fluorescence parameters including photosynthetic quantum yield, the apparent electron transport rate (ETR) and the ratio of variable fluorescence to maximal fluorescence (F_v/F_m) were determined for the *mtp8 vit1* line and the wild type cultivated under Fe and Mn deficiency (Figure 27). A significant difference was not found for any of these parameters.

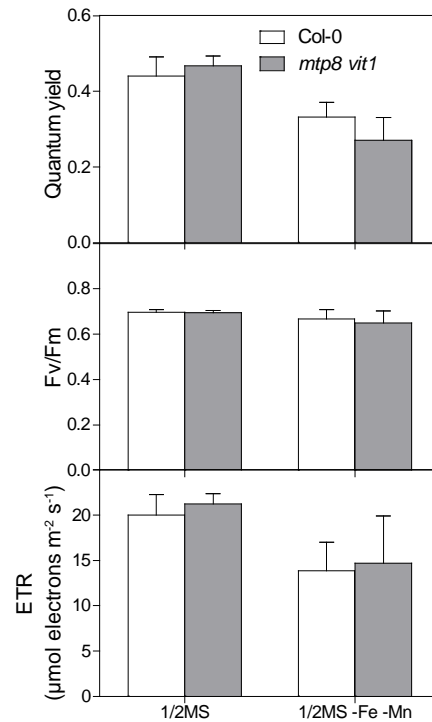


Figure 27. Photosynthetic parameters in germinating wild type and *mtp8 vit1* mutant seedlings.

Seeds were germinated without stratification on either ½ MS or ½ MS excluding Mn and Fe and cultivated for 5 days. The medium was solidified with 0.8% agarose and not supplemented with sucrose. Seedlings were dark-adapted for 2 hours before the measurements. Three independently propagated seed sets were used and comparable results were obtained. Bars represent means ± SD. Quantum yield, photosynthetic quantum yield; ETR, apparent electron transport rate; Fv/Fm ratio of variable fluorescence to maximum fluorescence.

The *vit1-1* mutant has been reported to grow poorly on calcareous soil (Kim et al., 2006). In order to validate this observation and to check for other growth phenotypes, *vit1* and *mtp8* single and double mutant lines were germinated and grown for 18 days on a calcareous substrate. However, no difference in growth could be observed (Figure 28). In an alternative approach, seeds from the same lines were germinated on Fe0/Mn0 medium and root fluorescence under UV was observed as a measure for the synthesis of coumarins. Again, no difference in the intensity of the fluorescence was apparent among the lines (Figure 28).

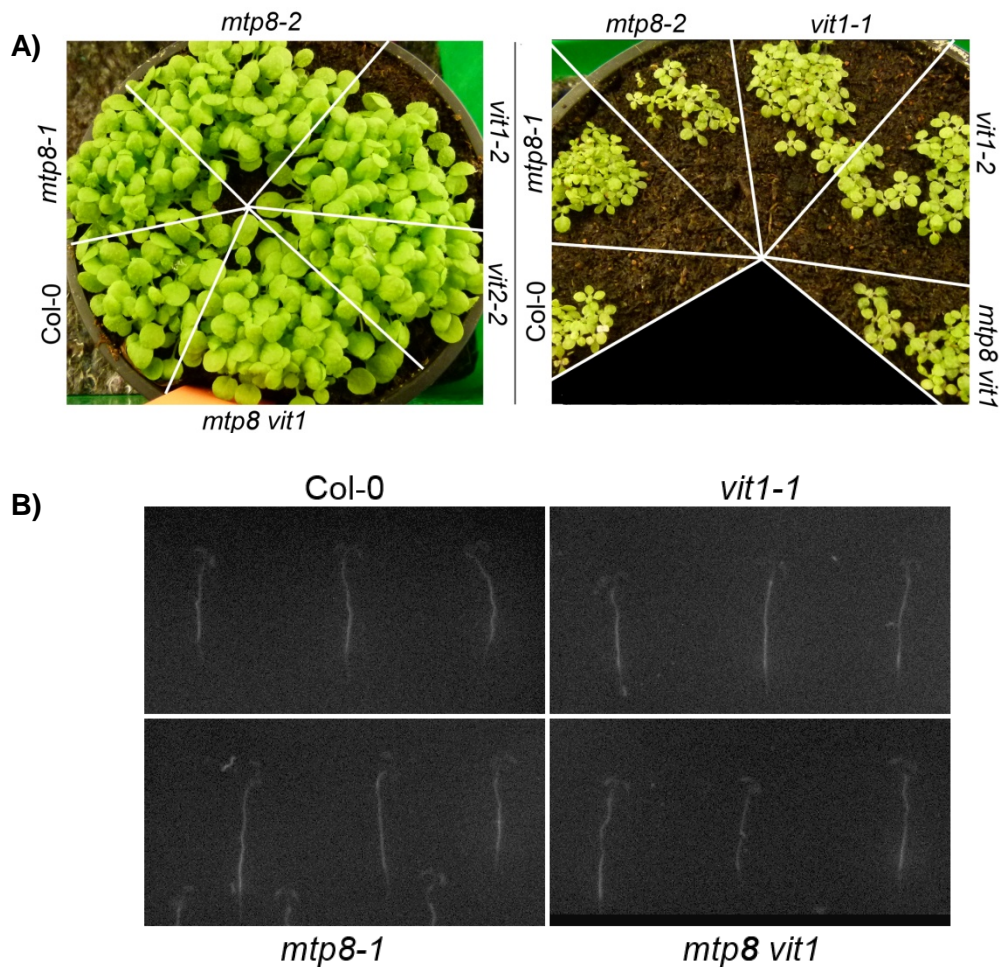


Figure 28. Phenotype of Col-0, *mtp8*, *vit1* and *mtp8 vit1* mutant lines when grown on low Fe availability.

A, phenotype of Col-0, *mtp8*, *vit1* and *mtp8 vit1* lines on a peat-based potting substrate without (left) or with (right) supplementation of 20 g CaCO₃ and 16g NaHCO₃ per kg of substrate. Seedlings were watered with dH₂O and cultivated for 18 days in the greenhouse. B, Fe-deficiency dependent, coumarin-based root fluorescence of seedlings which were grown for 6 days on Fe₀/Mn₀ medium.

4.3.5. Metal concentrations in rosette leaves and seeds of soil-grown plants

Since both, MTP8 and VIT1 have roles in Fe and Mn homeostasis in plants during their vegetative phase and/or during embryo development, elemental concentrations of leaves and seeds were determined in mutants. First, old leaves from the rosette of bolting plants were collected, dried, and Fe, Zn and Mn concentrations were assessed (Figure 29). ICP-OES results showed that in rosette leaves Fe and Zn concentrations were not significantly different between wild type and mutants, whereas Mn concentrations were approximately 3 to 5 times higher in the absence of MTP8. This observation was in agreement with the function of MTP8 in storing Mn in root vacuoles (Figure 15).

Seeds obtained from plants of the same culture were then analyzed for their metal concentrations. While the Zn concentration in seeds of all plants was similar, Fe concentrations were found to be approximately 25% higher in *mtp8* mutants. Likewise, seed Mn

concentrations were higher in *mtp8* single and *mtp8 vit1* double mutant lines. These observations suggested that MTP8 suppresses Fe and Mn accumulation in seeds.

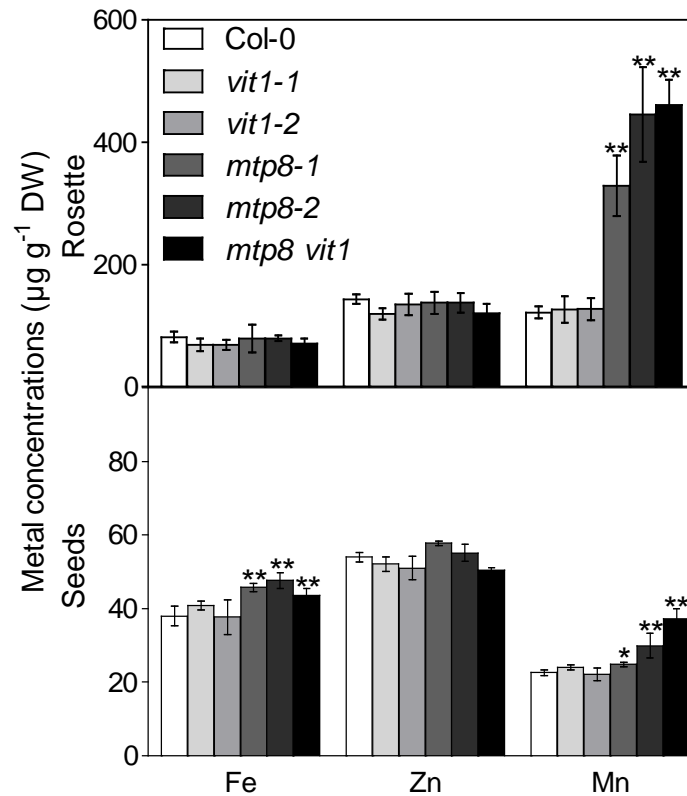


Figure 29. Concentrations of Fe, Zn and Mn in rosette leaves and seeds of Arabidopsis wild-type and *mtp8* and *vit1* single and double mutant lines.

Plants were cultivated in the greenhouse. At bolting the four oldest rosette leaves were excised and subjected to elemental analysis. Another set of plants continued to grow to maturity. Seeds were harvested and prepared for elemental analysis. Bars represent means \pm SD. Asterisks denote significant differences (*, $P < 0.05$; **, $P < 0.01$) of the respective mutant line to Col-0 according to Student's t-test ($n=4$).

5. Discussion

5.1. Screening Arabidopsis mutant lines on high-pH, low-Fe agar medium as a novel approach to isolate genes involved in Fe homeostasis

The most common practice to induce nutrient deficiencies in plant cultures is to decrease the concentration of the nutrient in the medium to the level that it cannot meet the nutrient demand of the plant. While the plant demand for macronutrients like P, K or Ca is high, it is low in the case of micronutrients, such as Fe, Mn, Zn or Cu. When the demand is low, even trace contaminations of a particular nutrient in the medium can be enough to avoid or revert the deficiency. In particular nutrients contained in commercial agar media have been found to be a major source of contamination and sometimes sufficient to meet the demand of the plant (Gruber et al., 2013). In the particular case of Fe, it became a common practice to aim for a completely Fe-free medium, which is prepared without adding any Fe compounds and supplementation of ferrozine, a strong chelator of Fe²⁺, making Fe unavailable to plants (Giehl et al., 2012; Séguéla et al., 2008).

Aiming at establishing screening conditions that allow the isolation of Arabidopsis genes involved in overcoming Fe deficiency-induced chlorosis, a medium was developed in which the availability of Fe was decreased by elevating medium pH. Growing wild-type plants on this medium induced Fe deficiency-dependent chlorosis in Arabidopsis seedlings (Figure 2), indicating that Fe derived from other sources like agar or impure chemicals was negligible. Fe deficiency-induced chlorosis could be easily reverted by increasing the supplementation of Fe(III)-EDTA, indicating that Fe, and not other pH-sensitive metal micronutrients, were causing the chlorotic phenotype. The newly developed medium allowed to fine-tune the extent of Fe deficiency-induced chlorosis by adjusting the concentration of added Fe(III)-EDTA and mimicked more adequately the Fe limitation found in alkaline soils where Fe is abundant, but sparingly available to plants. Therefore, this medium appeared advantageous over the commonly-used media in inducing Fe deficiency.

Parameters of the high-pH, low-Fe medium, which were shown in Figure 1, were adjusted to achieve a long-term Fe deficiency-dependent chlorosis in germinating Arabidopsis seedlings. Sowing density had a big impact on the development of Fe deficiency-induced chlorosis and necrosis (Figure 1C). Better growth of closely sown plants was attributed to an improved acquisition of Fe. Most likely, Fe availability at high sowing density was increased because closely located seedlings had larger regions in which the proton secretion of the roots could overlap and thus overcome the high pH-dependent low Fe availability. This may have led to a higher Fe acquisition, and consequently to a regreening and a higher biomass production of the plants. Light intensity during the screening procedure was also found to be a critical issue (Figure 1). Higher light intensities resulted in exacerbated Fe deficiency, which was reflected in higher coumarin-based fluorescence emission by the roots and in leaf necrosis. One possible explanation for the lower availability of Fe to the plant upon high light could be that an increase in light intensity caused an increase in EDTA oxidation in the growth medium, which resulted in unchelated, precipitated, and thus unavailable Fe for the plants (Hangarter and Stasinopoulos, 1991).

For the present approach, it was hypothesized that a plant carrying a T-DNA insertion in a gene which is essential for the Fe deficiency response would show a more severe Fe deficiency-dependent chlorosis compared to the wild type. The medium used in the screening was supplied with 28 μM Fe and 40 μM Mn (Fe28/Mn40 medium) and induced a mild chlorosis in wild-type plants, starting soon after germination and remaining present for more than two weeks (Figure 2). However, Fe deficiency-dependent chlorosis on Fe28/Mn40 medium disappeared completely after three weeks. Most likely, the medium pH was lowered by the continuous secretion of protons, allowing the roots to take up Fe more efficiently. The suitability of the Fe28/Mn40 medium for the screening of Fe deficiency-susceptible mutants was further validated by the extensive chlorotic or necrotic phenotype of the already characterized Fe deficiency-susceptible mutants *fro2*, *irt1*, *frd3* and *pye* (Figure 3).

Mutant lines can be differentiated as gain-of-function or loss-of-function mutants (Ichikawa et al., 2006). Gain-of-function mutants are lines that perform better than the wild type under a certain stress due to the mutation they carry. It was initially aimed to screen gain-of-function mutants in order to obtain plants that show chlorosis-free growth on Fe28/Mn40. For this purpose, the recently developed FOX seed collection was used, in which each line expresses ectopically one to two independent Arabidopsis full-length cDNAs (Ichikawa et al., 2006). However, this seed material resulted in the selection of too many false positives (Figure 4). The inhomogeneous growth of many of the FOX lines in the seed pool could have been due to differences in the seed age or other factors which caused high variability on seed performance. Therefore, an alternative and more consistent pool of mutant lines had to be sourced and was found in homozygous T-DNA insertion lines that are publicly accessible. To decrease the number of lines to be screened, lines were preselected according to the upregulation of the mutated gene in Fe-deficient wild-type plants (Figure 5). In contrast to the FOX lines, the variability of the chlorotic phenotype on Fe28/Mn40 was found to be much lower in the T-DNA insertion lines.

In a first screening round, the line SALK_019569C showed a repression of primary root growth on Fe28/Mn40 medium (Figure 6). However, newly propagated seeds from this line did not show such a phenotype when the growth experiment was repeated. This suggested that seed storage or seed propagation conditions may have been responsible for some of the false positives that were identified in the first round. Propagating all lines under the same conditions and using the newly propagated seeds in the screening procedure would have been ideal to reduce the number of false positives. However, due to time restrictions seeds directly obtained from the seed stock centers had to be used.

5.2. The vacuolar manganese transporter MTP8 determines tolerance to Fe deficiency-induced chlorosis in Arabidopsis

For a century it has been known that Fe nutrition in plants is antagonistically affected by Mn. In numerous classical studies, increased Mn availability induced Fe deficiency symptoms, irrespective of whether plants were grown in the field or on standard growth media (Gile, 1916; Hewitt, 1948; Sideris and Young, 1949; Somers and Shive, 1942; Twyman, 1951). Similar to Zn and Ni, which have been very occasionally reported to induce Fe deficiency when supplied in excess (Ghasemi et al., 2009; Hamlin and Barker, 2008), the negative interaction between Fe and Mn has been explained by their similar solubility characteristics in soil and by competition for uptake (Marschner, 2012). This was supported at the molecular level when

IRT1 was found to permeate also Mn, Zn, Ni, and Cd besides Fe (Korshunova et al., 1999; Vert et al., 2002). Searching for Arabidopsis genes involved in Fe acquisition, MTP8 was identified as a critical determinant of Fe deficiency tolerance whenever Mn is present. Unexpectedly, the physiological implications of MTP8 go far beyond the sequestration of Mn into the vacuole of root cells to detoxify cytosolic Mn because the regulation of MTP8 is not primarily linked with excess Mn supply, but rather with the induction of the Fe acquisition machinery under low Fe availability, i.e. high pH conditions. The data presented in this thesis indicate that Mn inhibits in particular the ferric chelate reductase activity in the absence of MTP8, making this transporter essential for Fe chlorosis tolerance whenever Mn is available during Fe acquisition.

5.2.1. MTP8 localizes to the tonoplast and transports Mn and Fe into the vacuole

Arabidopsis MTP8 belongs to the CDF family of metal transporters. This family has 12 members in Arabidopsis, of which only a few have been characterized so far (Gustin et al., 2011; Montanini et al., 2007; Ricachenevsky et al., 2013). An ortholog from a Mn-accumulating legume, *Stylosanthes hamata*, ShMTP8 (renamed from ShMTP1 for consistency; Montanini et al., 2007), is the founding member of the Mn subgroup in the CDF family (Delhaize et al., 2003) and contains an amino acid signature that coincides with Mn specificity (Montanini et al., 2007). Yeast complementation assays provided experimental evidence that also Arabidopsis MTP8 has a transport activity for Mn (Figure 10). Like ShMTP8, the Arabidopsis MTP8-EYFP fusion protein resided at the tonoplast (Figure 9). In accord with a function of Arabidopsis MTP8 in Mn detoxification, growth of *mtp8* mutants was impaired by high Mn (Figure 12), and *MTP8* expression was increased under excess Mn supply (Figure 12). Mn specificity and vacuolar localization were recently also demonstrated for MTP8 orthologs in cucumber (Migocka et al., 2014) and rice (Chen et al., 2013). The function of MTP8 to sequester Mn into vacuoles is therefore widely conserved across species, with the possible exception of barley, where MTP8 homologs have been localized to the Golgi apparatus (Pedas et al., 2014). However, the circumstances under which this function is employed may differ. Interestingly, unlike the Arabidopsis and cucumber orthologs, *OsMTP8.1* from rice is expressed almost exclusively in the shoot, so that shoots of an *osmtp8.1* mutant contained less Mn (Chen et al., 2013). Both findings are opposite to what is observed with Arabidopsis in the present study (Figure 13, Figure 15). The different functionality of MTP8 in the graminaceous species rice, as compared to the dicots Arabidopsis and cucumber, may be related to their Fe acquisition strategies or to the higher Mn availability in their agro-ecological environment. In lowland rice, reducing soil conditions often lead to a concomitant excess of Mn^{2+} and Fe^{2+} (Marschner, 2012), i.e. a situation where elevated Mn translocation to the shoot goes along elevated Fe availability and uptake. The additional expression of *OsMTP8.1* in leaves may then increase the whole-plant capacity of rice to compartmentalize Mn in vacuoles.

Ectopic overexpression of the *MTP8* gene under control of a 35S promoter led to an increase in the Mn concentration of the root when plants were grown on ½ MS or Fe28/Mn40 (Figure 11), further indicating a function for MTP8 in loading Mn into the vacuole. However, Fe concentration of the roots was not increased although MTP8 is capable to transport Fe (Figure 10, Figure 25). The reason for this could be due to veiling of excess precipitated Fe in the root apoplast. In plant roots, the apoplast contains a large pool of precipitated Fe (Kosegarten and Koyro, 2001; Mengel, 1994). Thus, even though the root symplast of 35S::*MTP8* lines might

have accumulated more Fe compared to that of the wild type, it can have a negligible impact on the total Fe concentration in the root.

Besides the evidence from the yeast complementation assay where MTP8 complemented a Fe-hypersensitive yeast mutant (Figure 10), convincing evidence suggesting Fe transport by MTP8 *in planta* came from the observation that Fe localization in the abaxial side of the cotyledons in the seeds was dependent on MTP8 in the *vit1* mutant background (Figure 25). Since MTP8 belongs to the Mn-CDFs, which have been predicted to transport specifically Mn but not Fe (Migeon et al., 2010; Montanini et al., 2007), it appears that MTP8 is the first member of Mn-CDFs capable of transporting Fe besides Mn.

In general, knock-out mutations do not necessarily result in phenotypes because other proteins may take over the same physiological function. It is noteworthy that Mn accumulation in the root sharply decreased in the Fe-deficient *mtp8-1* mutant line (Figure 15), indicating that other vacuolar Mn transporters in the root cells did not take over the function of MTP8 in sequestering Fe-accompanying Mn to the vacuole. These data indicate that, besides MTP8, which is indeed indirectly regulated by excess Mn (Figure 16), other tonoplast Mn transporters in the root are not highly responsive to Mn toxicity. Accordingly, other genes encoding for Mn transporters, like CAX2, CAX4, CAX5 and CCX3 have been reported to respond poorly to Mn toxicity, and knock-out lines of these genes do not exhibit striking Mn-related phenotypes (Cheng et al., 2002; Edmond et al., 2009; Hirschi et al., 2000; Mei et al., 2009; Morris et al., 2008).

Besides MTP8, MTP11 has been shown to be a major factor for tolerance of Arabidopsis to high Mn concentrations (Peiter et al., 2007). Unlike MTP8, MTP11 is present in a compartment that co-localizes with markers for the PVC (Delhaize et al., 2007) and the Golgi apparatus (Peiter et al., 2007). Based on mutant analyses and expression patterns, the MTP11 protein has been hypothesized to contribute to Mn secretion, rather than to intracellular compartmentalization (Peiter et al., 2007). On high Mn media, *mtp11* mutants were much more impaired in growth than *mtp8* mutants (compare Figure 14 and Peiter et al., 2007), which indicates that, at least in Arabidopsis, MTP8 makes only a minor contribution to Mn tolerance under non-limiting Fe conditions. Also, the expression patterns of *MTP8* and *MTP11* are very different: Whereas *MTP8* is highly expressed only in Fe-deficient roots except for the root tip, *MTP11* expression is most pronounced in the apical area of the root and also in hydathodes of leaves, which all contain cells that lack large vacuoles. This indicates that MTP8 and MTP11 have different, non-redundant and most likely complementary functions, and that MTP8 is employed to sequester Mn specifically in those cells that are involved in IRT1-mediated Fe uptake and thus face localized Mn influx.

5.2.2. MTP8 is part of the Fe acquisition machinery in Arabidopsis

In Fe-replete conditions, Arabidopsis *MTP8* was expressed at very low levels, while Fe depletion strongly induced its mRNA levels (Figure 16). This regulation is mediated by the major transcription factor of Fe acquisition mechanisms in Arabidopsis roots, FIT. Accordingly, *MTP8* expression was strongly enhanced during Fe deficiency in a FIT-dependent manner. This indicated that MTP8 is specifically recruited to detoxify Mn whenever Mn is taken up by IRT1 in superfluous amounts. This function was manifested by determining Mn concentrations in Fe-deficient plants, which were far higher in roots of the wild type than in roots of the mutant (Figure 15).

From the perspective of the low substrate selectivity of IRT1, it is not surprising how much the detoxification mechanisms for IRT1-permeated heavy metals resemble each other. During IRT1-dependent metal uptake, vacuolar loading of excess Zn, Co and Ni is mediated by MTP3 and IREG2 (Arrivault et al., 2006; Schaaf et al., 2006). However, while vacuolarization of Fe-accompanying heavy metals has been seen primarily as a means for detoxification, it was shown now for Mn that sequestration of the heavy metal is essential for the tolerance of a plant to Fe deficiency.

MTP8 is also induced by high Mn availability on standard growth media (Figure 12). Although the most straightforward explanation for this may be a Mn-specific regulation of the gene, it was found that the induction of *MTP8* is under complete control of the FIT transcription factor, which was confirmed by the loss of *MTP8* expression in Mn-exposed roots of a *fit* mutant (Figure 12). This indicated that not Mn, but rather the degree of Mn-induced Fe deficiency determines *MTP8* transcript levels. In summary, although MTP8 increases the tolerance of the plant to excess Mn, this is more an indirect consequence of the function of MTP8 to avoid Mn toxicity during Fe acquisition in Arabidopsis.

5.2.3. MTP8 prevents Mn from inhibiting Fe(III) reduction under Fe deficiency

The *mtp8* mutants displayed two distinct phenotypes. First, primary root elongation was reduced on high Mn media (Figure 12), which is indicative of Mn toxicity (Peiter et al., 2007). Second, *mtp8* mutants displayed severe chlorosis on Mn-containing media with low Fe availability (Figure 7); the latter occurred even before Mn-triggered root growth inhibition set in (Figure 14). This chlorosis went along with strongly decreased shoot Fe concentrations, confirming that these plants suffered from Fe deficiency-induced chlorosis (Figure 15). These observations raised the questions how Mn interferes with Fe nutrition and what role MTP8 plays to counteract the antagonistic Fe/Mn interaction.

One possible explanation for the diminished Fe concentration in *mtp8* shoots may lie in a direct competition of Fe and Mn for xylem loading. Once acquired by the outer root cells, Fe and Mn are translocated radially to the stele to be unloaded into the xylem. In the absence of intracellular Mn compartmentalization by MTP8, high Mn uptake from the medium via IRT1 will inevitably increase cytosolic Mn concentrations, which may competitively inhibit Fe export to the xylem, in particular if transport proteins of low specificity are involved. A restriction of Fe unloading into the xylem would likely result in an accumulation of Fe in roots, as seen in the *man1/frd3* mutant, which is defective in xylem loading of the Fe(III) chelator citrate (Delhaize, 1996; Durrett et al., 2007). However, an accumulation of Fe in *mtp8* roots was never observed (Figure 15).

Alternatively, the transcriptional response to Fe deficiency may be suppressed by Mn, which would then affect the activation of genes involved in Fe mobilization and uptake. This hypothesis was tested, but rather the opposite was found. A number of key transcriptional regulators and Fe acquisition genes were upregulated when Mn was included in low Fe medium, and this induction was even more pronounced in the *mtp8* mutant (Figure 16). Thus, the Fe acquisition machinery was upregulated in the *mtp8* mutant even to a higher level than in wild type roots, but it was obviously less efficient in the presence of Mn.

Arabidopsis plants growing under Fe deficiency accumulate coumarins, which can be detected by their fluorescence emission under UV light. Under Fe deficiency in the absence of

Mn, *mtp8-1* seedlings exhibited fluorescence in the roots to a similar extent as the wild type. However, in the presence of Mn, although the mutants were Fe deficient, they exhibited less fluorescence emission under UV light in the rhizosphere compared to the wild type (Figure 18). Coumarins chelate Fe(III), hence supporting its solubilization and reduction, and are an essential part of the Fe deficiency response of plants grown on calcareous soil (Schmid et al., 2014). Coumarin synthesis is increased under Fe deficiency via the MYB72 and F6'H1 proteins, and loss-of-function mutants of these proteins grew chlorotic leaves when Fe supply was low. In high-pH, low-Fe medium, Fe was provided already in chelated form, i.e. as Fe(III)EDTA complex. Therefore, secreted coumarins were not expected to play a role in the Fe acquisition of plants grown on the present medium. This is in accordance with the result of the experiment, where *myb72-1* and *f6'h1-1* knock-out lines were cultivated. Although these mutants were inefficient to accumulate and secrete coumarins, they did not develop chlorotic leaves on Fe28/Mn40 (Figure 17). From these observations it was concluded that *mtp8-1* mutants failed to accumulate fluorescence-emitting coumarins, but this was not the reason why they were Fe-deficient on low-Fe, high-pH medium in the presence of Mn.

Although the transcript levels of *FRO2* were even higher in *mtp8* than in the wild type, the mutant was unable to realize full ferric chelate reduction capacity in the presence of Mn (Figure 19). A possible explanation could lie in the low pH optimum of the enzyme, which requires an acidification of the apoplast for maximum activity (Susin et al., 1996). However, proton release by Fe-deficient *mtp8* roots was not diminished. Instead, the acidification of the root medium was even more intense (Figure 20). Apoplastic pH was therefore not likely limiting *FRO2* activity. Alternatively, the posttranscriptional or posttranslational regulation of *FRO2* may be affected. Evidence for the existence of such a mechanism comes from experiments, in which overexpression of the gene did not lead to an increase in ferric chelate reductase activity under Fe sufficiency (Connolly et al., 2003).

In order to explain both, the inefficiency of ferric chelate reduction and the lack of fluorescence in the roots of *mtp8*, two different scenarios are proposed. The first scenario depends on posttranslational regulation of *FRO2* and *F6'H1*. *IRT1* is posttranslationally regulated (Barberon et al., 2011). Although *IRT1* performs uptake of Fe across the plasma membrane, it is mostly accumulated in the Golgi network. Localization of the *IRT1* protein to the plasma membrane is inhibited by the presence of Fe-accompanying heavy metals in the medium (Barberon et al., 2014). This is based on the observation that most of the *IRT1* protein localizes to the plasma membrane only if plants are grown on nutrient medium lacking Fe-accompanying heavy metals. Otherwise, when the same lines are grown on nutrient medium containing Fe-accompanying heavy metals, *IRT1* targeting to the plasma membrane of the epidermis cells is disturbed, resulting in a decreased uptake of Fe. Such a mechanism may exist for *FRO2* and *F6'H1*, too. Then, imported Mn which cannot be sequestered in the epidermal cells of *mtp8-1* under Fe deficiency, can lead to posttranslational modifications that inactivates *FRO2* and *F6'H1*, decreasing ferric chelate reduction and coumarin production. The second scenario depends on an increased redox potential in epidermal and cortical cells of *mtp8* due to the excess of Mn not sequestered into the vacuoles. Theoretically, a high redox potential leads to the oxidation of coumarins, disrupting their fluorescent nature. A high redox potential also decreases the efficiency of Fe(III) reduction reaction which is carried out by *FRO2*. What may be the source of such a hypothetical high redox potential? One possibility is that part of the absorbed Mn^{2+} , which could not be sequestered into the vacuole by *MTP8*, is precipitated to $Mn(IV)$, a strong oxidizing agent. This hypothesis is named glass makers' hypothesis, because ancient glass

makers were using oxidized Mn in order to precipitate Fe to make colorless glass (Janssens, 2013; Quartieri et al., 2002).

Taken together, the Arabidopsis MTP8 protein takes in a special position among the set of vacuolar transporters that are required to compensate for the low specificity of IRT1. By loading Mn into root vacuoles MTP8 prevents the inhibition of ferric chelate reduction by Mn and warrants chlorosis-free growth. MTP8 is thus a key player to prevent the antagonistic interaction of Mn on Fe nutrition in Arabidopsis. The operation of MTP8 is considered crucial for plant survival under any conditions where Mn is present and Fe uptake depends on the induction of Fe acquisition mechanisms.

5.3. MTP8 is responsible for the specific Fe and Mn localization in subepidermal cells of the Arabidopsis embryo

Seeds store metals as well as other nutrients required for germination. The localization of three of these metals, namely Fe, Mn and Zn, was visualized for the first time by Kim et al. (2006) using X-ray synchrotron analysis. According to this study, Zn localized rather homogeneously throughout the seed, whereas Fe localized to the cells surrounding the prevascular tissue (Roschztardt et al., 2009) and Mn to the abaxial side of the cotyledons. Furthermore, Fe localization was found to be determined by the tonoplast transporter VIT1, as the restriction of Fe to vascular strands was lost in the *vit1-1* mutant (Kim et al., 2006). Following a similar logic, Mn localization on the abaxial side of the cotyledons was supposed to be determined by a yet unknown tonoplast transporter too. Interestingly, in the absence of VIT1, Fe colocalized with Mn on the abaxial side of the cotyledons (Kim et al., 2006), indicating that the candidate transporter determining the Mn localization might also determine Fe localization in *vit1-1*, provided that the candidate transporter transports both Mn and Fe (Roschztardt et al., 2009). Since MTP8 was shown to transport both of these elements (Figure 10), and its promoter was active during embryo development (Figure 21), it became a promising candidate to determine Fe and Mn localization on the abaxial side of the cotyledons. Therefore, the localization of several metals in *mtp8-1* and *mtp8-2* mutants was analyzed by X-ray synchrotron fluorescence (Figure 23). Mn was indeed mislocalized in the mutants. In contrast to the wild type, the main Mn signals in the mutant embryos shifted from the subepidermal cell layer to the endodermal cell layer, colocalizing with Fe. This observation indicated that MTP8 was responsible for the specific Mn localization in the subepidermal cells.

In order to investigate the role of MTP8 in Fe localization on the abaxial side of the cotyledons in *vit1*; a *mtp8 vit1* double knock-out line was generated. Perls/DAB staining showed that Fe localization in the *mtp8 vit1* was no longer restricted to the abaxial side of the cotyledons, but Fe was now homogeneously distributed (Figure 25). This diffuse distribution of Fe was similar to the distribution of Zn in wild-type seeds (Figure 23), which may indicate that Fe localization in the embryo is now determined by other yet uncharacterized transporters.

Although Fe and Mn localization was altered in the embryos of *mtp8 vit1*, the mutant line was apparently healthy, since the chlorophyll patterns during embryo development were not changed (Figure 26). Moreover, the double mutant was not hypersensitive to Fe or Mn deficiency during germination (Figure 27, Figure 28). It has been previously reported that *vit1-1* poorly grows on calcareous soil (Kim et al., 2006). The data presented in this thesis failed to

confirm Kim et al., and suggested that the specific localization of Fe and Mn in the embryo is not critical for seed development and germination, at least in the tested conditions.

Seed Fe and Mn concentrations were higher in the *mtp8* single and double mutant lines (Figure 29) which could have been due to an increase in Fe and Mn re-translocation from the shoot to the seeds. It can be assumed that in the absence of MTP8 a part of these metals might be shifted from vacuoles to the cytosol, which would support a higher mobilization of Fe to the seeds. In addition, in the *mtp8* mutants, Mn concentrations in the shoots were found to be more than 2 fold compared to those of wild type shoots (Figure 29) which can then elevate Mn concentrations in the seeds of *mtp8* mutants by re-translocation.

Expression of *VIT1* and *MTP8* during seed development was assessed by taking advantage of *promoterGENE::GUS* lines. According to the GUS staining patterns, both of the promoters were active during seed development, and *VIT1* was clearly activated earlier than *MTP8* (Figure 22). *VIT1* promoter activity was observed as soon as the prevascular strands appeared, contrasting to the promoter activity of *MTP8*, which was not seen earlier than at the green cotyledon stage (Figure 21, Figure 22). Another interesting point came from the study of Otegui et al. (2002), who showed that loading of Fe to the embryo set in earlier than the loading of Mn. Since *VIT1* was mainly responsible for Fe and *MTP8* for Mn localization in the seed, and since *VIT1* was induced earlier, it is speculated that a differential timing in the upregulation of these genes may correlate with the differential loading of the respective metals to the embryo.

In conclusion, an alternative screening medium with limited Fe availability caused by an elevated pH led to the identification of MTP8 as an essential component of the Fe deficiency response in the presence of Mn. Characterization of *mtp8* mutant lines suggested that Mn interferes with the Fe deficiency response in mutant seedlings affecting both, coumarin-dependent fluorescence accumulation and ferric chelate reduction. Furthermore, analysis of *vit1* and *mtp8* single and double mutant seeds showed that the interplay of *VIT1* and *MTP8* determines the localization of Fe and Mn in the embryos. This finding opened many critical research questions to be answered in future including: i) Why does MTP8 not affect the localization of Fe reserves in wild-type seeds although it does so in *vit1*? Why does *VIT1* not affect the localization of Mn reserves in wild-type seeds although it does so in *mtp8*? ii) Is there any physiological significance for the specific localization of these metals in the embryo? One of the great aims of plant Fe research is to manipulate plants in order to provide higher concentrations of Fe to the human diet. The present study showed that a substantial change in the localization of Fe reserves did not result in lethality or poorer growth of the plants (Figure 24, Figure 26, Figure 27, Figure 28). This observation may encourage the idea that the localization of seed Fe reserves might be further manipulated in order to improve Fe contents in the edible parts of the seeds, which may help to improve human nutrition in the future.

6. References

- Abadía, J., Vázquez, S., Rellán-Álvarez, R., El-Jendoubi, H., Abadía, A., Álvarez-Fernández, A., and López-Millán, A.F. (2011). Towards a knowledge-based correction of iron chlorosis. *Plant Physiol. Biochem.* *49*, 471–482.
- Alonso, J.M., Stepanova, A.N., Leisse, T.J., Kim, C.J., Chen, H., Shinn, P., Stevenson, D.K., Zimmerman, J., Barajas, P., Cheuk, R., et al. (2003). Genome-wide insertional mutagenesis of *Arabidopsis thaliana*. *Science* *301*, 653–657.
- Alvarez-Tinaut, M.C., Leal, A., and Martínez, L.R. (1980). Iron-manganese interaction and its relation to boron levels in tomato plants. *Plant Soil* *55*, 377–388.
- Antebi, A., and Fink, G.R. (1992). The yeast Ca (2+)-ATPase homologue, PMR1, is required for normal Golgi function and localizes in a novel Golgi-like distribution. *Mol. Biol. Cell* *3*, 633–654.
- Arrivault, S., Senger, T., and Krämer, U. (2006). The *Arabidopsis* metal tolerance protein AtMTP3 maintains metal homeostasis by mediating Zn exclusion from the shoot under Fe deficiency and Zn oversupply. *Plant J.* *46*, 861–879.
- Baker, N.R. (2008). Chlorophyll fluorescence: a probe of photosynthesis in vivo. *Annu Rev Plant Biol* *59*, 89–113.
- Barberon, M., Zelazny, E., Robert, S., Conéjéro, G., Curie, C., Friml, J., and Vert, G. (2011). Monoubiquitin-dependent endocytosis of the IRON-REGULATED TRANSPORTER 1 (IRT1) transporter controls iron uptake in plants. *Proc. Natl. Acad. Sci.*
- Barberon, M., Dubeaux, G., Kolb, C., Isono, E., Zelazny, E., and Vert, G. (2014). Polarization of IRON-REGULATED TRANSPORTER 1 (IRT1) to the plant-soil interface plays crucial role in metal homeostasis. *Proc. Natl. Acad. Sci.* *111*, 8293–8298.
- Bauer, P., Ling, H.-Q., and Guerinot, M.L. (2007). FIT, the FER-like iron deficiency induced transcription factor in *Arabidopsis*. *Plant Physiol. Biochem.* *45*, 260–261.
- Blaudez, D., Kohler, A., Martin, F., Sanders, D., and Chalot, M. (2003). Poplar metal tolerance protein 1 confers zinc tolerance and is an oligomeric vacuolar zinc transporter with an essential leucine zipper motif. *Plant Cell* *15*, 2911–2928.
- Bloss, T., Clemens, S., and Nies, D.H. (2002). Characterization of the ZAT1p zinc transporter from *Arabidopsis thaliana* in microbial model organisms and reconstituted proteoliposomes. *Planta* *214*, 783–791.
- Bolte, S., Lanquar, V., Soler, M.-N., Beebo, A., Satiat-Jeunemaitre, B., Bouhidel, K., and Thomine, S. (2011). Distinct Lytic Vacuolar Compartments are Embedded Inside the Protein Storage Vacuole of Dry and Germinating *Arabidopsis thaliana* Seeds. *Plant Cell Physiol.* *52*, 1142–1152.
- Brash, A.R. (1999). Lipoxygenases: occurrence, functions, catalysis, and acquisition of substrate. *J. Biol. Chem.* *274*, 23679–23682.
- Chance, B., Estabrook, R.W., and Yonetani, R. (1966). Hemes and hemoproteins. *Science* *152*, 1409–1411.
- Chen, Z., Fujii, Y., Yamaji, N., Masuda, S., Takemoto, Y., Kamiya, T., Yusuyin, Y., Iwasaki, K., Kato, S., Maeshima, M., et al. (2013). Mn tolerance in rice is mediated by MTP8.1, a member of the cation diffusion facilitator family. *J. Exp. Bot.* *64*, 4375–4387.
- Cheng, N., Pittman, J.K., Shigaki, T., and Hirschi, K.D. (2002). Characterization of CAX4, an *Arabidopsis* H⁺/Cation Antiporter. *Plant Physiol.* *128*, 1245–1254.
- Clemens, S. (2006). Toxic metal accumulation, responses to exposure and mechanisms of tolerance in plants. *Biochimie* *88*, 1707–1719.
- Clough, S.J., and Bent, A.F. (1998). Floral dip: a simplified method for *Agrobacterium*-mediated transformation of *Arabidopsis thaliana*. *Plant J.* *16*, 735–743.
- Colangelo, E.P., and Guerinot, M.L. (2004). The essential basic helix-loop-helix protein FIT1 is required for the iron deficiency response. *Plant Cell Online* *16*, 3400–3412.
- Connolly, E.L., Fett, J.P., and Guerinot, M.L. (2002). Expression of the IRT1 metal transporter is controlled by metals at the levels of transcript and protein accumulation. *Plant Cell Online* *14*, 1347–1357.
- Connolly, E.L., Campbell, N.H., Grotz, N., Prichard, C.L., and Guerinot, M.L. (2003). Overexpression of the FRO2 ferric chelate reductase confers tolerance to growth on low iron and uncovers posttranscriptional control. *Plant Physiol.* *133*, 1102–1110.
- Curie, C., Panaviene, Z., Loulergue, C., Dellaporta, S.L., Briat, J.-F., and Walker, E.L. (2001). Maize yellow stripe1 encodes a membrane protein directly involved in Fe (III) uptake. *Nature* *409*, 346–349.
- Curie, C., Cassin, G., Couch, D., Divol, F., Higuchi, K., Le Jean, M., Misson, J., Schikora, A., Czernic, P., and Mari, S. (2009). Metal movement within the plant: contribution of nicotianamine and yellow stripe 1-like transporters. *Ann. Bot.* *103*, 1.
- Delhaize, E., Kataoka, T., Hebb, D.M., White, R.G., and Ryan, P.R. (2003). Genes Encoding Proteins of the Cation Diffusion Facilitator Family That Confer Manganese Tolerance. *Plant Cell Online* *15*, 1131–1142.
- Delhaize, E., Gruber, B.D., Pittman, J.K., White, R.G., Leung, H., Miao, Y., Jiang, L., Ryan, P.R., and Richardson, A.E. (2007). A role for the AtMTP11 gene of *Arabidopsis* in manganese transport and tolerance. *Plant J.* *51*, 198–210.
- DiDonato, R.J., Roberts, L.A., Sanderson, T., Eisley, R.B., and Walker, E.L. (2004). *Arabidopsis* Yellow Stripe-Like2 (YSL2): a metal-regulated gene encoding a plasma membrane transporter of nicotianamine-metal complexes. *Plant J.* *39*, 403–414.
- Divol, F., Couch, D., Conéjéro, G., Roschztardt, H., Mari, S., and Curie, C. (2013). The *Arabidopsis* YELLOW STRIPE LIKE4 and 6 Transporters Control Iron Release from the Chloroplast. *Plant Cell Online* *25*, 1040–1055.
- Donner, E., Punshon, T., Guerinot, M.L., and Lombi, E. (2012). Functional characterisation of metal(loids) processes in planta through the integration of synchrotron techniques and plant molecular biology. *Anal. Bioanal. Chem.* *402*, 3287–3298.
- Durrett, T.P., Gassmann, W., and Rogers, E.E. (2007). The FRD3-Mediated Efflux of Citrate into the Root Vasculature Is Necessary for Efficient Iron Translocation. *Plant Physiol.* *144*, 197–205.
- Edmond, C., Shigaki, T., Ewert, S., Nelson, M.D., Connorton, J.M., Chalova, V., Noordally, Z., and Pittman, J.K. (2009). Comparative analysis of CAX2-like cation transporters indicates functional and regulatory diversity. *Biochem. J.* *418*, 145.
- Fourcroy, P., Sisó-Terraza, P., Sudre, D., Savirón, M., Reyt, G., Gaymard, F., Abadía, A., Abadía, J., Álvarez-Fernández, A., and Briat, J.-F. (2014). Involvement of the ABCG37 transporter in secretion of scopoletin and derivatives by *Arabidopsis* roots in response to iron deficiency. *New Phytol.* *201*, 155–167.
- Frigerio, L. (2008). Response to Rogers Letter. *Plant Physiol.* *146*, 1026–1027.
- Frigerio, L., Hinz, G., and Robinson, D.G. (2008). Multiple vacuoles in plant cells: rule or exception? *Traffic* *9*, 1564–1570.

- Ghasemi, R., Ghaderian, S.M., and Krämer, U. (2009). Interference of nickel with copper and iron homeostasis contributes to metal toxicity symptoms in the nickel hyperaccumulator plant *Alyssum inflatum*. *New Phytol.* *184*, 566–580.
- Giehl, R.F.H., Lima, J.E., and Wirén, N. von (2012). Localized Iron Supply Triggers Lateral Root Elongation in Arabidopsis by Altering the AUX1-Mediated Auxin Distribution. *Plant Cell Online* *24*, 33–49.
- Gile, P.L. (1916). Chlorosis of pineapples induced by manganese and carbonate of lime. *Science* *44*, 855–857.
- Gleave, A.P. (1992). A versatile binary vector system with a T-DNA organisational structure conducive to efficient integration of cloned DNA into the plant genome. *Plant Mol. Biol.* *20*, 1203–1207.
- Glusker, J.P. (1991). Structural Aspects of Metal Liganding to Functional Groups in Proteins. In *Advances in Protein Chemistry*, J.T.E., Frederic M. Richards and David S. Eisenberg C.B. Anfinsen, ed. (Academic Press), pp. 1–76.
- Grillet, L., Ouerdane, L., Flis, P., Hoang, M.T.T., Isaure, M.-P., Lobinski, R., Curie, C., and Mari, S. (2014). Ascorbate Efflux as a New Strategy for Iron Reduction and Transport in Plants. *J. Biol. Chem.* *289*, 2515–2525.
- Gruber, B.D., Giehl, R.F., Friedel, S., and von Wirén, N. (2013). Plasticity of the Arabidopsis root system under nutrient deficiencies. *Plant Physiol.* *163*, 161–179.
- Grusak, M.A. (1994). Iron transport to developing ovules of *Pisum sativum* (I. Seed import characteristics and phloem iron-loading capacity of source regions). *Plant Physiol.* *104*, 649–655.
- Gustin, J.L., Zanis, M.J., and Salt, D.E. (2011). Structure and evolution of the plant cation diffusion facilitator family of ion transporters. *BMC Evol. Biol.* *11*, 76.
- Hall, J.L., and Williams, L.E. (2003). Transition metal transporters in plants. *J. Exp. Bot.* *54*, 2601–2613.
- Hamlin, R.L., and Barker, A.V. (2008). Nutritional alleviation of zinc-induced iron deficiency in Indian mustard and the effects on zinc phytoremediation. *J. Plant Nutr.* *31*, 2196–2213.
- Hangerter, R.P., and Stasinopoulos, T.C. (1991). Effect of Fe-catalyzed photooxidation of EDTA on root growth in plant culture media. *Plant Physiol.* *96*, 843–847.
- Haydon, M.J., and Cobbett, C.S. (2007). A novel major facilitator superfamily protein at the tonoplast influences zinc tolerance and accumulation in Arabidopsis. *Plant Physiol.* *143*, 1705–1719.
- Hewitt, E.J. (1948). Relation of manganese and some other metals to the iron status of plants. *Nature* *161*, 489–489.
- Higuchi, K., Suzuki, K., Nakanishi, H., Yamaguchi, H., Nishizawa, N.-K., and Mori, S. (1999). Cloning of nicotianamine synthase genes, novel genes involved in the biosynthesis of phytosiderophores. *Plant Physiol.* *119*, 471–480.
- Hirschi, K.D., Korenkov, V.D., Wilganowski, N.L., and Wagner, G.J. (2000). Expression of Arabidopsis CAX2 in tobacco. Altered metal accumulation and increased manganese tolerance. *Plant Physiol.* *124*, 125–134.
- Hopkins, E.F. (1930a). The necessity and function of manganese in the growth of *Chlorella* sp. *Science* *72*, 609–610.
- Hopkins, E.F. (1930b). Manganese as an essential element for green algae. *Amer J Bot* *17*, 205–210.
- Hunter, P.R., Craddock, C.P., Di Benedetto, S., Roberts, L.M., and Frigerio, L. (2007). Fluorescent Reporter Proteins for the Tonoplast and the Vacuolar Lumen Identify a Single Vacuolar Compartment in Arabidopsis Cells. *Plant Physiol.* *145*, 1371–1382.
- Ichikawa, T., Nakazawa, M., Kawashima, M., Iizumi, H., Kuroda, H., Kondou, Y., Tsuchida, Y., Suzuki, K., Ishikawa, A., Seki, M., et al. (2006). The FOX hunting system: An alternative gain-of-function gene hunting technique. *Plant J.* *48*, 974–985.
- Ivanov, R., Brumbarova, T., Blum, A., Jantke, A.-M., Fink-Straube, C., and Bauer, P. (2014). SORTING NEXIN1 Is Required for Modulating the Trafficking and Stability of the Arabidopsis IRON-REGULATED TRANSPORTER1. *Plant Cell Online* *26*, 1294–1307.
- Jakoby, M., Wang, H.Y., Reidt, W., Weisshaar, B., and Bauer, P. (2004). FRU (BHLH029) is required for induction of iron mobilization genes in Arabidopsis thaliana. *FEBS Lett.* *577*, 528–534.
- Janssens, K.H. (2013). *Modern Methods for Analysing Archaeological and Historical Glass* (Wiley).
- Jean, M.L., Schikora, A., Mari, S., Briat, J.-F., and Curie, C. (2005). A loss-of-function mutation in AtYSL1 reveals its role in iron and nicotianamine seed loading. *Plant J.* *44*, 769–782.
- Jefferson, R.A., Burgess, S.M., and Hirsh, D. (1986). beta-Glucuronidase from *Escherichia coli* as a gene-fusion marker. *Proc. Natl. Acad. Sci.* *83*, 8447–8451.
- Johnson, M.O. (1917). Manganese as a Cause of the Depression of the Assimilation of Iron by Pineapple Plants. *Ind. Eng. Chem.* *9*, 47–49.
- Kadish, K.M., Smith, K.M., and Guillard, R. (1999). *The porphyrin handbook* (Elsevier).
- Kai, K., Mizutani, M., Kawamura, N., Yamamoto, R., Tamai, M., Yamaguchi, H., Sakata, K., and Shimizu, B. (2008). Scopoletin is biosynthesized via ortho-hydroxylation of feruloyl CoA by a 2-oxoglutarate-dependent dioxygenase in Arabidopsis thaliana. *Plant J.* *55*, 989–999.
- Kelley, W.P. (1909). Manganese in Some of Its Relations to the Growth of Pineapples. *Ind. Eng. Chem.* *1*, 533–538.
- Kennedy, M.C., Emptage, M.H., Dreyer, J.-L., and Beinert, H. (1983). The role of iron in the activation-inactivation of aconitase. *J. Biol. Chem.* *258*, 11098–11105.
- Kim, S.A., and Guerinot, M.L. (2007). Mining iron: iron uptake and transport in plants. *FEBS Lett.* *581*, 2273–2280.
- Kim, S.A., Punshon, T., Lanzirrotti, A., Li, L., Alonso, J.M., Ecker, J.R., Kaplan, J., and Guerinot, M.L. (2006). Localization of iron in Arabidopsis seed requires the vacuolar membrane transporter VIT1. *Science* *314*, 1295.
- Klimovitskaya, Z.M., Lobanova, Z.I., and Prokopivnyuk, L.M. (1969). Physicochemical properties of RNA and DNA of plants with manganese deficiency. *Physiol. Biochem. Cultiv. Plants* *1*, 269–275.
- Kobae, Y., Uemura, T., Sato, M.H., Ohnishi, M., Mimura, T., Nakagawa, T., and Maeshima, M. (2004). Zinc transporter of Arabidopsis thaliana AtMTP1 is localized to vacuolar membranes and implicated in zinc homeostasis. *Plant Cell Physiol.* *45*, 1749–1758.
- Kobayashi, T., and Nishizawa, N.K. (2012). Iron uptake, translocation, and regulation in higher plants. *Annu. Rev. Plant Biol.* *63*, 131–152.
- Kobayashi, T., Nakayama, Y., Itai, R.N., Nakanishi, H., Yoshihara, T., Mori, S., and Nishizawa, N.K. (2003). Identification of novel cis-acting elements, IDE1 and IDE2, of the barley IDS2 gene promoter conferring iron-deficiency-inducible, root-specific expression in heterogeneous tobacco plants. *Plant J. Cell Mol. Biol.* *36*, 780–793.
- Kobayashi, T., Ogo, Y., Itai, R.N., Nakanishi, H., Takahashi, M., Mori, S., and Nishizawa, N.K. (2007). The transcription factor IDEF1 regulates the response to and tolerance of iron deficiency in plants. *Proc. Natl. Acad. Sci. U. S. A.* *104*, 19150–19155.
- Kobayashi, T., Itai, R.N., Ogo, Y., Kakei, Y., Nakanishi, H., Takahashi, M., and Nishizawa, N.K. (2009). The rice transcription factor IDEF1 is essential for the early response to iron deficiency, and induces vegetative expression of late embryogenesis abundant genes. *Plant J. Cell Mol. Biol.* *60*, 948–961.
- Kobayashi, T., Itai, R.N., Aung, M.S., Senoura, T., Nakanishi, H., and Nishizawa, N.K. (2012). The rice transcription factor IDEF1 directly binds to iron and other divalent metals for sensing cellular iron status. *Plant J.* *69*, 81–91.

- Kobayashi, T., Nagasaka, S., Senoura, T., Itai, R.N., Nakanishi, H., and Nishizawa, N.K. (2013). Iron-binding haemerythrin RING ubiquitin ligases regulate plant iron responses and accumulation. *Nat. Commun.* 4.
- Koike, S., Inoue, H., Mizuno, D., Takahashi, M., Nakanishi, H., Mori, S., and Nishizawa, N.K. (2004). OsYSL2 is a rice metal-nicotianamine transporter that is regulated by iron and expressed in the phloem. *Plant J.* 39, 415–424.
- Korshunova, Y.O., Eide, D., Clark, W.G., Guerinot, M.L., and Pakrasi, H.B. (1999). The IRT1 protein from *Arabidopsis thaliana* is a metal transporter with a broad substrate range. *Plant Mol. Biol.* 40, 37–44.
- Kosegarten, H., and Koyro, H.-W. (2001). Apoplastic accumulation of iron in the epidermis of maize (*Zea mays*) roots grown in calcareous soil. *Physiol. Plant.* 113, 515–522.
- Kurtz Jr, D.M. (1997). Structural similarity and functional diversity in diiron-oxo proteins. *JBIC J. Biol. Inorg. Chem.* 2, 159–167.
- Lan, P., Li, W., Wen, T.-N., Shiao, J.-Y., Wu, Y.-C., Lin, W., and Schmidt, W. (2011). iTRAQ protein profile analysis of *Arabidopsis* roots reveals new aspects critical for iron homeostasis. *Plant Physiol.* 155, 821–834.
- Lanquar, V., Lelièvre, F., Bolte, S., Hamès, C., Alcon, C., Neumann, D., Vansuyt, G., Curie, C., Schröder, A., Krämer, U., et al. (2005). Mobilization of vacuolar iron by AtNRAMP3 and AtNRAMP4 is essential for seed germination on low iron. *EMBO J.* 24, 4041–4051.
- Le, B.H., Cheng, C., Bui, A.Q., Wagmaister, J.A., Henry, K.F., Pelletier, J., Kwong, L., Belmonte, M., Kirkbride, R., and Horvath, S. (2010). Global analysis of gene activity during *Arabidopsis* seed development and identification of seed-specific transcription factors. *Proc. Natl. Acad. Sci.* 107, 8063–8070.
- Lindner, R.C., and Harley, C.P. (1944). Nutrient interrelations in lime-induced chlorosis. *Plant Physiol.* 19, 420.
- Ling, H.Q., Bauer, P., Bereczky, Z., Keller, B., and Ganai, M. (2002). The tomato fer gene encoding a bHLH protein controls iron-uptake responses in roots. *Proc. Natl. Acad. Sci.* 99, 13938.
- Lingam, S., Mohrbacher, J., Brumbarova, T., Potuschak, T., Fink-Straube, C., Blondet, E., Genschik, P., and Bauer, P. (2011). Interaction between the bHLH Transcription Factor FIT and ETHYLENE INSENSITIVE3/ETHYLENE INSENSITIVE3-LIKE1 Reveals Molecular Linkage between the Regulation of Iron Acquisition and Ethylene Signaling in *Arabidopsis*. *Plant Cell Online* 23, 1815–1829.
- Lobreaux, S., and Briat, J.-F. (1991). Ferritin accumulation and degradation in different organs of pea (*Pisum sativum*) during development. *Biochem J* 274, 601–606.
- Long, T.A., Tsukagoshi, H., Busch, W., Lahner, B., Salt, D.E., and Benfey, P.N. (2010). The bHLH transcription factor POPEYE regulates response to iron deficiency in *Arabidopsis* roots. *Plant Cell Online* 22, 2219.
- Lu, M., and Fu, D. (2007). Structure of the zinc transporter YiiP. *Science* 317, 1746–1748.
- Ma, J.F., Shinada, T., Matsuda, C., and Nomoto, K. (1995). Biosynthesis of phytosiderophores, mugineic acids, associated with methionine cycling. *J. Biol. Chem.* 270, 16549–16554.
- Marschner, H. (2012). *Marschner's mineral nutrition of higher plants* (Academic press).
- Marschner, H., and Römhild, V. (1994). Strategies of plants for acquisition of iron. *Plant Soil* 165, 261–274.
- Mäser, P., Thomine, S., Schroeder, J.I., Ward, J.M., Hirschi, K., Sze, H., Talke, I.N., Amtmann, A., Maathuis, F.J., Sanders, D., et al. (2001). Phylogenetic relationships within cation transporter families of *Arabidopsis*. *Plant Physiol.* 126, 1646–1667.
- Meguro, R., Asano, Y., Odagiri, S., Li, C., Iwatsuki, H., and Shoumura, K. (2007). Nonheme-iron histochemistry for light and electron microscopy: a historical, theoretical and technical review. *Arch. Histol. Cytol.* 70, 1–19.
- Mei, H., Cheng, N.H., Zhao, J., Park, S., Escareno, R.A., Pittman, J.K., and Hirschi, K.D. (2009). Root development under metal stress in *Arabidopsis thaliana* requires the H⁺/cation antiporter CAX4. *New Phytol.* 183, 95–105.
- Mengel, K. (1994). Iron availability in plant tissues-iron chlorosis on calcareous soils. *Plant Soil* 165, 275–283.
- Migeon, A., Blaudez, D., Wilkins, O., Montanini, B., Campbell, M.M., Richaud, P., Thomine, S., and Chalot, M. (2010). Genome-wide analysis of plant metal transporters, with an emphasis on poplar. *Cell. Mol. Life Sci.* 67, 3763–3784.
- Migocka, M., Papierniak, A., Maciaszczyk-Dziubińska, E., Poźdźik, P., Posyniak, E., Garbiec, A., and Filleur, S. (2014). Cucumber metal transport protein MTP8 confers increased tolerance to manganese when expressed in yeast and *Arabidopsis thaliana*. *J. Exp. Bot.* 65, 5367–5384.
- Mladěnka, P., Macáková, K., Zatloukalová, L., Řeháková, Z., Singh, B.K., Prasad, A.K., Parmar, V.S., Jahodář, L., Hrdina, R., and Saso, L. (2010). In vitro interactions of coumarins with iron. *Biochimie* 92, 1108–1114.
- Montanini, B., Blaudez, D., Jeandroz, S., Sanders, D., and Chalot, M. (2007). Phylogenetic and functional analysis of the Cation Diffusion Facilitator (CDF) family: improved signature and prediction of substrate specificity. *BMC Genomics* 8, 107.
- Mori, S. (1999). Iron acquisition by plants. *Curr. Opin. Plant Biol.* 2, 250–253.
- Morris, J., Tian, H., Park, S., Sreevidya, C.S., Ward, J.M., and Hirschi, K.D. (2008). AtCCX3 Is an *Arabidopsis* Endomembrane H⁺-Dependent K⁺ Transporter. *Plant Physiol.* 148, 1474–1486.
- Murata, Y., Ma, J.F., Yamaji, N., Ueno, D., Nomoto, K., and Iwashita, T. (2006). A specific transporter for iron(III)-phytosiderophore in barley roots. *Plant J.* 46, 563–572.
- Nies, D.H., and Silver, S. (1995). Ion efflux systems involved in bacterial metal resistances. *J. Ind. Microbiol.* 14, 186–199.
- Ogo, Y., Kobayashi, T., Nakanishi, Itai, R., Nakanishi, H., Kakei, Y., Takahashi, M., Toki, S., Mori, S., and Nishizawa, N.K. (2008). A novel NAC transcription factor, IDEF2, that recognizes the iron deficiency-responsive element 2 regulates the genes involved in iron homeostasis in plants. *J. Biol. Chem.* 283, 13407–13417.
- Otegui, M.S., Capp, R., and Staehelin, L.A. (2002). Developing Seeds of *Arabidopsis* Store Different Minerals in Two Types of Vacuoles and in the Endoplasmic Reticulum. *Plant Cell Online* 14, 1311–1327.
- Patrick, J.W., and Offler, C.E. (2001). Compartmentation of transport and transfer events in developing seeds. *J. Exp. Bot.* 52, 551–564.
- Paulsen, I.T., and Saier Jr, M.H. (1997). A novel family of ubiquitous heavy metal ion transport proteins. *J. Membr. Biol.* 156, 99–103.
- Pedas, P., Stokholm, M.S., Hegelund, J.N., Ladegaard, A.H., Schjoerring, J.K., and Husted, S. (2014). Golgi Localized Barley MTP8 Proteins Facilitate Mn Transport. *PLoS One* 9, e113759.
- Peiter, E., Maathuis, F.J., Mills, L.N., Knight, H., Pelloux, J., Hetherington, A.M., and Sanders, D. (2005a). The vacuolar Ca²⁺-activated channel TPC1 regulates germination and stomatal movement. *Nature* 434, 404–408.
- Peiter, E., Fischer, M., Sidaway, K., Roberts, S.K., and Sanders, D. (2005b). The *Saccharomyces cerevisiae* Ca²⁺ channel Cch1pMid1p is essential for tolerance to cold stress and iron toxicity. *FEBS Lett.* 579, 5697–5703.
- Peiter, E., Montanini, B., Gobert, A., Pedas, P., Husted, S., Maathuis, F.J., Blaudez, D., Chalot, M., and Sanders, D. (2007). A secretory pathway-localized cation diffusion facilitator confers plant manganese tolerance. *Proc. Natl. Acad. Sci.* 104, 8532–8537.
- Porra, R.J., Thompson, W.A., and Kriedemann, P.E. (1989). Determination of accurate extinction coefficients and simultaneous equations for assaying chlorophylls a and b extracted with four different solvents: verification of the concentration of chlorophyll standards by atomic absorption spectroscopy. *Biochim. Biophys. Acta BBA-Bioenerg.* 975, 384–394.

- Punshon, T., Ricachenevsky, F.K., Hindt, M.N., Socha, A.L., and Zuber, H. (2013). Methodological approaches for using synchrotron X-ray fluorescence (SXRF) imaging as a tool in ionomics: examples from *Arabidopsis thaliana*. *Metallomics* 5, 1133–1145.
- Quartieri, S., Triscari, M., Sabatino, G., Boscherini, F., and Sani, A. (2002). Fe and Mn K-edge XANES study of ancient Roman glasses. *Eur. J. Mineral.* 14, 749–756.
- Raboy, V. (2003). myo-Inositol-1,2,3,4,5,6-hexakisphosphate. *Phytochemistry* 64, 1033–1043.
- Ramakrishnan, U. (2002). Prevalence of Micronutrient Malnutrition Worldwide. *Nutr. Rev.* 60, S46–S52.
- Ramos, M.S., Khodja, H., Mary, V., and Thomine, S. (2013). Using PIXE for quantitative mapping of metal concentration in *Arabidopsis thaliana* seeds. *Front. Plant Sci.* 4.
- Ravet, K., Touraine, B., Boucherez, J., Briat, J., Gaymard, F., and Cellier, F. (2009). Ferritins control interaction between iron homeostasis and oxidative stress in *Arabidopsis*. *Plant J.* 57, 400–412.
- Ricachenevsky, F.K., Menguer, P.K., Sperotto, R.A., Williams, L.E., and Fett, J.P. (2013). Roles of plant metal tolerance proteins (MTP) in metal storage and potential use in biofortification strategies. *Front. Plant Sci.* 4.
- Rippel, A. (1923). The iron chlorosis in green plants caused by manganese. *Biochem Z* 140, 315–323.
- Robinson, N.J., Procter, C.M., Connolly, E.L., and Guerinot, M.L. (1999). A ferric-chelate reductase for iron uptake from soils. *Nature* 397, 694–697.
- Rodríguez-Celma, J., Lin, W.-D., Fu, G.-M., Abadía, J., López-Millán, A.-F., and Schmidt, W. (2013). Mutually exclusive alterations in secondary metabolism are critical for the uptake of insoluble iron compounds by *Arabidopsis* and *Medicago truncatula*. *Plant Physiol.* 162, 1473–1485.
- Roschztardt, H., Conéjéro, G., Curie, C., and Mari, S. (2009). Identification of the Endodermal Vacuole as the Iron Storage Compartment in the *Arabidopsis* Embryo. *Plant Physiol.* 151, 1329–1338.
- Roschztardt, H., Séguéla-Arnaud, M., Briat, J.-F., Vert, G., and Curie, C. (2011). The FRD3 Citrate Effluxer Promotes Iron Nutrition between Symplastically Disconnected Tissues throughout *Arabidopsis* Development. *Plant Cell Online* 23, 2725–2737.
- Santi, S., and Schmidt, W. (2009). Dissecting iron deficiency-induced proton extrusion in *Arabidopsis* roots. *New Phytol.* 183, 1072–1084.
- Schaaf, G. (2004). Molecular and biochemical characterization of plant transporters involved in the cellular homeostasis of Mn and Fe. *Der Andere Verlag*.
- Schaaf, G., Ludewig, U., Erenoglu, B.E., Mori, S., Kitahara, T., and von Wirén, N. (2004). ZmYS1 functions as a proton-coupled symporter for phytosiderophore- and nicotianamine-chelated metals. *J. Biol. Chem.* 279, 9091–9096.
- Schaaf, G., Honsbein, A., Meda, A.R., Kirchner, S., Wipf, D., and von Wirén, N. (2006). AtIREG2 Encodes a Tonoplast Transport Protein Involved in Iron-dependent Nickel Detoxification in *Arabidopsis thaliana* Roots. *J. Biol. Chem.* 281, 25532–25540.
- Schmid, N.B. (2014). Identification and characterization of *Arabidopsis* genes involved in tolerance to Fe deficiency-mediated chlorosis. Halle (Saale), Universitäts- und Landesbibliothek Sachsen-Anhalt, Diss., 2014.
- Schmid, W.E., and Gerloff, G.C. (1961). A naturally occurring chelate of iron in xylem exudate. *Plant Physiol.* 36, 226.
- Schmid, M., Davison, T.S., Henz, S.R., Pape, U.J., Demar, M., Vingron, M., Schölkopf, B., Weigel, D., and Lohmann, J.U. (2005). A gene expression map of *Arabidopsis thaliana* development. *Nat. Genet.* 37, 501–506.
- Schmid, N.B., Giehl, R.F., Döll, S., Mock, H.-P., Strehmel, N., Scheel, D., Kong, X., Hider, R.C., and von Wirén, N. (2014). Feruloyl-CoA 6'-Hydroxylase1-Dependent Coumarins Mediate Iron Acquisition from Alkaline Substrates in *Arabidopsis*. *Plant Physiol.* 164, 160–172.
- Séguéla, M., Briat, J.-F., Vert, G., and Curie, C. (2008). Cytokinins negatively regulate the root iron uptake machinery in *Arabidopsis* through a growth-dependent pathway. *Plant J.* 55, 289–300.
- Shin, L.-J., Lo, J.-C., Chen, G.-H., Callis, J., Fu, H., and Yeh, K.-C. (2013). IRT1 DEGRADATION FACTOR1, a RING E3 Ubiquitin Ligase, Regulates the Degradation of IRON-REGULATED TRANSPORTER1 in *Arabidopsis*. *Plant Cell Online* 25, 3039–3051.
- Shive, J.W. (1941). Significant roles of trace elements in the nutrition of plants. *Plant Physiol.* 16, 435.
- Sideris, C.P., and Young, H.Y. (1949). Growth and chemical composition of *Ananas comosus* (L.) Merr., in solution cultures with different iron-manganese ratios. *Plant Physiol.* 24, 416.
- Sivitz, A., Grinvalds, C., Barberon, M., Curie, C., and Vert, G. (2011). Proteasome-mediated turnover of the transcriptional activator FIT is required for plant iron-deficiency responses. *Plant J.* 66, 1044–1052.
- Somers, I.I., and Shive, J.W. (1942). The iron-manganese relation in plant metabolism. *Plant Physiol.* 17, 582.
- Stacey, M.G., Patel, A., McClain, W.E., Mathieu, M., Remley, M., Rogers, E.E., Gassmann, W., Blevins, D.G., and Stacey, G. (2008). The *Arabidopsis* AtOPT3 protein functions in metal homeostasis and movement of iron to developing seeds. *Plant Physiol.* 146, 589–601.
- Stadler, R., Lauterbach, C., and Sauer, N. (2005). Cell-to-Cell Movement of Green Fluorescent Protein Reveals Post-Phloem Transport in the Outer Integument and Identifies Symplastic Domains in *Arabidopsis* Seeds and Embryos. *Plant Physiol.* 139, 701–712.
- Stephan, U.W., and Scholz, G. (1993). Nicotianamine: mediator of transport of iron and heavy metals in the phloem? *Physiol. Plant.* 88, 522–529.
- Susin, S., Abadía, A., González-Reyes, J.A., Lucena, J.J., and Abadía, J. (1996). The pH requirement for in vivo activity of the iron-deficiency-induced "Turbo" ferric chelate reductase (a comparison of the iron-deficiency-induced iron reductase activities of intact plants and isolated plasma membrane fractions in sugar beet). *Plant Physiol.* 110, 111–123.
- Takagi, S., Nomoto, K., and Takemoto, T. (1984). Physiological aspect of mugineic acid, a possible phytosiderophore of graminaceous plants. *J. Plant Nutr.* 7, 469–477.
- Takahashi, M., Yamaguchi, H., Nakanishi, H., Shioiri, T., Nishizawa, N.-K., and Mori, S. (1999). Cloning two genes for nicotianamine aminotransferase, a critical enzyme in iron acquisition (Strategy II) in graminaceous plants. *Plant Physiol.* 121, 947–956.
- Tauris, B., Borg, S., Gregersen, P.L., and Holm, P.B. (2009). A roadmap for zinc trafficking in the developing barley grain based on laser capture microdissection and gene expression profiling. *J. Exp. Bot.* 60, 1333–1347.
- Tejos, R.I., Mercado, A.V., and Meisel, L.A. (2010). Analysis of chlorophyll fluorescence reveals stage specific patterns of chloroplast-containing cells during *Arabidopsis* embryogenesis. *Biol. Res.* 43, 99–111.
- Tottingham, W.E., and Beck, A.J. (1916). Antagonism between manganese and iron in the growth of wheat. *Plant World* 19, 359–370.
- Twyman, E.S. (1951). The iron and manganese requirements of plants. *New Phytol.* 50, 210–226.
- Ulker, B., Peiter, E., Dixon, D.P., Moffat, C., Capper, R., Bouché, N., Edwards, R., Sanders, D., Knight, H., and Knight, M.R. (2008). Getting the most out of publicly available T-DNA insertion lines. *Plant J.* 56, 665–677.

- Vert, G., Grotz, N., Dédaldéchamp, F., Gaymard, F., Guerinot, M.L., Briat, J.-F., and Curie, C. (2002). IRT1, an Arabidopsis Transporter Essential for Iron Uptake from the Soil and for Plant Growth. *Plant Cell Online* 14, 1223–1233.
- Waters, B.M., Chu, H.-H., DiDonato, R.J., Roberts, L.A., Easley, R.B., Lahner, B., Salt, D.E., and Walker, E.L. (2006). Mutations in Arabidopsis Yellow Stripe-Like1 and Yellow Stripe-Like3 Reveal Their Roles in Metal Ion Homeostasis and Loading of Metal Ions in Seeds. *Plant Physiol.* 141, 1446–1458.
- Weber, G., Neumann, G., and Römheld, V. (2002). Speciation of iron coordinated by phytosiderophores by use of HPLC with pulsed amperometric detection and AAS. *Anal. Bioanal. Chem.* 373, 767–771.
- Wei, Y., and Fu, D. (2006). Binding and transport of metal ions at the dimer interface of the Escherichia coli metal transporter YiiP. *J. Biol. Chem.* 281, 23492–23502.
- White, P.J., and Broadley, M.R. (2009). Biofortification of crops with seven mineral elements often lacking in human diets—iron, zinc, copper, calcium, magnesium, selenium and iodine. *New Phytol.* 182, 49–84.
- Von Wirén, N., Marschner, H., and Römheld, V. (1995). Uptake kinetics of iron-phytosiderophores in two maize genotypes differing in iron efficiency. *Physiol. Plant.* 93, 611–616.
- Von Wirén, N., Klair, S., Bansal, S., Briat, J.-F., Khodr, H., Shioiri, T., Leigh, R.A., and Hider, R.C. (1999). Nicotianamine chelates both FeIII and FeII. Implications for metal transport in plants. *Plant Physiol.* 119, 1107–1114.
- Wu, B., and Becker, J.S. (2012). Imaging techniques for elements and element species in plant science. *Metallomics* 4, 403.
- Yeung, E.C., and Meinke, D.W. (1993). Embryogenesis in Angiosperms: Development of the Suspensor. *Plant Cell Online* 5, 1371–1381.
- Yi, X., McChargue, M., Laborde, S., Frankel, L.K., and Bricker, T.M. (2005). The Manganese-stabilizing Protein Is Required for Photosystem II Assembly/Stability and Photoautotrophy in Higher Plants. *J. Biol. Chem.* 280, 16170–16174.
- Yuan, Y., Wu, H., Wang, N., Li, J., Zhao, W., Du, J., Wang, D., and Ling, H.Q. (2008). FIT interacts with AtbHLH38 and AtbHLH39 in regulating iron uptake gene expression for iron homeostasis in Arabidopsis. *Cell Res.* 18, 385–397.
- Van der Zaal, B.J., Neuteboom, L.W., Pinas, J.E., Chardonens, A.N., Schat, H., Verkleij, J.A., and Hooykaas, P.J. (1999). Overexpression of a novel Arabidopsis gene related to putative zinc-transporter genes from animals can lead to enhanced zinc resistance and accumulation. *Plant Physiol.* 119, 1047–1056.
- Zhai, Z., Gayomba, S.R., Jung, H., Vimalakumari, N.K., Piñeros, M., Craft, E., Rutzke, M.A., Danku, J., Lahner, B., Punshon, T., et al. (2014). OPT3 Is a Phloem-Specific Iron Transporter That Is Essential for Systemic Iron Signaling and Redistribution of Iron and Cadmium in Arabidopsis. *Plant Cell Online tpc* – 114.
- Zinder, B., Furrer, G., and Stumm, W. (1986). The coordination chemistry of weathering: II. Dissolution of Fe (III) oxides. *Geochim. Cosmochim. Acta* 50, 1861–1869.

7. Abbreviations

°C	degree Celsius	iTRAQ	isobaric tags for relative and absolute quantitation
%	percent	LB	left border
μ	micro	M	molar
μM	micromolar	MES	2-(<i>N</i> -morpholino) ethanesulfonic acid, buffer
μg	microgram	ml	milliliter
μl	microlitre	Mn	manganese
μM	micromolar	MS	murashige and Skoog medium
CaMV	cauliflower mosaic virus	NA	nicotianamine
bp	base pair	Ni	nickel
cDNA	complementary DNA	P	p-value
Co	cobalt	PS	phytosiderophores
Col-0	Columbia-0	PSV	protein storage vacuole
DNA	deoxyribonucleic acid	PCR	polymerase chain reaction
DW	dry weight	RB	right border
EDTA	ethylenediaminetetraacetic acid	RNA	ribonucleic acid
Fe	iron	ROS	reactive oxygen species
Fe28/Mn40	½ MS based medium supplemented with 28 μM Fe and 40 μM Mn	SAIL	syngenta <i>Arabidopsis</i> Insertion Library
FW	fresh weight	SALK	Salk Institute for biological studies
FeSOD	Fe-dependent superoxide dismutase	SD	standart deviation
GUS	β-glucuronidase, is a reporter gene system	t-test	student's <i>t</i> distribution test
GFP	green fluorescent protein	UV	ultra-violet light
h	hour	WT	wild type
ICP-OES	inductively coupled plasma opticaemission pectrometry	Zn	zinc

8. Affirmation

I hereby declare that the submitted work has been completed by me, the undersigned, and that I have not used any other than permitted reference sources or materials or engaged any plagiarism. All the references and the other sources used in the presented work have been appropriately acknowledged in the work. I further declare that the work has not been previously submitted for the purpose of academic examination, either in its original or similar form, anywhere else.

Hiermit erkläre ich, dass ich diese Arbeit selbständig verfasst und keine anderen als die angegebenen Quellen und Hilfsmittel verwendet habe. Die den benutzten Hilfsmitteln wörtlich oder inhaltlich entnommenen Stellen habe ich unter Quellenangaben kenntlich gemacht. Die vorliegende Arbeit wurde in gleicher oder ähnlicher Form noch keiner anderen Institution oder Prüfungsbehörde vorgelegt.

Seçkin Eroğlu

Gatersleben 12th February, 2015

9. Acknowledgements

My entire story in IPK started with the acceptance of Nico; therefore, I am greatly thankful to him giving me the opportunity to conduct a PhD study in his group. It required a great effort for me to discipline myself to work in a systematic way rather than in a free style, forming my ideas as well-built arguments for discussion rather than letting them fly in the air, conducting the same experiment over and over again in order to create state-of-the-art data sets. Yet, I understand this is the requirement to justify earning the philosophy of a doctorate's degree in natural sciences. I am thankful to him for his continuous support and guidance in my professional and private life during the PhD.

I thank our collaborators Dr. Edgar Peiter and Bastian Meier, with whom I worked intensively with a great pleasure. I also thank Dr. Michiko Takahashi and Dr. Yasuko Terada for the X-ray fluorescence analysis which added a lot to my work. Thanks to Dr. Michael Melzer and Marion Benneke for their support at the microscopy, Susanne Reiner for the elemental analysis and Mr. Geyer and Mrs. Braun for taking care of the Arabidopsis plants in the greenhouse.

I thank Dr. K. Humbeck and Dr. T. Buckhout for accepting to evaluate my thesis.

I would like to thank all members of the Molecular Plant Nutrition group esp. the Fe-specialized guys like Ricardo, Nicole and Ben for fruitful discussions as well as other colleagues as Alexandra, Siva, Seyed, MT Ben, Alex, Rongli, Fanghua, Fengying, Diana, Elis, Lisa, Julia, Heike, Melanie, Andrea, Polet, Baris, Dima, Zhaojun, Takao, Markus, Ying, Kai, Mo, Dagmar, Wally and everyone else for their friendship and support.

For financial support during my PhD I would like to acknowledge the Federal Ministry of Education and Research (BMBF) and the IPK Gatersleben.

Besides, thanks to the all the people working in the administration and maintenance, especially Dr. Leps, Brigitte and our lovely department secretary Elmarie.

Thanks to the friends for not leaving me isolated in this small place called Gatersleben, revolutionist ones from Hannover: Çınar, Dilruba, Güven, Selin, Gamze, Uygur and musician ones from Halle: İlker, Onur, Hami, Özgür, Gözde. Special thanks to Gülhas for her extensive support and to Helmut and Susanne Knüpffer for their warm friendliness and cultural conversations.

Seçkin Eroğlu

Nationality: Turkish

Date and Place of Birth: 30.08.1985 Izmir

Address:

Mavisehir Mah., Erkin Usman sok,

Selcuk 2blok, 3/28

Karsiyaka/Izmir Turkey

Telephone: +905062164786

Email: erogluseckin@gmail.com

EDUCATION:

2010-...

PhD candidate

Leibniz Institute of Plant Genetics and Crop Plant
Research, Gatersleben, Germany

2008- 2010

MSc:

Yeditepe University, Istanbul, Turkey

Biotechnology program

CGPA: 3.65 / 4.00

2003-2008

BSc-Major:

Middle East Technical University, Ankara, Turkey

Molecular Biology&Genetics

CGPA: 3.10 / 4.00

SCHOLARSHIP:

TUBITAK (Turkish Academy of Sciences) Scholarship for MSc students

Yeditepe University Scholarship for MSc students.

PUBLISHED PAPERS:

Eroglu, S., Sahin, U., Tunc, T., and Sahin, F. (2012). Bacterial application increased the flow rate of CaCO₃-clogged emitters of drip irrigation system. *Journal of Environmental Management* 98, 37–42. (Patent pending, application no: 15162520.0-1401)

Sahin, U., Tunc, T., and Eroğlu, S. (2012). Evaluation of CaCO₃ clogging in emitters with magnetized saline waters. *Desalination and Water Treatment* 40, 168–173.)

Sahin, U., Eroğlu, S., and Sahin, F. (2011). Microbial application with gypsum increases the saturated hydraulic conductivity of saline–sodic soils. *Applied Soil Ecology* 48, 247–250.

Eroglu, S., Ozbek, H., and Sahin, F. (2010). First Report of Group 16SrXII Phytoplasma Causing Stolbur Disease in Potato Plants in the Eastern and Southern Anatolia Regions of Turkey. *Plant Disease* 94, 1374–1374.

Seçkin Eroğlu (2010). Molecular identification and characterization of phytoplasmas causing stolbur disease on potato and tomato plants in turkey. Yeditepe University.

İşeri, Ö.D., Kars, M.D., Eroğlu, S., and Gündüz, U. (2009). Drug Resistant MCF-7 Cell Lines Also Developed Cross-Resistance to Structurally Unrelated Anticancer Agents. *International Journal of Hematology & Oncology* 19, 1–8.

POSTER PRESENTATIONS:

Developing screening strategies to identify genes involved in Fe homeostasis in plants.

16th International Symposium on Iron Nutrition and Interactions in Plants, Amherst, USA, June, 2012

Characterization of a Mn transporter essential for Fe efficiency in *Arabidopsis thaliana*.

17th International Plant Nutrition Colloquium, İstanbul, Turkey, August, 2013(Best poster prize)

A Mn transporter essential for Fe efficiency in *Arabidopsis*.

17th International Symposium on Iron Nutrition and Interactions in Plants, Gatersleben, Germany, July , 2014

LANGUAGES:

- Turkish (Native)
- English (Fluent, 101 on TOEFL ibt[2009])
- German (B1 certificate [2011])